NDA-2140-2

METALLURGY AND CERAMICS

CARBIDE FUEL DEVELOPMENT

Phase I Report—Period of May 15 to September 15, 1959

By

R. Bolomey
S. Lazerus
J. Sapir
G. Sofer
H. Steinmetz
A. Strasser
J. Weisman
R. Dial
C. McMurtry
F. Saulino
K. Taylor

October 15, 1959

Nuclear Development Corporation of America
White Plains New York

and

The Carborundum Company
Niagara Falls, New York

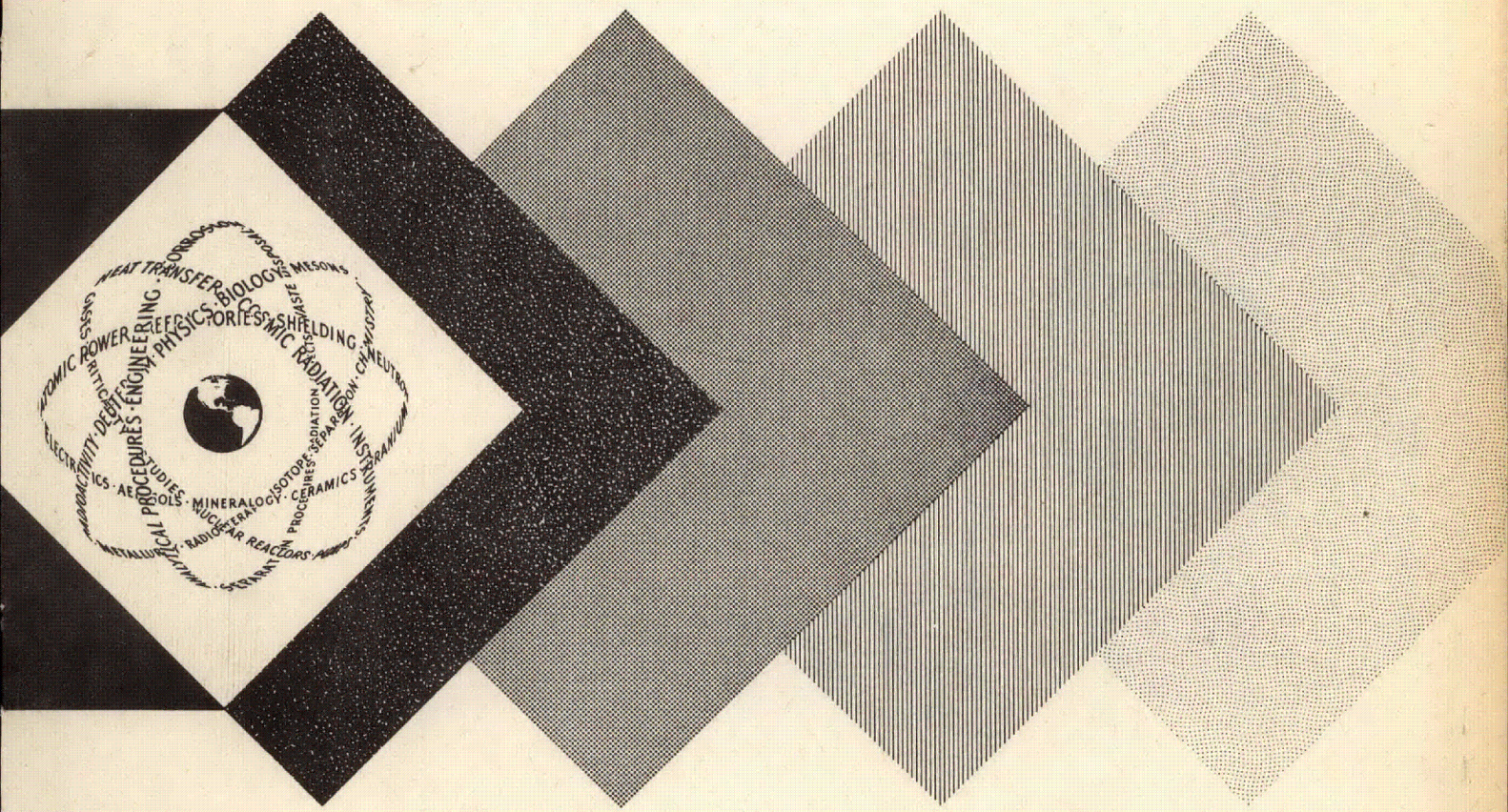

UNITED STATES ATOMIC ENERGY COMMISSION
Technical Information Service

LEGAL NOTICE

Printed in USA. Price $2.50. Available from the Office of Technical Services, Department of Commerce, Washington 25, D. C.

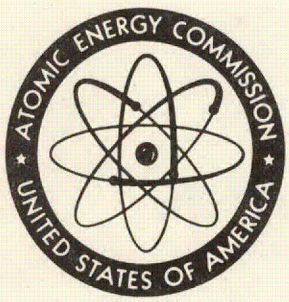

AEC Technical Information Service Extension
Oak Ridge, Tennessee

NDA 2140-2

CARBIDE FUEL DEVELOPMENT

Phase I Report
Period of May 15 to September 15, 1959

Project Engineer: A. Strasser

NDA Authors	Carborundum Co. Authors
R. Bolomey	R. Dial
S. Lazerus	C. McMurtry
J. Sapir	F. Saulino
G. Sofer	K. Taylor
H. Steinmetz	
A. Strasser	
J. Weisman	

October 15, 1959

Work Performed under Project IV, Contract AT(30-1)-2303
for the United States Atomic Energy Commission

Prime Contractor
NUCLEAR DEVELOPMENT CORPORATION OF AMERICA
White Plains, New York

Subcontractor
THE CARBORUNDUM COMPANY
Niagara Falls, N. Y.

FOREWORD

The Carbide Fuel Development project is part of the AEC Fuel Cycle Development Program. The prime contractor is the Nuclear Development Corporation of America (NDA), and the subcontractor is The Carborundum Company. NDA is performing the conceptual design, fuel evaluation, fuel irradiation, and irradiated fuel reprocessing. The Carborundum Company is fabricating the fuel and reprocessing unirradiated fuel. Both companies are designing and building plutonium handling facilities.

Phase I covers the period May 15-November 7, 1959. This report covers the period May 15-September 15, 1959. The work accomplished includes the complete Conceptual Design task, and the initial results of the tasks on Facility Design and Fabrication, Fuel Fabrication and Evaluation, and Fuel Reprocessing.

ABSTRACT

A combination of UC and PuC is proposed as a fuel which has the potential for reducing the fuel cycle cost of fast breeder reactors. A $3\frac{1}{2}$ year development program is outlined, the purpose of which is to fabricate the fuel and evaluate the fuel properties having the most significant effect on fuel cycle cost.

Technical progress in the first four months of Phase I consisted of:

1. Conceptual Design

   Analytical evaluation of PuC-UC in existing fast breeder reactors was completed with respect to heat transfer, physics, and cost. It was found that if certain reasonable fuel performance goals can be achieved, a fuel cycle cost reduction of a factor of 2 to 3 is possible.

2. Plutonium Facility Design

   Facilities to handle and irradiate plutonium were designed and partially constructed. The facilities will be capable of synthesis and fabrication of carbides by dry powder techniques, chemical analysis, x-ray diffraction, metallography, fuel-clad compatibility studies, hardness testing, thermal cycling. Irradiation capsules were designed to irradiate clad fuel rod sections to 2% burnup at maximum fuel temperatures >1900°F.

3. Fuel Fabrication and Evaluation

   High purity, better than 99 w/o, UC pellets have been fabricated by pressing and sintering. Evaluation studies [listed in (2)] have been initiated.

4. Reprocessing

   The ease of dissolution of unirradiated UC was confirmed. Dissolution studies of UC with simulated fission products were initiated.

CONTENTS

TABLES

FIGURES

1. INTRODUCTION

Fuel made of a combination of UC and PuC has a potential of reducing the fuel cycle cost of existing fast breeder reactors. The fuel cycle cost reduction is anticipated for two major reasons: increased burnup and increased power generation capability of PuC-UC compared to presently available metallic fuels. The effect of high burnup and high power generation rate on the stability of UC or PuC-UC is not known. However, based on UC irradiation tests to low burnups, there is justifiable optimism that carbide fuels will be dimensionally more stable than metallic fuels, and based on the high melting point and good thermal conductivity of UC, there is further expectation that carbide fuels will be capable of high power generation rates.

The Carbide Fuel Development Program is to study the technology of the entire PuC-UC fuel cycle. The major goal of the program is to produce PuC-UC, and to obtain data on the irradiation behavior of PuC-UC for long burnups, and at high power generation rates. In addition, other areas of the fuel cycle are being explored to discover potential problems. The program is planned for a period of about $3\frac{1}{2}$ years. Specifically, the following will be accomplished:

1. Conceptual Design

An analytical study of the effect of substitution of PuC-UC fuel in existing fast breeder reactors on heat transfer, physics, and cost will be made. A conceptual, rod-type, fuel element configuration will be proposed which can be substituted directly in an existing reactor.

2. Facility Design and Fabrication

The experimental facility to handle plutonium will be designed and built.

3. Fuel Fabrication and Evaluation

Various methods of fuel preparation and fabrication into cylindrical pellets will be explored. The pellets will be evaluated by density measurement, chemical analysis, x-ray diffraction, hardness, and metallography. Fuel-cladding compatibility will be studied. Cermets with small amounts of uranium metal will be cycled thermally.

4. Fuel Irradiation

Clad fuel samples will be irradiated, with burnup and maximum fuel temperature as variables; a post-irradiation examination will be made.

5. Fuel Reprocessing

A study of the reprocessing of both unirradiated and irradiated fuel will be made.

6. Full Scale Fuel Assembly

The design and construction of a full scale fuel element assembly for irradiation in an existing fast breeder reactor will be completed.

2. SUMMARY AND CONCLUSIONS

2.1 CONCEPTUAL DESIGN

Heat transfer, nuclear and preliminary cost studies were conducted to evaluate the potential of carbide fuels in fast breeder power reactors. In these studies carbide fuel elements were substituted in the core of the Enrico Fermi Fast Breeder Reactor (EFFBR) and their effect on the reactor heat transfer characteristics, nuclear characteristics, and fuel cycle cost was calculated and compared to U-10% Mo and PuO_2-UO_2 fuels.

2.1.1 Conclusion

The calculations indicate that carbide fuels offer the promise of significant reduction in the fuel cycle cost of fast breeder power reactors by virtue of (1) their favorable heat transfer characteristics, i.e., high thermal conductivity and high melting point, and (2) their high burnup potential, as shown by the results summarized in Table 2.1.

2.1.2 Summary

Heat Transfer Effects

A factor of two increase in fuel pin diameter and a factor of four decrease in the number of fuel pins appear possible with UC or PuC, compared to U-10% Mo, at a maximum carbide temperature well below the melting point. With PuO_2-UO_2 fuel, the low thermal conductivity requires a reduction in fuel pin size below that of U-10% Mo, coupled with a large increase in the number of fuel pins required.

Nuclear Effects

Uranium carbide yields a somewhat smaller critical mass (kg U^{235}) than does U-10% Mo alloy. However, because of the lower fuel density and the softer neutron spectrum caused by the introduction of carbon, a slight (3%) reduction in breeding ratio is obtained. With PuC-UC fuel an increase in the breeding ratio and a decrease in critical mass is achieved, as might be expected from the use of plutonium as the fissile material. The PuO_2-UO_2 fuel is characterized by a lower breeding ratio than the PuC-UC fuel because of its lower fuel density. The critical mass for PuO_2-UO_2 fuel, however, is somewhat lower than for PuC-UC fuel, because of the necessary reduction of U^{238} in the core.

Effect on Fuel Cost

The fuel cost of the EFFBR with a UC core is expected to be lower than with U-10% Mo, even if burnup were unchanged. This is primarily the result of savings realized in the fuel fabrication steps, reflecting the larger fuel pin diameter of UC. With the higher burnup expected of UC, the

Table 2.1 — Summary of Conceptual Design Results

Reactor	A Reference EFFBR U-10% Mo Core	B EFFBR UC Core			C EFFBR PuC-UC Core		D EFFBR PuO_2-UO_2 Core
Heat Transfer Characteristics							
Number of fuel pins per subassembly	144	36			36		225
Fuel pin diameter, in.	0.148	0.289			0.289		0.104
Corresponding maximum fuel temperature, °F	1135	2900			2900		3900
Nuclear Characteristics							
Calculated breeding ratio	1.12	1.09			1.57		1.48
Critical mass, kg U^{235} or Pu^{239}	433	397			279		253
Estimated Fuel Costs							
Fuel fabrication cost, $/kg (U+Pu)	540	←——340*——→			←550*→		2200*
Assumed burnup, a/o of (U+Pu)	1.25	1.25	2.0	5.0	2.0	5.0	2.0
Fuel cost, mills/kwh (Pu at $30/g)	8.8	7.3	4.7	2.1	6.4	2.9	18.1
Fuel cost, mills/kwh (Pu at $12/g)	11.7	10.0	7.4	4.9	5.9	3.4	16.4

* Based on pressing, sintering, and grinding pellets. Relaxation of tolerances to eliminate grinding will reduce fuel cycle costs more on Pu cores than others.

fuel cost goes down to a fraction of the cost with U-10% Mo. The relative costs of the PuC-UC and UC fuel cycles depend on the Pu costs. The $30/g cost gives a high credit for breeding, but also increases the cost due to increased fabrication losses, reprocessing losses, working capital, and fuel lease charges. The $12/g cost decreases the credit for breeding but also decreases the cost of losses, working capital, and fuel lease charges. At $30/g the balance of costs favors UC; at $12/g the balance of costs favors PuC-UC. It should be noted that reduction in the number and complexity of fabrication operations, such as elimination of pellet grinding, will result in greater cost reductions for PuC-UC than UC. Fuel costs are expected to be much higher for PuO_2-UO_2 fuel than PuC-UC, mainly because of the large number of small pins needed to satisfy the heat transfer requirements. The fabrication cost estimate for PuO_2-UO_2 fuel is based on pelletizing and grinding, which may be entirely impractical for this fuel; a more economical fabrication method is required without a sacrifice in fuel density.

2.2 FUEL FABRICATION AND EVALUATION

2.2.1 Fuel Fabrication

A study of the reaction of uranium oxides (UO_2 and U_3O_8) and carbon has been made. Uranium monocarbide having a UC content of about 97% has been produced by heating a stoichiometric mixture of UO_2 and carbon in vacuum or in an inert atmosphere at 1800°C. The UC content was increased to about 99% by milling the product to a fine powder, pressing into pellets, and sintering in an inert atmosphere at 1800°C.

Uranium monocarbide pellets having a density of about 10 g/cc (theoretical density 13.63 g/cc) were obtained by milling the powder to an average particle size of 5 microns, pressing at 40,000 psi with a Carbowax binder and sintering at 1800 to 1900°C in vacuum or an inert atmosphere. In order to achieve higher density, variations in fabrication procedure, such as milling to finer particle size, hot pressing, increasing soak period, and adding minor amounts of uranium metal, have been initiated.

A few experiments indicated that a small amount of nitrogen in the atmosphere probably aids sintering. In this case, however, the sintered shape contains nitrogen, presumably as uranium nitride in solid solution.

Uranium carbide, in fine powder form, is pyrophoric and readily hydrolizes when exposed to moisture. Therefore, in the synthesis and fabrication of UC, careful control of the atmosphere is required if a high purity product is to be obtained.

2.2.2 Fuel Evaluation

A study of chemical analysis methods has been completed and selection has been made of specific procedures to be used in the present project. Uranium, carbon, and impurity analyses have been initiated.

Studies of the metallography of carbide fuels have been initiated. Experiments on the compatibility of carbide fuels with potential cladding materials have been planned, and the equipment and materials for tests with UC have been prepared. Experiments on the thermal cycling behavior of carbide fuels with small amounts of excess uranium have been planned, and the equipment for tests with UC-U has been set up.

2.3 REPROCESSING

A review of the literature on decladding has been completed.

Preliminary experiments on the dissolution of UC pellets indicate that the crushed pellets dissolve readily in dilute nitric acid. The rate of solution is dependent upon particle size, concentration of the acid, and temperature.

A study has been initiated to determine the effect of added simulated fission products on the solubility of UC pellets. Preliminary experiments indicate that such pellets are not completely soluble in nitric acid. The residue is being analyzed for uranium content.

2.4 FACILITY DESIGN

The design for the Carborundum plutonium facility has been completed and the various components are under construction. All equipment for use inside the facility has either been received or is on order. The glove-boxes and gas purification train have been designed and are being fabricated. It is anticipated that the facility and equipment fabrication will be completed during November 1959.

The design of the NDA plutonium facility has been essentially completed. Three chemistry glove-boxes have been fabricated; a fourth glove-box is nearly complete. All equipment for the chemistry glove-boxes has been received or is on order. It is anticipated that the facility and equipment fabrication will be completed during March 1960.

Eight capsules have been planned for the irradiation test program. The initial two capsules will contain UC specimens and will be irradiated in 1960. The design of the two experiments is about 70% complete. Six capsules will contain PuC-UC specimens, and will be irradiated in 1961. Initial reliability tests on capsule heaters have been made.

3. CONCEPTUAL DESIGN

3.1 INTRODUCTION

In order to evaluate the future potential of carbide fuels for fast breeder power reactors,the characteristics of several carbide-fueled reactors of this type were investigated. Heat transfer, nuclear, and cost studies were performed for both uranium carbide (UC) and plutonium-uranium carbide combinations (PuC-UC). In these studies, carbide fuel elements were substituted for the presently planned fuels in the current designs of several fast reactors. Overall reactor performance and design characteristics, such as power output, core size, coolant temperatures, and coolant flow rate were kept constant, so that a direct comparison could be made of the effects of fuel substitution. The number and size of fuel element subassemblies were also kept constant to obtain a design which permits testing of individual carbide fuel subassemblies in the parent reactor. Since this approach imposes some restrictions on the utilization of carbide fuels, the benefits obtained are expected to fall short of the maximum benefits possible with design optimizations based on carbide fuels alone

Heat transfer calculations were performed for the Enrico Fermi Fast Breeder Reactor (EFFBR) and the Experimental Breeder Reactors (EBR-I and II). The number of fuel pins required per subassembly, and the corresponding pin diameter were determined as a function of maximum fuel temperature. Nuclear calculations of critical mass, enrichment, and breeding ratio were performed for the EFFBR. Order of magnitude fuel cost studies were made comparing carbide fuel at several burnups to the reference U-10% Mo EFFBR and a hypothetical EFFBR fueled with combined uranium-plutonium oxide. The EFFBR was selected for the nuclear and cost calculations because more data are available on fuel costs for this reactor than for the EBR's.

3.2 DESIGN STUDIES

3.2.1 Heat Transfer Studies

Effect of Heat Transfer on Configuration

The number of fuel rods needed to deliver a given amount of power depends upon the physical properties of the fuel elements as well as the design characteristics of the reactor. In this study, carbide fuel elements were substituted in several present reactor designs, using the same fuel subassembly external dimensions and the same coolant flow area per subassembly as in the reference reactor. The number of carbide elements required is a function primarily of the maximum allowable carbide temperature. The high melting point (~4500 °F), high permissible operating temperature (~1800 °F min.) and good thermal conductivity of uranium carbide suggest the possibility of using fewer – and larger – rods than in the reference metallic uranium designs.

The results of the heat transfer analysis are summarized in Table 3.1. The number of rods

Table 3.1 — Results of the Heat Transfer Study

	EFFBR					
Fuel	U-10% Mo	UC or PuC-UC				PuO_2-UO_2
Maximum fuel temp, °F	1135	1670	1890	2910	3650	3900
Thermal bond	Metallurgical bond	10 mils NaK	←0.5 mil He→			
Fuel thermal conductivity, Btu/hr-°F-ft*	~16.2	12.1	12.1	12.1	12.1	1.0
Number of fuel rods per subassembly	144	81	81	36	25	225
Fuel rod diameter, in.	0.148	0.172	0.190	0.289	0.348	0.104

	EBR-II					EBR-I	
Fuel	U-Fissium	UC or PuC-UC				U-2% Zr	UC or PuC-UC
Maximum fuel temp, °F	1190	1600	1800	2400	3600	740	1700
Thermal bond	6 mils NaK	10 mils NaK	←0.5 mil He→			Metallurgical bond	1 mil He
Fuel thermal conductivity, Btu/hr-°F-ft*	~17	12.1	12.1	12.1	12.1	~15.5	12.1
Number of fuel rods per subassembly	91	61	61	37	19	36	6
Fuel rod diameter, in.	0.144	0.173	0.191	0.249	0.355	0.364	0.853

*The out-of-pile, UC thermal conductivity at 1400°F was used for the UC and PuC-UC rods. The best estimate for UO_2 thermal conductivity at high temperatures was used for the PuO_2-UO_2 rods.

required per subassembly and the corresponding pin diameter for the EFFBR and EBR-II are plotted as functions of maximum fuel temperature in Figs. 3.1 and 3.2 respectively. An increase in the maximum fuel temperature permits a greater temperature drop across the fuel pin. Because the heat generated per unit length of fuel rod is directly proportional to the temperature drop across the fuel and is independent of the rod diameter, the number of rods required to produce a given power will decrease as the maximum fuel temperature is allowed to increase. The pin diameters given in Table 3.1 and Figs. 3.1 and 3.2 were chosen to yield the same flow area and, therefore, the same coolant temperatures and flow velocity as the reference reactors. Standard heat transfer equations were used in the analysis.

Because of the lack of experience with carbide fuels, the maximum permissible fuel temperature is uncertain. Several maximum fuel temperatures were, therefore, assumed and the corresponding number of fuel rods per subassembly and fuel rod diameter were calculated. The results have been shown in Table 3.1, and cross-sectional views of the fuel subassemblies are presented in Figs. 3.3 through 3.6.

While the present EFFBR subassembly design uses 144 metallic uranium fuel rods, the most conservative carbide design, in which the maximum carbide temperature is under 2000°F (1090°C), requires only 81 rods. A design allowing a 2900°F (1590°C) maximum carbide temperature further reduces the required number of rods to 36. Finally, at a maximum temperature of 3650°F (2010°C), still well below the carbide melting point, only 25 carbide rods are needed. In contrast to the uranium carbide elements, 225 rods per subassembly would be required with PuO_2-UO_2 fuel for a maximum temperature of 3900°F (2150°C). The greatly increased number of rods is due to the lower thermal conductivity of PuO_2-UO_2.

The present EBR-II design uses 91 metallic uranium fuel rods. Carbide designs with maximum temperatures of 1800°F (980°C), 2400°F (1320°C), and 3600°F (1980°C) would require 61, 37, and 19 rods, respectively.

The results of heat transfer calculations for the EBR-I indicate that six uranium carbide fuel rods, with a maximum temperature of 1700°F (930°C), may be substituted for the 36 metallic uranium rods in each fuel subassembly. (See Fig. 3.6.) Since the EBR-I is a relatively low specific power, low temperature reactor, there is less incentive to utilize the high specific power, high temperature potential of carbide fuel in this reactor.

The thermal conductivity of a number of the fuels is unknown. It was necessary to make some assumptions of thermal conductivity values, in order to do the above heat transfer analyses. The thermal conductivity of UC is known only to 1400°F (760°C). Since the variation between room temperature and 1400°F is slight, the same thermal conductivity was assumed up to 3600°F (1980°C). The PuC-UC thermal conductivity is unknown, and it was assumed to be similar to that of UC. The PuO_2-UO_2 thermal conductivity is also unknown, and it was assumed to be similar to that of UO_2. In the event the thermal conductivities are found to be appreciably different from the assumptions, the heat transfer analyses would change accordingly.

Effect of Fuel to Clad Gap

A 0.5 mil radial helium gap between the carbide and inner clad surface was assumed in obtaining the above heat transfer results. A larger gap would result in an excessive temperature drop across the helium, which would reduce the efficient utilization of the high fuel temperature. (See Table 3.2.) A smaller gap is impractical. The temperature drop across the cladding and the coolant film is comparatively small and its influence is therefore subordinated to that of the helium gap.

Several approaches can be taken to design the fuel to clad gap. Initial ceramic fuel element designs, such as PWR UO_2 rods, considered the relative expansion of fuel and cladding. By specifying very close dimensional tolerances on the OD of the fuel (±0.0005 in. for PWR) and ID of the cladding, the fuel and cladding were designed to just touch at operating conditions. The fuel rods designed on this principle performed well, but were expensive to fabricate.

Recent irradiation experience on UO_2 with less stringent dimensional tolerances has served as the basis for a less conservative approach in the design of the fuel to clad gap; Runnalls[1] and Robertson have reported that the surface temperature of UO_2 starting with a 0.017 in. diametral, cold, fuel-clad gap did not rise during irradiation more than 210°F (100°C) over that of UO_2 starting with a 0.005 in. diametral, cold, fuel-clad gap. Tests were with 0.67 in. diameter pellets clad in Zircaloy-2; center temperatures were near the melting point. The explanation proposed was that cracked segments of oxide shift radially outwards and contact the cladding. The fuel-to-clad temperature drop then becomes a function of contact pressure and the surface condition of fuel and cladding. Ability of fuel to relocate itself from an unfavorable heat transfer position to a more favorable one has been noted by Bates and Roake.[2] They irradiated UO_2 powder packed to 4 g/cc in Zircaloy-2, at heat fluxes as high as 700,000 Btu/hr/ft^2 at central melting temperatures. The fuel sintered to at least 9.3 g/cc during irradiation, and the shrinkage was taken axially. The dense UO_2 filled the cladding radially. It is reasonable to assume that UC will behave in the same manner as UO_2. The coefficient of expansion of UO_2 is similar to that of UC, and although the thermal conductivity of UC is considerably better than that of UO_2, UC is still expected to crack at operating temperature gradients (see next section). The decreased allowable tolerances would decrease the fuel cycle costs below the estimates made in Section 3.3.

An additional method of circumventing the problem of strict tolerance is the use of a low melting point metal bond between the fuel and cladding. Sodium or NaK are compatible with fuel and cladding; initial experiments with lead show some promise. The experience with low melting

point metal bonds and ceramic fuels operating above the boiling points of the bonds is very limited. The ceramic fuels will crack, and the bond material could become heated above its boiling point. The behavior of the fuel element under such circumstances is a development problem in itself, and should be separated from carbide fuel development. Designs where the maximum fuel temperature does not appreciably exceed the boiling point of the metal bond, are more reasonable at this date.

Upon substituting a 10 mil NaK bond (radial gap) for the helium in the low temperature UC designs of the EFFBR and EBR-II, the maximum carbide temperature is reduced from 1900°F and 1800°F to 1670°F and 1600°F respectively. The advantages gained did not seem to justify the attendant development problems, and it was decided to design and test helium-filled fuel rods.

Since the less conservative design approach is supported by relatively little experimental data, the more conservative approach was also studied.

The room temperature gap which would yield a one mil diametral clearance at operating temperatures, and the maximum room temperature gap which would produce an interference fit at operating temperatures were calculated on the basis of expansion coefficients for stainless steel, niobium, and Zircaloy-2 clad materials. The results are given in Table 3.3, along with the linear expansion coefficients used in the calculations. The room temperature pellet tolerances required to insure a one mil diametral gap or less at operating temperature are shown in Table 3.4. Case A represents an extreme condition in which no variation is permitted on the clad ID, and no clearance is required for insertion. Under these unrealistic conditions stainless steel cladding would be permissible in conjunction with ground pellets. More realistic assumptions of 1 mil diametral tolerance on the clad ID and 1 mil clearance required for insertion (Case B) would limit the cladding to zirconium or niobium unless a stretch-forming or swaging technique is used subsequent to insertion of pellets, or a 3650°F carbide temperature is permitted. In any case, grinding of the carbide pellets appears necessary in order to achieve the desired tolerances. The design of the initial specimens for irradiation is a compromise between cost of holding close tolerances and performance reliability. It is planned to grind the pellets to tolerances of ±0.001 and obtain tubing with an ID clearance of ±0.0005.

Effect of Thermal Stresses

The high power and large temperature differentials of the fuel will cause large thermal stresses in the fuel. Thermal stresses tend to crack materials with low ductility and high moduli of elasticity. Thermal stress cracking has been observed in all dense UO_2 fuel elements which have operated at useful power levels. An estimate was made to determine if thermal stress cracking should be expected in UC. The results are presented in Fig. 3.7.

UC (and presumably PuC-UC) pellets will almost certainly crack in the EFFBR and EBR-II designs. Thermal stresses above 100,000 psi are expected in the 36-rod EFFBR design; thermal stresses above 60,000 psi are expected in the 81-rod EFFBR design with and without an NaK bond. The tensile strength of UC is not known; however, a review of the tensile strength of other oxides and carbides shows that at 1200°F (650°C) the maximum strengths are not above 40,000 psi. The majority of the ceramics have strength in the 10,000 to 20,000 psi range.

The modulus of elasticity (E) and Poisson's ratio (ν) of UC at elevated temperatures is unknown. A review of the effect of temperature on the E of other oxides and carbides provided the basis for the estimate that E for UC might decrease by 15% at 2000°F (1090°C) and by 40% at 3000°F (1650°C). E for UC has been measured as 31.5×10^6 psi at room temperature. The ν was assumed to be 0.3. As can be seen in Fig. 3.7, the lower E will probably not prevent thermal stress cracking in the EFFBR design.

If cracking of UC is to be avoided, temperature differentials would have to be kept below 200°F (90°C), and probably below 100°F (40°C). An EFFBR UC fuel rod with a ΔT of 200°F, would

Table 3.2 — Temperature Drop Across Fuel and Helium Gap for UC-Fueled EFFBR

Maximum Fuel Temperature, °F	Temperature Drop Across Fuel, °F		Temperature Drop Across He Gap, °F		Number of Rods Required per Subassembly		Diameter of Carbide Pellet, in.	
	0.5-mil radial He Gap	1-mil radial He Gap	0.5-mil radial He Gap	1-mil radial He Gap	0.5-mil radial He Gap	1-mil radial He Gap	0.5-mil radial He Gap	1-mil radial He Gap
2000	615	392	450	740	75	117	0.198	0.154
3000	1316	930	640	1080	35	49	0.299	0.249
4000	2070	1520	785	1360	22	30	0.383	0.324

Table 3.3 — Maximum Permissible Room Temperature Diametral Clearance

Maximum Operating Fuel Temperature, °F	Room Temperature Carbide Pellet Diameter, in.	Room Temperature Diametral Clearance Yielding 1-mil Diametral Clearance at Operating Temperature, mils			Maximum Room Temperature Diametral Clearance Yielding Interference Fit at Operating Temperatures, mils		
		Stainless Steel	Niobium	Zircaloy-2	Stainless Steel	Niobium	Zircaloy-2
1890	0.190	1.4	2.3	2.4	0.4	1.3	1.4
2910	0.289	2.6	4.1	4.2	1.6	3.1	3.2
3650	0.348	3.8	5.6	5.8	2.8	4.6	4.8

Linear Expansion Coefficients, in./in.-°F

UC (arc cast)	6.44×10^{-6}*
Stainless Steel	10.0×10^{-6}
Niobium	4.2×10^{-6}
Zircaloy-2	3.61×10^{-6}

*Recent measurements for sintered UC give a value of 7.88×10^{-6} (Reference 27, Section 4.8), which would decrease required tolerances considerably.

have a fuel diameter of 0.109 in.; 225 rods would be required per subassembly, raising the fabrication cost to prohibitive levels.

3.2.2 Nuclear Studies

Comparison of Carbide with Uranium Alloy and Oxide Designs

The nuclear characteristics of the EFFBR were estimated by one-dimensional, ten-group, diffusion-theory calculations. The purpose of these calculations was to uncover significant differences between metallic, carbide and oxide fuels, rather than to determine accurate absolute values of critical mass and breeding ratio. A one-dimensional, spherical model was used, and suitable correction factors were applied to allow for deviation from the actual EFFBR geometry.

Table 3.4 — Pellet Tolerances Required to Insure One-Mil Diametral Gap at Operating Temperatures

Case A – 1 mil diametral clearance at operating temperatures
±0.000 tolerance on ID of clad
±0.000 clearance on insertion

Maximum Operating Fuel Temperature, °F	Nominal Pellet Diameter, in.	Pellet Tolerances Required, in.		
		Stainless Steel	Niobium	Zircaloy-2
1890	0.190	±0.0007	±0.001	±0.001
2910	0.289	±0.001	±0.002	±0.002
3650	0.348	±0.002	±0.003	±0.003

Case B – 1 mil diametral clearance at operating temperatures
±0.0005 tolerance on ID of clad
0.001 minimum clearance on insertion

Maximum Operating Fuel Temperature, °F	Nominal Pellet Diameter, in.	Pellet Tolerances Required, in.		
		Stainless Steel	Niobium	Zircaloy-2
1890	0.190	–	±0.000	±0.000
2910	0.289	±0.000	±0.001	±0.001
3650	0.348	±0.001	±0.002	±0.002

In this study all reactors were calculated cold, clean, and with control rods withdrawn. The critical mass was adjusted to yield an excess reactivity of approximately one dollar. The important parameters calculated were critical mass, enrichment, and breeding ratio. The significant results of the nuclear analysis are presented in Table 3.5, following a listing of the physical characteristics of the designs in question.

Reactor A represents the present EFFBR design. The core of this reactor is fueled with a U-10% Mo alloy encased in a Zircaloy-2 clad. The calculated critical mass of 433 kg is in fair

Table 3.5 — Reactor Characteristics

Reactor	A Reference EFFBR U-10% Mo Core	B EFFBR UC Core	C EFFBR PuC-UC Core	D EFFBR PuO_2-UO_2 Core
Physical Characteristics				
Core				
Power, MW	265	265	265	265
Volume, ft^3	11.65	11.65	11.65	11.65
Fuel material diam., in.	0.148	0.289	0.289	0.104
Cladding material	Zr	SS	SS	SS
Cladding thickness, in.	0.005	0.013	0.013	0.010
No. of pins per subassembly	144	36	36	225
No. of fuel subassemblies	91	91	91	91
Volume fractions, %				
Fuel material	33.7	33.1	33.1	27.3
Cladding	4.9	5.5	5.5	11.3
Coolant	47.2	47.2	47.2	47.2
Subassembly walls	14.2	14.2	14.2	14.2
Blanket				
Power, MW	35	35	35	35
Volume, ft^3	174	174	174	174
Fuel material	U-2.75% Mo	U-2.75% Mo	U-2.75% Mo	U-2.75% Mo
Fuel material diam., in.	0.415	0.415	0.415	0.415
Cladding material	SS	SS	SS	SS
Cladding thickness, in.	0.010	0.010	0.010	0.010
Nuclear Characteristics				
k_{eff}	1.008	1.008	1.006	1.005
Critical mass, kg U^{235} or Pu^{239}	433	397	279	253
Enrichment, %				
Core	25.0	27.9	19.4	28.1
Blanket	0.35	0.35	0.35	0.35
Breeding ratio				
Core	0.32	0.28	0.48	0.30
Blanket	0.80	0.81	1.09	1.18
Total	1.12	1.09	1.57	1.48
Total, normalized to 1.2 for reactor A	1.20	1.17	1.68	1.59
$\overline{\alpha}$	0.23	0.25	0.22	0.23
$\overline{\eta}$	2.00	1.97	2.37	2.36
ϵ	1.07	1.06	1.07	1.04
$\overline{\eta}\epsilon$	2.13	2.08	2.53	2.45
A_1	0.03	0.02	0.03	0.04
A_2	0.03	0.03	0.04	0.04
L	0.75	0.75	1.00	1.08
Δ^{235}	–	–	0.02	0.01
C	1.06	1.07	1.09	1.09
$\overline{D}_{core}$	1.41	1.42	1.37	1.36
$\overline{\Sigma}_{a_{core}}^{235 \text{ or } 239}$	6.73×10^{-3}	6.76×10^{-3}	4.93×10^{-3}	4.52×10^{-3}
$\frac{L}{\overline{D}_{core}/\overline{\Sigma}_{a_{core}}^{235 \text{ or } 239}}$	3.58×10^{-3}	3.57×10^{-3}	3.59×10^{-3}	3.59×10^{-3}

agreement with 444 kg reported by APDA.[3] A breeding ratio of 1.12* was calculated compared with 1.20 reported by APDA.[3]† The breeding ratio expected in the EFFBR appears to be uncertain, as a value of 1.12 was reported in a publication[4] equally recent to Reference 3. Breeding ratios are given in Table 3.5 as determined from the 10-group calculations, and also normalized to a breeding ratio of 1.20 for the reference EFFBR.

Reactor B represents an EFFBR which contains UC fuel. Because the blanket rods of the reference EFFBR are relatively large and their burnup at discharge is well below the metallurgical limit, carbide blanket elements do not offer any significant advantage. The use of carbide elements in the blanket might result in a decrease of the U^{238} captures because of the lower uranium density. The reference reactor blanket design was, therefore, maintained in all reactors considered.

The important changes caused by the fuel substitution in the core are (1) introduction of carbon in the fuel, (2) removal of molybdenum alloying material, and (3) a necessary increase in enrichment (ratio of U^{235}/U^{238}) resulting from the lower density of the carbide fuel. These changes tend to increase reactivity and thereby reduce the critical mass.

The slowing down characteristics of the carbon result in an increase in reactivity by shifting the neutron energy spectrum to regions of higher importance. The relative importance of core neutrons as a function of energy for the EFFBR is shown in Fig. 3.8.[3] Up to the U^{238} fission threshold (1 Mev) the importance is a decreasing function of energy, because a higher energy results in a higher leakage probability. The effect of carbon in softening the neutron spectrum of UC-fueled reactors may be seen from Figs. 3.9 and 3.10. In these figures the calculated neutron spectrum averaged over the core and blanket, respectively, are shown for the four reactors examined. Molybdenum acts primarily as a neutron absorber and its removal tends to improve neutron economy and increase reactivity. Finally, U^{238} in the core also acts as neutron absorber, capturing more neutrons than it produces by fast fissions. Hence its removal causes an increase in reactivity. Removal of U^{238} also leads to reduced inelastic scattering and, therefore, a slight "hardening" of the neutron spectrum in the region between 1 to 5 Mev, as may be seen from Figs. 3.9 and 3.10.

The net result is that the calculated critical mass in the uranium carbide reactor is 397 kg, or about 8% less than in the reference reactor. Because of the lower uranium content in the carbide reactor, an increase in enrichment from 25.0 to 27.9% is required.

The effect of replacing the fuel of EFFBR with uranium carbide is not beneficial in all respects, as it leads to a somewhat lower breeding ratio. The breeding ratio of reactor B was calculated as 1.09, which is about 3% less than the breeding ratio of the reference design. This decrease is due to a 13% decrease in the core breeding ratio, the blanket breeding ratio remaining essentially unchanged. The decrease in breeding ratio may be understood in the light of the following equations

$$\text{Core breeding ratio} = \overline{\eta}\epsilon - 1 - A_1 - A_2 - L + \Delta^{235} \tag{3.1}$$

$$\text{Blanket breeding ratio} = CL \tag{3.2}$$

$$\text{Total breeding ratio} = \overline{\eta}\epsilon - 1 - A_1 - A_2 - (1-C)L + \Delta^{235} \tag{3.3}$$

---

*Defined as U^{238} captures per U^{235} core absorption.

† The reported APDA critical mass and breeding ratio may be based, at least in part, on past calculations performed by NDA for APDA. However, these NDA calculations were made using a different multigroup code than in the present work.

where $\overline{\eta}$ = average number of neutrons produced per neutron absorbed in fissile material, i.e., U^{235} or Pu^{239}

ϵ = total fission neutrons born – minus neutrons absorbed in U^{238} fissions – per fission neutron from fissile material

L = number of neutrons leaking from the core per neutron absorbed in fissile material

A_1 = number of parasitic absorptions in the core per neutron absorbed in fissile material (not including captures in U^{238} and U^{235})

A_2 = number of excess neutrons available for absorption in control rods per neutron absorbed in fissile material

C = ratio of U^{238} captures in the blanket to all neutrons leaking into the blanket

Δ^{235} = net additional neutrons available from U^{235} fission per neutron absorbed in Pu^{239}.

The quantity C is expected to be essentially constant for the following reasons.

1. The blanket captures practically all neutrons leaking from the core.
2. The blanket is unchanged in composition or thickness.
3. A shift in the energy spectrum of the neutrons leaking from the core does not materially influence the distribution of captures in the blanket.

C is larger than one because of the multiplication resulting from fissions in the blanket (U^{235} and U^{238}).

The total breeding ratio will therefore depend on $\overline{\eta}$, ϵ, A_1 and, to some extent, on L.

The changes caused by the substitution of UC for U-10% Mo result in the following effects on the quantities which determine the breeding ratio.

1. $\overline{\eta}$ is reduced by virtue of the degradation of the core spectrum (see Table 3.5) which increases the capture to fission ratio in U^{235}.
2. ϵ is reduced because of the lower ratio of U^{238} to U^{235}. (An opposite but smaller effect results from the slight hardening of spectrum above the threshold of fission of U^{238}, i.e., 1 Mev.)
3. A_1, which stands for parasitic absorptions, tends to decrease because of removal of molybdenum and to increase because of the spectral shift. The net effect is a decrease in A_1.
4. The leakage per U^{235} absorption, L, is qualitatively proportional to $\overline{D}/\overline{\Sigma}_a^{235}$ where $\overline{D}$ is the average core diffusion coefficient, $(1/3)(\overline{D}/\Sigma_{tp})$, and $\overline{\Sigma}_a^{235}$ is the average U^{235} macroscopic absorption cross section in the core. Both $\overline{D}$ and $\overline{\Sigma}_a$ will depend on core composition and spectrum. A downward spectral shift will tend to increase the microscopic absorption and transport cross sections, thereby decreasing $\overline{D}$, increasing $\overline{\Sigma}_a$, and resulting in a lower leakage. The composition changes from reactor A to B, however, lead to an opposite effect tending to increase L. The two effects appear to cancel each other leading essentially to no change in L.

The net effect of the above is to decrease the breeding ratio.

The next reactor examined is an EFFBR with Pu-UC core (reactor C). The uranium in the core is depleted uranium from diffusion plant tailings containing 0.37% U^{235}. The calculated Pu^{239} critical mass, 279 kg, is 30% smaller than the U^{235} critical mass of reactor B. The reduced critical mass is characteristic of plutonium-fueled reactors, and is caused primarily by the higher value of ν for plutonium.

The effect on breeding ratio of changing from a UC core to a PuC-UC core is as follows.

1. $\overline{\eta}$ is increased because of the use of Pu.
2. ϵ increases slightly because of a higher ratio of U^{238}/Pu^{239}.
3. A_1 is increased because of a somewhat softer neutron spectrum.

L is increased appreciably because of an appreciable decrease in $\overline{\Sigma}_a^{239}$ from the corresponding $\overline{\Sigma}_a^{235}$ for reactor B. This change in L, however, does not influence the breeding ratio appreciably.

The net effect is a breeding ratio of 1.57, approximately 40% greater than the UC and the reference reactors.

The next reactor is an EFFBR fueled with a PuO_2-UO_2 mixture (reactor D). Because of the small rod diameter required, the volume fraction of cladding is a factor of two larger than in reactor C, leaving a smaller volume for the oxide fuel. In addition, the density of U (or Pu) in mixed oxide is about 20% less than the density of U (or Pu) in the combined carbide. Therefore, the total number of heavy atoms (U+Pu) in reactor D is 38% less than in reactor C. This leads to a substantially higher plutonium enrichment for reactor D than in reactor C, i.e., a substantial reduction of the U^{238}/Pu^{239} ratio. This removal of U^{238} from the core tends to increase the reactivity of the core, resulting in a lower critical mass. The critical mass calculated for the PuO_2 reactor is 253 kg of Pu^{239} which is 9% less than the corresponding critical mass for the PuC reactor.

The breeding ratio of reactor D is 1.48 or 6% lower than that for the PuC reactor. This is the result of the following factors.

1. $\overline{\eta}$ is affected only slightly.
2. ϵ is substantially reduced because of a lower U^{238}/Pu^{239} ratio.
3. A_1 is increased because of increased cladding volume.
4. L is increased because of a decrease in $\overline{\Sigma}_a^{239}$, tending to increase the breeding ratio.

The net effect is to decrease the breeding ratio.

Compensation for Reactivity Loss at High Burnup

One of the important advantages of carbide fuels is their high burnup potential. Whereas metallic uranium alloys are presently limited to approximately 1% burnup, it is believed that the burnup limit of carbide might be 3 or 4 times as great.

The length of time that individual fuel subassemblies are allowed to remain in the reactor core is determined by the metallurgical fission damage the fuel elements can withstand. Because of the small excess reactivity available to compensate for fuel element burnup and growth, the time between successive refueling shutdowns is considerably shorter than the allowable fuel residence time, even in the case of U-10% Mo fuel. In order to compensate for reactivity losses, partial reloadings are employed so that individual subassemblies may be irradiated to their maximum metallurgical burnup. In the reference EFFBR partial reloadings are planned at bi-weekly intervals. The number of fuel subassemblies which are withdrawn at each shutdown is 16 out of 91 core subassemblies for 1¼% burnup. As the metallurgical burnup is increased, the number of fuel subassemblies withdrawn may be proportionately decreased.

To compensate for large losses in reactivity resulting from fission product buildup and fuel growth, additional U^{235} or Pu may be added to the core. It was estimated[3] by APDA that an increase in core loading of 1.65% over the clean cold value for each 1¼% burnup would be required for the U-10% Mo-fueled reactor. It should be noted that this increase in core loading cannot be introduced at startup, but must be achieved gradually as the average core burnup increases, by adding additional subassemblies at the edge of the core. A similar increase in the core loading would be required in the carbide-fueled reactors.

Temperature Coefficients of Reactivity

An estimate of the magnitude of the coefficients of reactivity was made for the UC-fueled EFFBR. This estimate was based on extrapolations from values reported for the reference EFFBR. The various effects are discussed below.

1. Axial Fuel Expansion

The effect of axial fuel expansion is to reduce fuel density. This has a negative effect on reactivity. It is partially offset by the increase in the length of the core which would tend to reduce leakage. The net effect is negative for the U-10% Mo and is given[3] as -2.8×10^{-6} $\Delta k/k/°C$. Since the linear expansion coefficient for UC is about 11.6×10^{-6} in./in.-°C compared with 18×10^{-6} in./in.-°C for U-10% Mo fuel, it might be expected that the net effect of axial fuel expansion for the UC carbide designs would be negative but smaller in magnitude than the U-10% Mo figure.

2. Ejection of Coolant by Fuel Radial Expansion

Since the danger coefficient of sodium is positive throughout the core (Fig. 30 of Reference 3), the expulsion of sodium due to radial expansion of fuel should have a negative effect on reactivity. The temperature coefficient of reactivity for this effect is given[3] as -0.5×10^{-6} $\Delta k/k/°C$ for U-10% Mo fuel. Again, because of the smaller linear expansion coefficient of the carbide fuel, it might be expected that this effect for UC would be negative but smaller in magnitude.

3. Reduced Sodium Density

Heating of the sodium results in reduced sodium density and, as in the radial expansion of the fuel, the effect on reactivity is negative. In a UC-fueled EFFBR this effect should also be negative and of about the same order of magnitude as for U-10% Mo fuel which is given[3] as -3.0×10^{-6} $\Delta k/k/°C$.

4. Radial Expansion of the Core

The radial expansion of the core results from the expansion of stainless steel fuel subassembly walls which are made to touch each other by pads provided to prevent bowing of individual subassemblies. The corresponding coefficient of reactivity is expected to be negative and of nearly the same magnitude as the U-10% Mo fuel, which is given[3] as -3.0×10^{-6} in./in.-°C.

5. Doppler Broadening

An increase in core temperature results in broadening of resonances of U^{238} captures (negative effect on reactivity) and U^{235} fissions (positive effect). These effects counterbalance each other at approximately 50% enrichment. For U-10% Mo, the effect is given[3] as -1.6×10^{-6} $\Delta k/k/°C$. Since a somewhat higher enrichment is used with UC fuel, the effect is somewhat smaller in magnitude, but again negative.

The net result of the above considerations is that all temperature coefficients for UC fuel are negative though the overall temperature coefficient of reactivity is smaller in magnitude than for U-10% Mo fuel. Best estimates for UC fuel are given in Table 3.6.

Table 3.6 — Isothermal Core Temperature Coefficients of Reactivity

	$\Delta k/k/°C$	
	U-10% Mo (Reference 3)	UC
Axial Fuel Expansion	-2.8×10^{-6}	$\sim -1.6 \times 10^{-6}$
Ejection of Sodium	-0.5×10^{-6}	$\sim -0.3 \times 10^{-6}$
Reduced Sodium Density	-6.1	$\sim -6 \times 10^{-6}$
Radial Expansion of Core	-3.0	$\sim -3 \times 10^{-6}$
Doppler Effect Total Core	-1.6	$\sim -1.5 \times 10^{-6}$
Total Core	-14.0×10^{-6}	$\sim -12 \times 10^{-6}$

It may be stated that all temperature coefficients for the PuC-fueled reactor are also negative. However, the magnitude of individual coefficients could not be directly estimated from the data on the reference EFFBR.

3.3 COST STUDIES

The results of the heat transfer and nuclear studies were used to estimate and compare fuel cycle costs for the EFFBR fueled with metallic, carbide, and oxide fuels. The physical and nuclear characteristics of the reactors considered in the cost comparison are given in Table 3.5. Breeding ratios normalized to 1.2 for the reference reactor were used in the calculations.

One of the most important factors affecting nuclear fuel costs is the allowable burnup of the fuel material. A 1¼% burnup corresponding to the presently anticipated value for the EFFBR was assumed for the reference reactor.* Although burnup capabilities of uranium carbide are unknown, it is believed that burnups considerably greater than 1¼% can be attained. Therefore several burnups ranging from 1¼% to 5% were considered in the cost estimate of the UC reactor. The cost calculations were patterned after the method outlined by the Edison Electric Institute,[5] and the results of the calculations are given in terms of quantities defined in Reference 5.

Because of the many uncertainties connected with nuclear fuel costs, the reliability of the comparison will depend on the assumptions made. The important fuel cost assumptions used in this study are presented in Table 3.7. Perhaps both the most important and the most uncertain cost is the fuel fabrication cost. The fabrication costs, given in Table 3.7 include the cost of conversion of UF_6 to fuel material, fabrication of fuel material into the finished fuel element and inspection of the final fuel elements. Fabrication costs for the reference U-10% Mo reactor were calculated from data published by APDA in Reference 6. Carbide fabrication costs were obtained partly from The Carborundum Company and partly by extrapolation from data available for UO_2, corrected for the size, number, and enrichment of the fuel rods. The carbide fabrication method assumed was preparation of carbide powder by the oxide-carbon reaction and pressing-sintering the powder into pellets. Allowance was made for higher conversion cost from UF_6 to UC than UF_6 to UO_2. The lower fabrication cost of UC elements compared to the reference is primarily due to the fewer number of fuel rods required.

Because of its high alpha activity and toxicity, handling and fabrication of plutonium is expected to be more expensive than corresponding operations with uranium. Therefore, although the number and size of fuel elements are the same for the UC and PuC-fueled reactors, fabrication costs for PuC will be higher. Because of the relatively large number of rods required, fabrication cost for the PuO_2-fueled reactor is expected to be very high.

The results of the cost studies are presented in Table 3.8. By virtue of a smaller fabrication cost, the UC reactor, even at 1¼% burnup, has a lower fuel cost than the reference reactor. At 2% burnup, which should easily be achieved with carbide fuels, the fuel cycle cost of the uranium carbide-fueled reactor is approximately one-half of the corresponding reference cost, and at 5% burnup the UC cost is less than one-fourth the reference cost.

Although at corresponding burnups a larger net fuel material credit is obtained in the PuC reactor, increased fabrication costs and lease charges cause a slightly higher total fuel cycle cost than that obtained with the corresponding UC reactor. The cost is, however, still considerably less than the reference reactor. The extremely high fabrication costs cause the fuel costs of the PuO_2 design to be more than twice that of the reference.

Fuel cycle costs using $12/g as the value of plutonium are also given in Table 3.8.

---

*Burnup defined as the atom percent of the heavy isotopes (U+Pu) fissioned. In U-10% Mo, 1.26% uranium burnup corresponds to 1% alloy burnup.

Table 3.7 — Fuel Cost Assumptions for EFFBR

	Core A (U-10% Mo)	Core B (UC)	Core C (PuC-UC)	Core D (PuO_2-UO_2)	Blanket
Fuel Fabrication Cost, C_f, $/kg (U+Pu)					
UF_6 to fuel material	145	110	12	5	11
Pu nitrate to fuel material	–	–	145	141	–
Powder to pellets (excluding losses)	–	11	33	38	–
Fabrication (including labor assembly, inspection, cladding material)	304	123	243	1853	51
Losses during fabrication and pelletizing, assumed at 2% (Pu at $30/g)	87	91	118	172	–
Shipping fresh fuel	2	2	2	2	2
Total	538	337	553	2211	64

Fuel Material Losses, %	
Conversion UF_6 to fuel material	1.5
Pelletizing	2.0
Reprocessing	1.5
Plutonium recovery	1.0
Fuel Cycle Working Capital Charges, %/yr*	12
Fuel Material Lease Charge, %/yr	4
Plant Factor, %	80
Plant Efficiency, %	33
Reprocessing Charges, $/day for a 1000 kg U/day capacity plant	15,300

*Applied to fuel fabrication cost of one reactor loading, and value of purchased depleted uranium.

Table 3.8 — Total Fuel Cycle Costs for EFFBR, mills/ekwh*

	Reactor A U-10% Mo 1¼% Burnup	Reactor B-1 UC 1¼% Burnup	Reactor B-2 UC 2% Burnup	Reactor B-3 UC 5% Burnup	Reactor C PuC-UC 2% Burnup	Reactor C PuC-UC 5% Burnup	Reactor D PuO_2-UO_2 2% Burnup
Fissionable Material Destroyed or Lost, M_U†	3.36	3.49	2.99	2.53	4.84	4.32	5.57
Credit for Pu Formed, M_{Pu}	-4.73	-4.57	-4.57	-4.56	-6.55	-6.55	-6.28
Net Fuel Material Cost, M_m	-1.37	-1.08	-1.58	-2.03	-1.71	-2.23	-0.71
Fuel Fabrication Cost, M_f‡	6.19	4.25	3.04	1.82	4.33	2.34	14.26
Spent Fuel Processing Cost, M_p	1.37	1.40	1.16	0.98	1.27	1.08	1.24
Fuel Cycle Working Capital Cost, M_c	0.63	0.55	0.55	0.55	0.61	0.61	0.81
Fuel Material Lease Cost, M_ℓ	2.00	2.15	1.50	0.82	1.90	1.05	2.50
Total Fuel Cost, M_t (Pu at $30/g)	8.82	7.27	4.70	2.14	6.40	2.85	18.10
Total Fuel Cost (Pu at $12/g)	11.66	10.02	7.44	4.88	5.85	3.38	16.41

*Reactors B, C, and D not optimized for respective fuels. For reactor descriptions see Table 3.5.

† Symbols correspond to definitions given by the Edison Institute.[5]

‡ Based on pressing, sintering, and grinding pellets. Relaxation of tolerances to eliminate grinding would reduce costs more on Pu cores than others. See Table 3.7 for additional details.

3.4 REFERENCES FOR SECTION 3

1. O. J. C. Runnalls, UO_2-Fabrication and Properties, Nucleonics, 17(5):110 (May 1959).
2. J. L. Bates and W. E. Roake, Irradiation of Fuel Elements Containing UO_2 Powder, Preprint V-90 of paper presented at the Nuclear Engineering and Science Conference, April, 1959.
3. Enrico Fermi Atomic Power Plant, APDA-124 (Jan. 1959).
4. "Directory of Nuclear Reactors," Vol. I Power Reactor, International Atomic Energy Agency (1959)
5. Survey of Initial Fuel Costs of Large U.S. Nuclear Power Stations, Edison Electric Institute, EEI-59-150 (Dec. 1958).
6. A. Amorosi and J. G. Yevick, "An Appraisal of the Enrico Fermi Reactor," A/Conf. 15/P/2427, Second International Conference on the Peaceful Uses of Atomic Energy (June 1958).

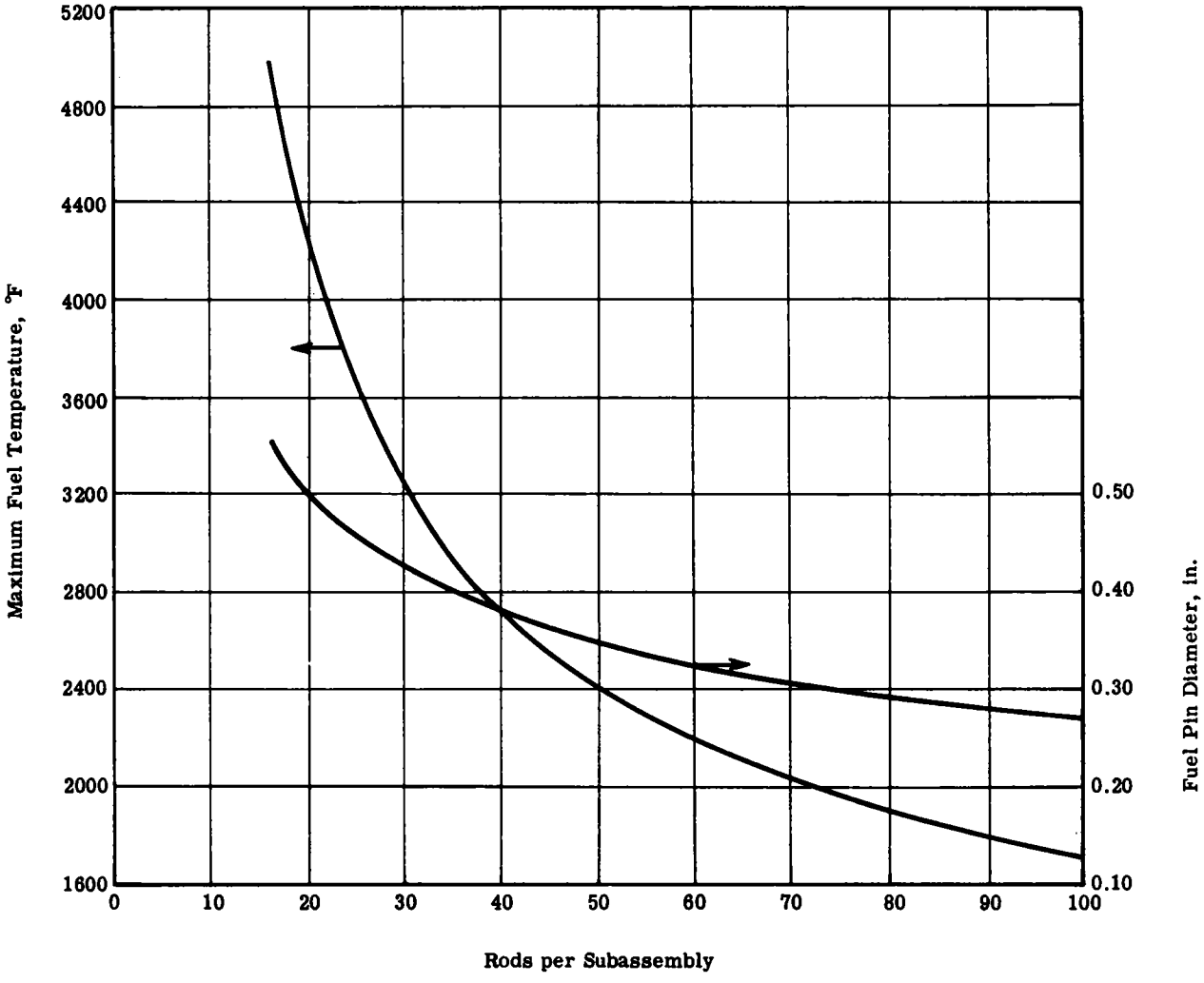

Fig. 3.1 — Maximum fuel temperature and fuel pin diameter vs number of rods per subassembly – EFFBR. Fuel = UC; k = 12.1 Btu/hr-ft-°F; radial gap = 0.5 mil He. Reactor power, coolant temperature, flow rate, and flow area same as present EFFBR design.

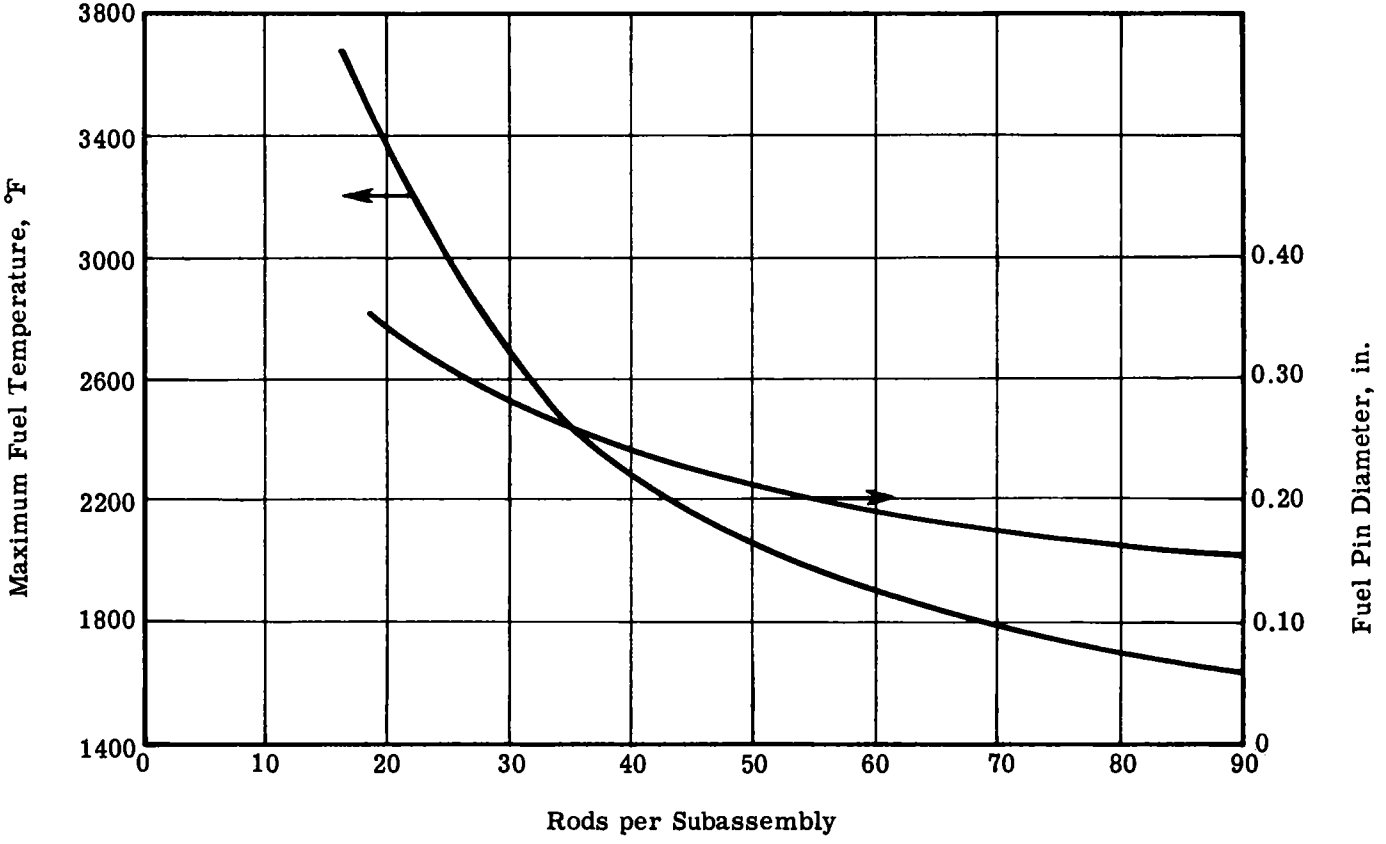

Fig. 3.2 — Maximum fuel temperature and fuel pin diameter vs number of rods per subassembly – EBR-II. Fuel = UC; k = 12.1 Btu/hr-ft-°F; radial gap = 0.5 mil He. Reactor power, coolant temperature, flow rate, and flow area same as present EBR-II design.

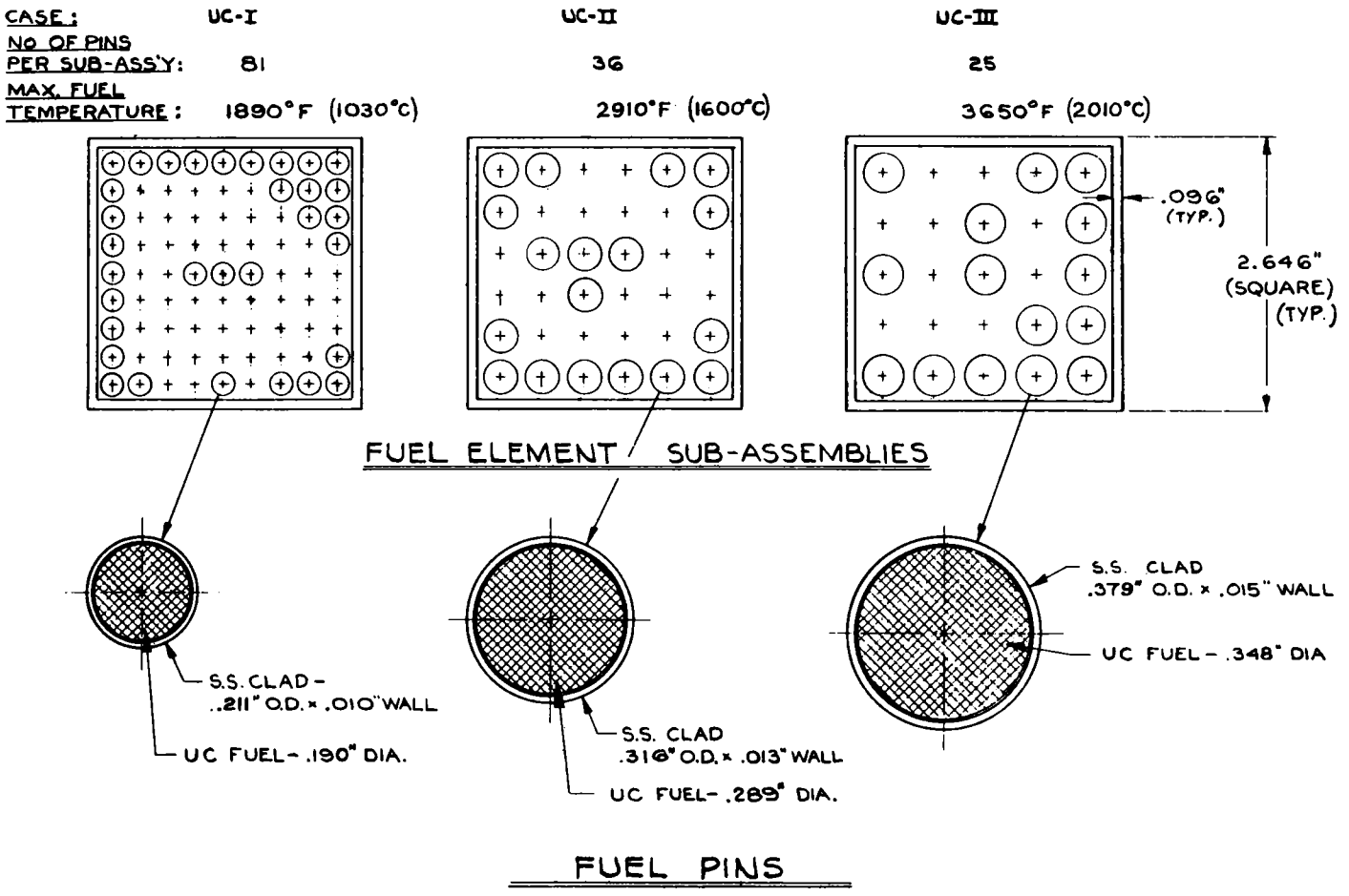

Fig. 3.3 — EFFBR fuel elements – UC-I, UC-II, UC-III. k = 12.1 Btu/hr-ft-°F; radial gap = 0.5 mil He at operating temperature. Reactor power, coolant temperature, flow rate, and flow area same as Reference Design.

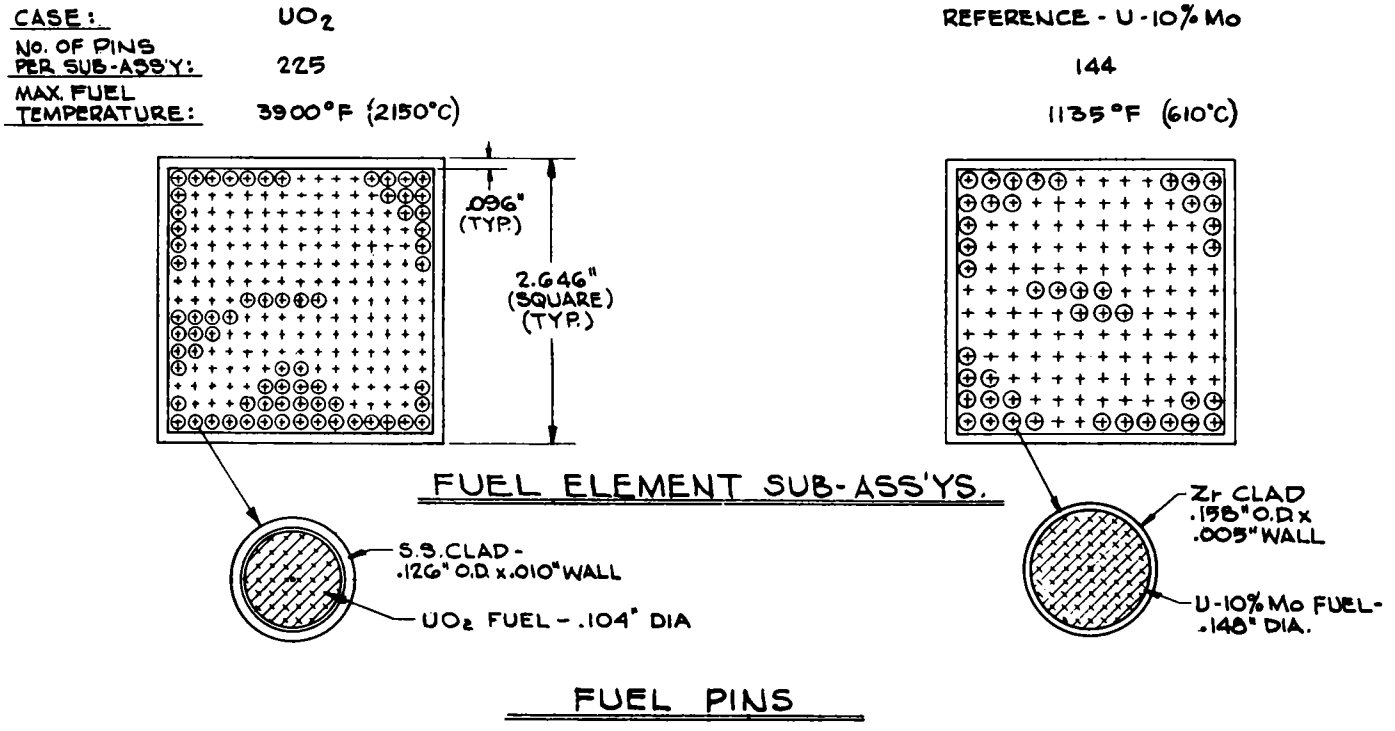

Fig. 3.4 — EFFBR fuel elements – UO_2, Reference: U-10% Mo. k = 1.0 Btu/hr-ft-°F; radial gap = 0.5 mil He at operating temperature. Reactor power, coolant temperature, flow rate, and flow area same as Reference Design.

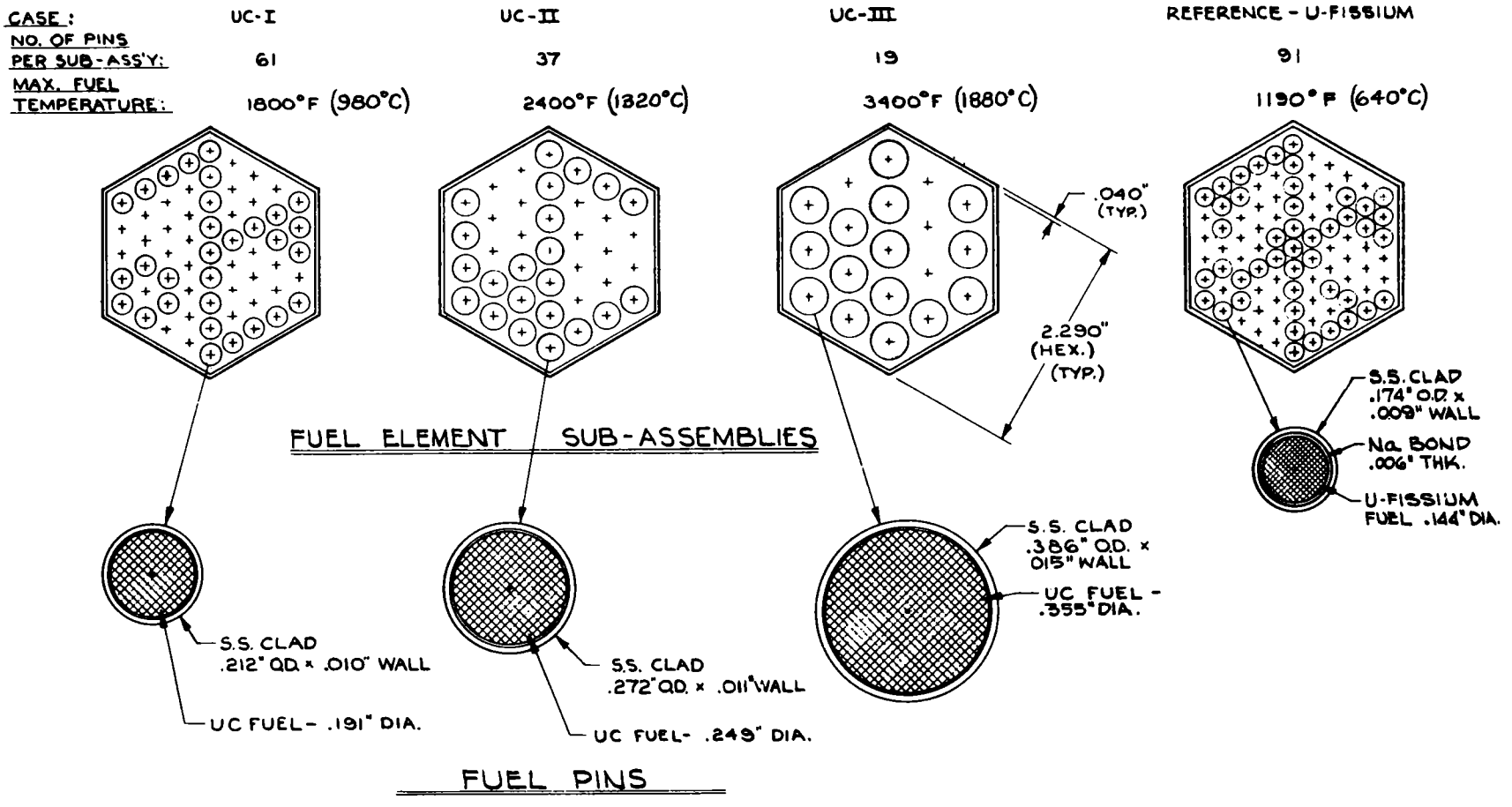

Fig. 3.5 — EBR-II fuel elements – UC-I, UC-II, UC-III, Reference: U-fissium. k = 12.1 Btu/hr-ft-°F; radial gap = 0.5 mil He at operating temperature. Reactor power, coolant temperature, flow rate, and flow area same as Reference Design.

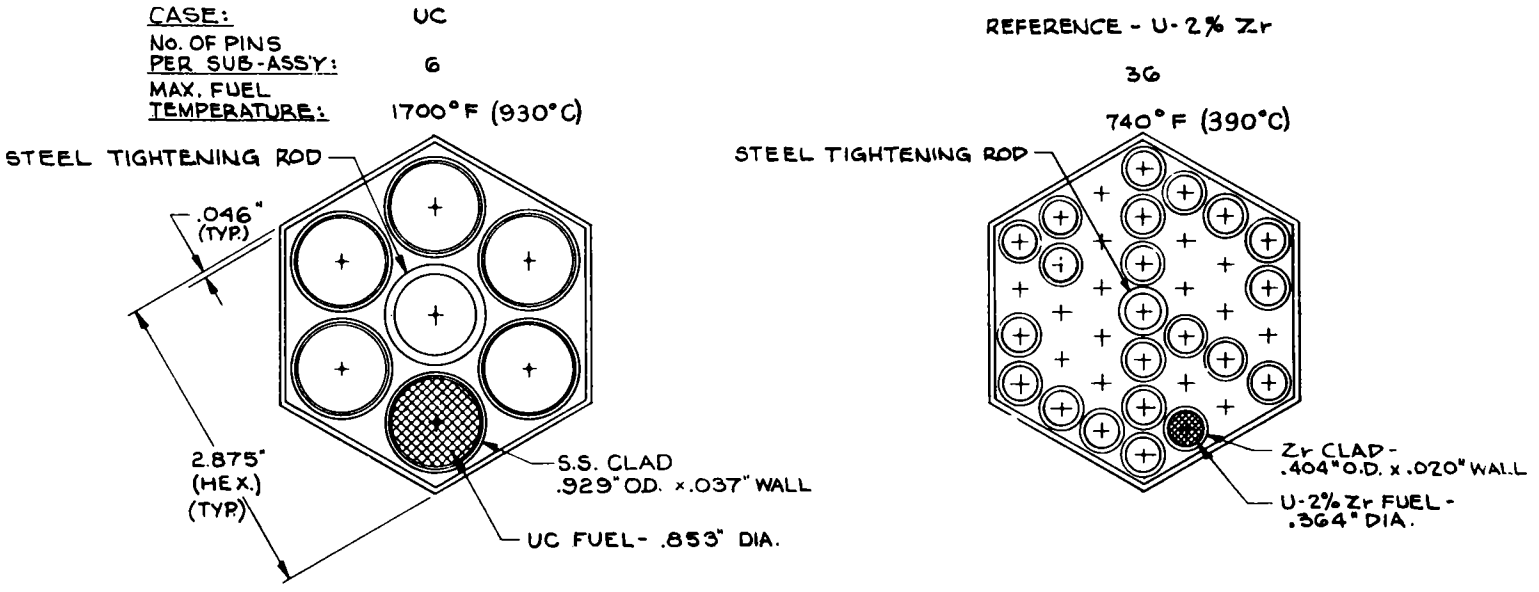

Fig. 3.6 — EBR-I fuel elements – UC, Reference: U-2% Zr. k = 12.1 Btu/hr-ft-°F; radial gap = 1.0 mil He at operating temperature. Reactor power, coolant temperature, flow rate, and flow area same as Reference Design.

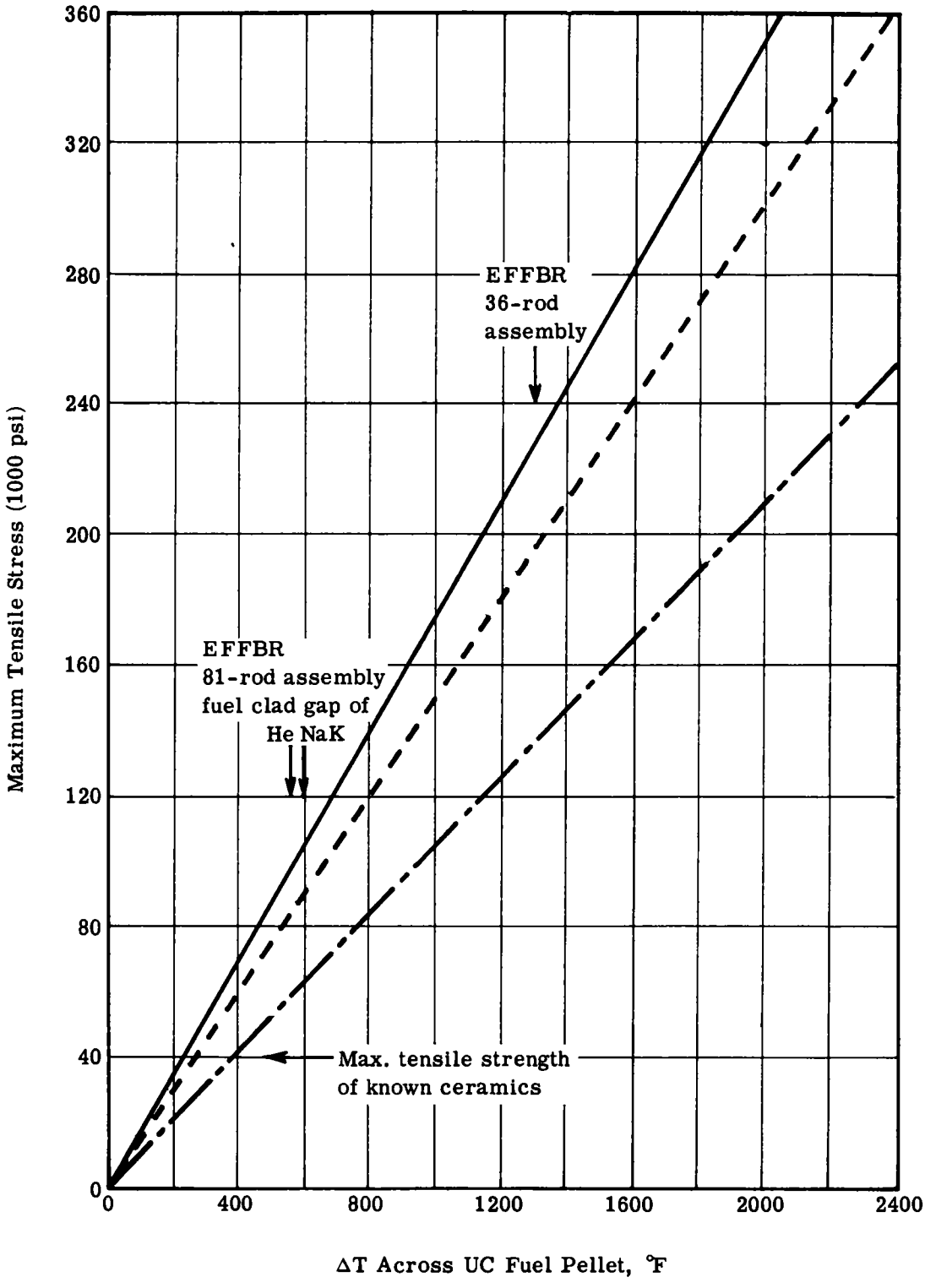

Fig. 3.7 — Thermal stresses in UC. ——— E at 80°F; - - - - E estimated at 2000°F; —— - —— E estimated at 3000°F.

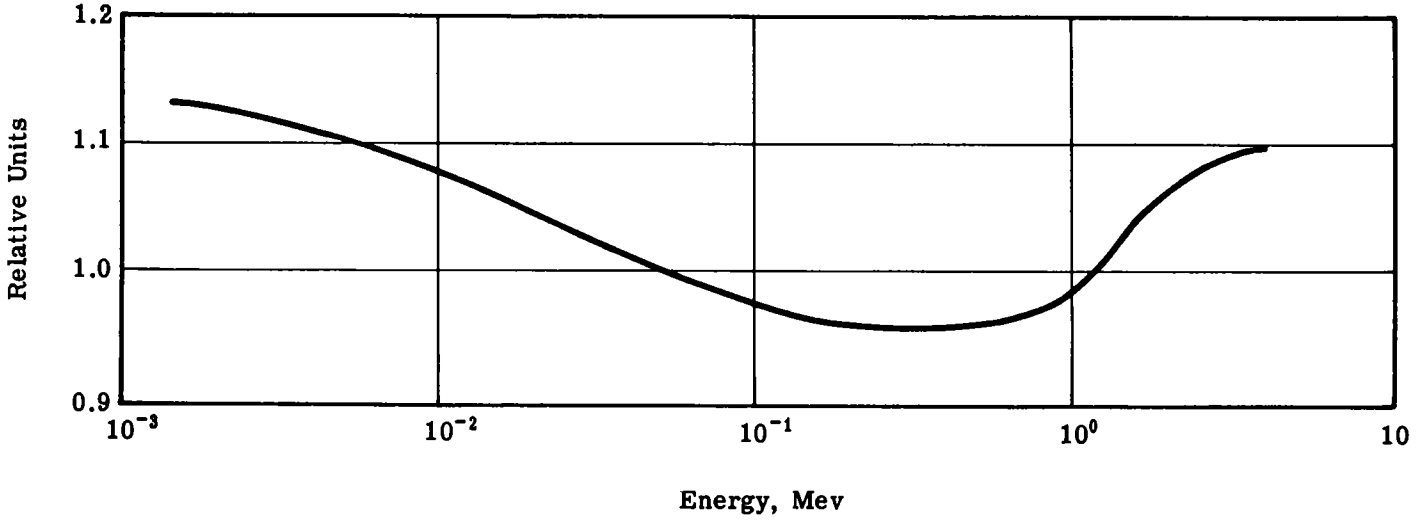

Fig. 3.8 — Relative importance of core neutrons as a function of energy (from APDA-124)

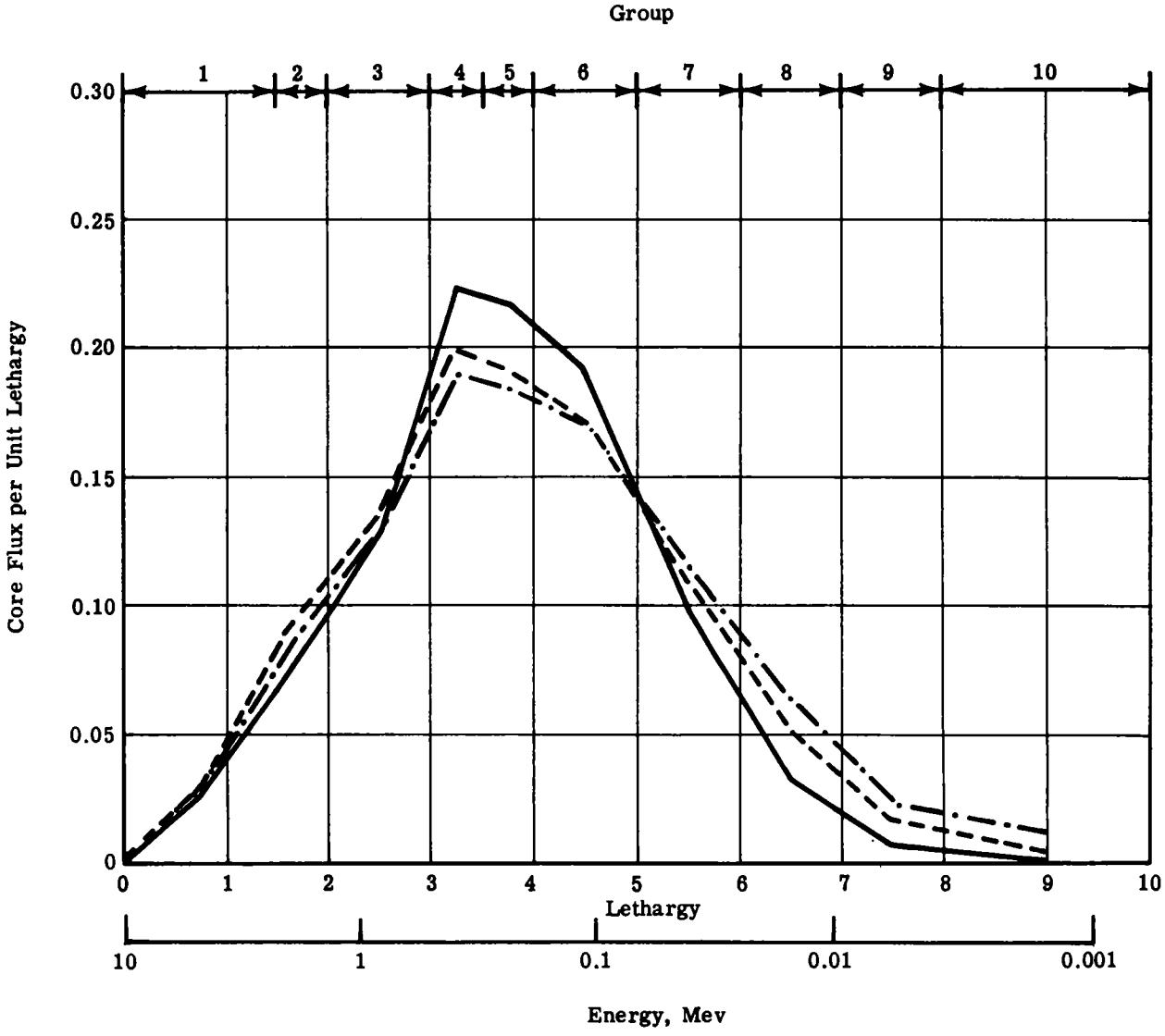

Fig. 3.9 — Average neutron flux spectrum in core – EFFBR.
———U-10% Mo; - - - - -UC; — — —PuC-UC + PuO_2-UO_2.

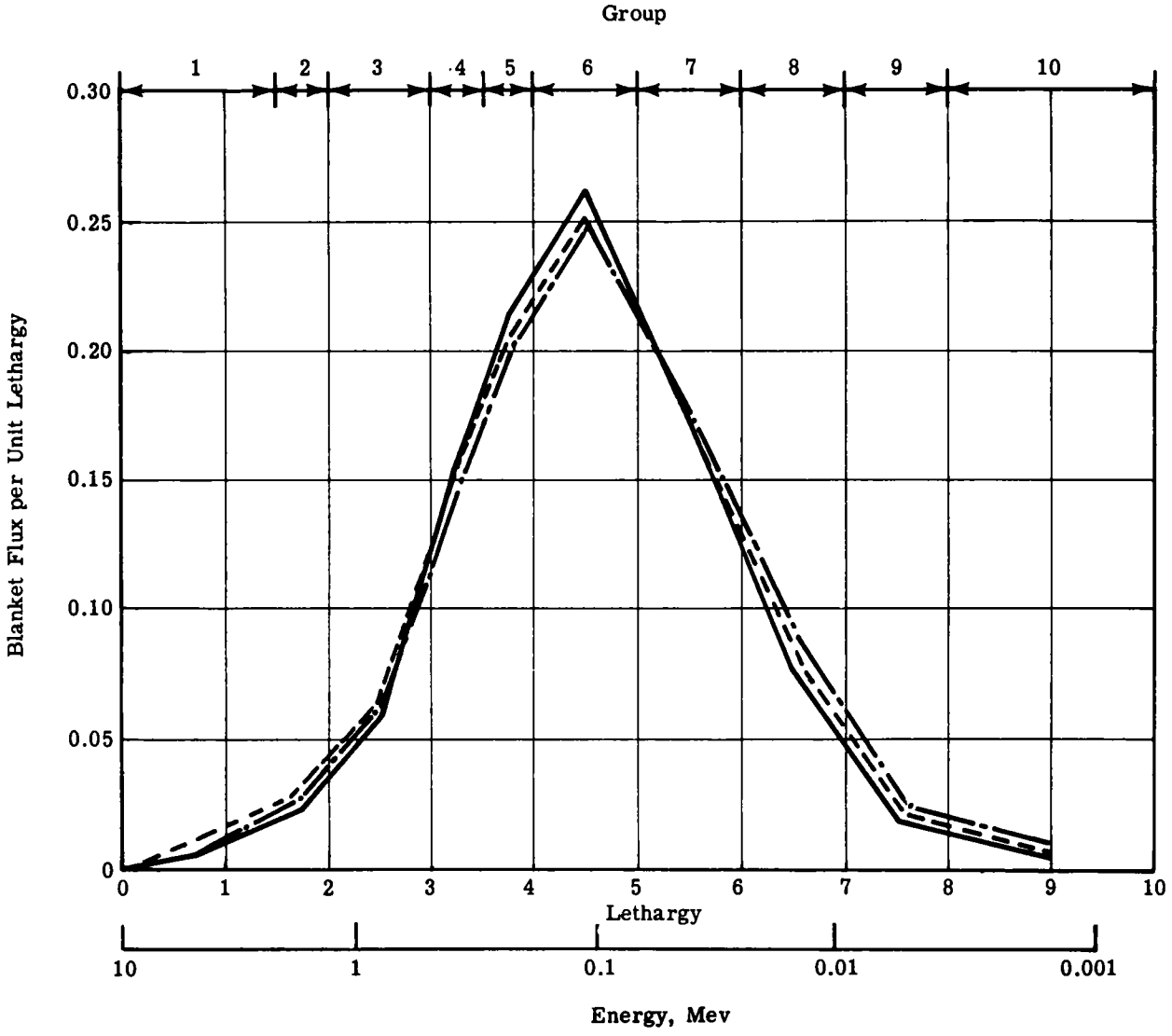

Fig. 3.10 — Average neutron flux spectrum in blanket – EFFBR.
———U-10% Mo; - - - - -UC; — - —PuC-UC + PuO_2-UO_2.

4. FUEL FABRICATION AND EVALUATION

4.1 INTRODUCTION

The goal of the fabrication studies is to produce a high density combination of stoichiometric PuC and UC by powder fabrication techniques. The monocarbides are the most desirable of the fuel carbides, since they have the highest fuel density, and they are the most stable at the proposed operating conditions. A high physical density (about 95% of theoretical) is desired to minimize fission gas release, as well as give a high fuel density. Some fuel is planned to be fabricated with excess uranium metal, to increase sinterability and achievable density, as well as to increase thermal conductivity.

The goal of the evaluation tests is to identify the material as well as possible, by density measurement, chemical analysis, x-ray diffraction, metallography and hardness. Additional out-of-pile tests of fuel-clad compatibility and thermal cycling of fuel containing excess uranium metal will survey some of the properties, knowledge of which is valuable for in-pile tests.

Current studies are limited to UC for lack of plutonium handling facilities. Fabrication and evaluation procedures developed for UC will be tried on PuC-UC as soon as the plutonium handling facilities are completed. The major effort in UC preparation has been on the uranium oxide-carbon reaction. Other preparation methods being studied are the uranium metal-carbon and ammonium diuranate-carbon reactions. The major effort in UC fabrication has been on pressing and sintering UC powder.

4.2 SUMMARY OF FUEL CARBIDE PROPERTIES

A summary was made of fuel carbide properties available in the literature to supply necessary information to the program and point to areas where information is lacking.

The combination of PuC and UC has apparently not been studied to date. The two carbides will probably form solid solutions. The prediction can be made with reasonable assurance, based on the similarity of their crystal structures. The lattice parameter of UC is 4.955 Å while that of PuC is 4.910-4.97 Å; both carbides have a face centered cubic structure of the NaCl type.

4.2.1 Physical and Mechanical Properties

Density (Theoretical at 25°C)

	g/cc	Reference
UC	13.63	1
U_2C_3	12.88	2
UC_2	11.68	3
PuC	13.99 ± 0.05	4
Pu_2C_3	12.70	5
PuC_2		

Melting Point

	°C	Reference
UC	2500 ± 25	6
	(Reported range 2250-2640)	7, 1, 8, 9, 10, 11
U_2C_3	Transforms to UC+UC_2 at 1750-1820	6, 12
UC_2	2445	6
	(Reported range 2350-2475)	7, 9, 13, 14, 10, 15, 11
PuC	1850	16
	Decomposes at >1400°C	17
Pu_2C_3	1900	16
PuC_2		

Boiling Point

	°C	
UC_2	4100-4370 at 760 mm Hg	9, 13, 14

Crystal Structure

	Type	Lattice Parameters (Å at 25°C)	
UC	Face centered cubic, NaCl type	a = 4.955	6
		a = 4.955	18*
		a = 4.951 ± 0.001	19
		a = 4.951 ± 0.004	20
U_2C_3	Body centered cubic	a_0 = 8.088 ± 0.001	2,*21
		carbon-carbon bond distance = 1.35 ± 0.05	21
UC_2	Face centered tetragonal in pairs, CaC_2 type	a = 3.524 c = 5.999	3, 11
		a = 3.54 c = 5.99	18*
		a = 3.517 ± 0.001 c = 5.987 ± 0.001	19, 3
		carbon-carbon bond distance = 1.34 ± 0.02	21
PuC	Face centered cubic, NaCl type	a = 4.910 ± 0.005	22
		a = 4.966 ± 0.004	23
		a = 4.97 ± 0.001	23
Pu_2C_3	Body centered cubic, 8 molecules/unit cell	a = 8.129 ± 0.001	5*

*Spacings and intensities tabulated in reference.

Electrical Properties

Resistivity

	ohm-cm × 10^{-6}	Reference
UC (arc welded)	41 (4.8 w/o C)	24
Other U-C alloys	40 (0.02 w/o C) 46 (2.4 w/o C) 45 (4.5 w/o C) 42-35 (5.0 w/o C) 45 (5.9 w/o C) 51 (6.8 w/o C) 57 (7.3 w/o C) 72 (8 w/o C) 83 (8.8 w/o C) 129 (9.3 w/o C)	24
UC	35-44 depending on impurities of Fe, Si, W, N, O, H_2	25
UC (10.2 g/cc)	10 ± 4 (4.8 w/o C)	20
UC (as sintered)	100 °C 60 500 °C 230-270 (differed for heating and cooling) 700 °C 180	46
(sintered and annealed 7 hr at 1100 °C)	100 °C 25 500 °C 60 850 °C 100	

Electrochemical Potential

	mv	Reference
UC	+320 ± 50	20

Coefficient of Thermal Expansion

	°C	/°C × 10^6		Reference
UC	mean 20-950	11.4		
		Heating	Cooling	
Arc cast UC (5 w/o C)	20-100	9.5	10.3	26
	100-200	10.1	10.6	
	200-300	10.7	11.1	
	300-400	11.1	11.7	
	400-500	11.4	12.2	
	500-600	11.6	12.4	
	600-700	12.1	12.8	
	700-800	12.2	13.1	
	800-900	12.6	13.4	
	900-950	13.0	13.6	

	°C	/°C × 10^6				Reference
	mean 20-980	14.2				
		1st Heating	1st Cooling	2nd Heating	2nd Cooling	
Sintered UC	20-93	12.42	12.06	12.78	12.60	27
	20-205	12.60	12.60	12.78	12.78	
	20-316	12.96	12.96	13.14	12.96	
	20-427	13.14	13.14	13.68	13.50	
	20-538	13.68	13.50	13.87	13.87	
	20-649	13.68	13.68	14.22	14.04	
	20-760	13.68	13.87	14.22	14.22	
	20-871	13.68	14.22	14.4	14.4	
	20-982	13.32	14.58	14.4	14.58	

Thermal Conductivity

	°C	cal/sec-cm-°C	Reference
UC (5.2 w/o C)	100	0.060	26
	150	0.058	
	200	0.056	
	250	0.055	
	300	0.054	
	350	0.053	
	400	0.053	
	450	0.053	
	500	0.054	
	550	0.055	
	600	0.057	
	650	0.058	
	700	0.060	
	735	0.061	
UC (4.8 w/o C, 10.2 g/cc)	60	0.080	20
	115	0.074	
	195	0.061	
	265	0.050	
UC (hot pressed, min. 98% of theoretical density)	119	0.046 ± 0.003	46
	181	0.047 ± 0.003	
	226	0.043 ± 0.003	
	236	0.044 ± 0.003	
UC_2	50	0.082 (density 10 g/cc)	9

Heat Capacity

	cal/gm mole °K	Reference
UC	$C_p = 7.6 + 2.85 \times 10^{-3}$ T(298-2400 °K)	27
UC_2	$C_p = 8.92 + 3.95 \times 10^{-3}$ T(15 cal/g mole at 1940 °K)	20

Modulus of Elasticity

	psi × 10^6	Reference
UC (arc cast)	31.5 (at 25°C)	26

Modulus of Rupture

	°C	tsi	
UC	25	5(12% porosity)	29
	25	20-25 (UC+5/10 w/o U)	
	100	10-15 (UC+5/10 w/o U)	

Hardness

	Method of Fabrication	Hardness	
UC	arc cast, 5.4 w/o C	600 VHN	30
	arc cast, 5.2 w/o C, 1 hr at 1000°C	563 VHN	30
	above plus 1 hr at 1500 °C	763 VHN	30
	above plus 5 min. at 1650 °C	776 VHN	30
	sintered	700 VHN	31
	sintered	750-800 VHN	29
	sintered (10.84 g/cc)	700±150 VHN	20
	sintered (10.2 g/cc)	550±50 VHN	20
UC_2	arc cast	620 Knoop, 100 g load	27
	sintered	500 Knoop	27

Mechanical Strength

UC	Rupture strength of arc cast UC in compression(at 25°C): 54,500 psi with 0.17% total strain		26
	Bend strength (at 25°C): 30-40 kg/mm^2		29
	Crushing strength (at 25°C):		
	parallel to direction of pressing 30 ± 4 kg/mm^2		20
	perpendicular to direction of pressing 13 ± 2 kg/mm^2		20
UC alloys	Creep strength:		
	800 psi at 810°C up to 20 min	0.05% C some improvement over U	32
		0.10% C considerable improvement over U	
		2% C vast improvement, little deformation	
	80 psi at 1070-1100°C up to 60 min	2% C, 3% C little deformation at 1070°C, increasing twofold at 1090°C	
		At 1110°C creep rate is high, with 2% C having distinctly higher rate	

		Reference
UC	Resistance to thermal cycling:	
	4.5 to 5 w/o C arc cast samples were cycled 100 times to 900°and 1100°C (15 min. cycles) with no evidence of fracturing	33,34
	4.8 w/o C, 10.2 g/cc samples were cycled between 100 and 750°C 2000 times without detectable changes. No changes took place on repeated quenching from 1000°C to 25°C in vacuum	20
UC-U	UC-25% U was thermally cycled 1000 times from 200 to 1000°C without appreciable change in external appearance or microstructure	35
	3 w/o C cycled 1000 times between 20 and 520°C was dimensionally stable	31
	Transverse breaking strength (at 25°C) 24,200 psi (4.8 w/o C) 15,300 psi (5.0 w/o C) The effect of Fe, Si, W, N, O, H_2 impurities were studied. Hydrogen and silicon are detrimental.	25

4.2.2 Chemical Reactivity

Thermodynamic Properties of UC

ΔH_{298}	-20 ± 5.0 K cal/mole	27
	-20 ± 1 K cal/mole	6
	-25 K cal/mole	10
ΔH_{298}	-43 K cal	10
ΔS_{298}	-2 cal/deg	10
ΔF_{25}	-41 K cal/g mole	15
ΔF_T	$U(\alpha) + C^* \rightarrow UC(s)(298\text{-}935°K)$ $-19{,}190-0.25T \log T+1.55 \times 10^{-3}T^2+0.70\times10^5 T^{-1} + 0.37 T$	27
	$U(\beta) + C^* \rightarrow UC(s)(935\text{-}1045°K)$ $-17{,}070 + 15.39T \log T - 2.46 \times 10^{-3} T^2 + 0.35 \times 10^5 T^{-1} - 44.68T$	27
	$U(\gamma) + C^* \rightarrow UC(s)(1045\text{-}1405°K)$ $-19{,}240 + 13.13T \log T - 2.46 \times 10^{-3} T^2 + 0.35\times 10^5 T^{-1} - 35.78T$	27
	$U(\ell) + C^* \rightarrow UC(s)(1405\text{–above})$ $-22{,}440 + 13.13T \log T - 2.46 \times 10^{-3} T^2 + 0.35 \times 10^5 T^{-1} - 33.50T$	27

ΔF_f° (cal/mole) for $U(\beta,\gamma,\ell) + C \rightarrow UC(s)$

1000°K	-18,010	27
1100°K	-17,620	
1200°K	-17,170	
1300°K	-16,730	
1400°K	-16,300	
1500°K	-15,610	

*Graphite

Thermodynamic Properties of UC_2

Reference

ΔH_{298} - 36 K cal — 10

ΔS_{298} - 5 cal/deg — 10

ΔF_{25} - 38 K cal/g mole — 15

$\Delta F = -36 - 5T$ can be used to obtain free energy of formation at high temperatures — 10

$\Delta F_f^\circ = A + TB$ — 36

A	B	°K		
-42,200	3.7	298-1400	$UO_2 + 4C \rightarrow UC_2 + 2CO$	37
-27,000	-2.8	298		38

$U + 2C \rightarrow UC_2$

$-\Delta F_0 = 3.925 + 6.3T \log T - 3.48 \times 10^{-3} T^{-2} + 7.545 \times 10^4 T^{-1} + 19.85T$ cal/g atom of U — 3

$-\Delta H_{298} = 3.92$ K cal/g atom U
$-\Delta F_{298} = 9.83$ K cal/g atom U
$\Delta S_{298} = 19.8$ ev

$U(\alpha) + 2C^* \rightarrow UC_2(s)$(935-1045 °K)
$\Delta F_T = -37.540 + 21.79T \log T - 0.96 \times 10^{-3} T^2 - 2.10 \times 10^5 T^{-1} - 66.72\ T$ — 27

$U(\gamma) + 2C^* \rightarrow UC_2(s)$(1045-1405 °K)
$\Delta F_T = -39.710 + 19.53T \log T - 0.96 \times 10^{-3} T^2 - 2.10 \times 10^5 T^{-1} - 66.72T$ — 27

$U(\ell) + 2C^* \rightarrow UC_2(s)$(1405 °K and above) — 27
$\Delta F_T = -42,910 + 19.53T \log T - 0.96 \times 10^{-3} T^2 - 2.10 \times 10^5 T^{-1} - 55.56T$ — 27

$UO_2 + 4C \rightarrow UC_2 + 2CO$

$-\Delta H = -188,540 - 0.8T + 4.05 \times 10^{-3} T^2 + 4.68 \times 10^5 T^{-1}$ cal/g at. of U — 3

$-\Delta F = -188,540 + 1.842T \log T - 4.05 \times 10^{-3} T^2 + 2.34 \times 10^5 T^{-1} + 93.4T$ cal/g at. of U — 3

$\Delta S_{298} = 23.6$ ev

$\Delta F_0 = -202,500 - 16.17T \log T - 2.775 \times 10^{-3} T^2 + 3.475 \times 10^5 T^{-1} + 156.75T$ K cal/g at. of U — 3

$\Delta F_{298} = -166.8$ K cal/g atom U — 3

$\Delta S_{298} = 108$ ev — 3

Thermodynamic Properties of U_2C_3

$\Delta F_{25} = -7.5$ K cal/g mole — 10

$\Delta S_{298} = -8$ cal/deg. — 10

$\Delta H_{298} = -76$ K cal — 10

---

*Graphite

Reactions with Solids

U-C Phase Diagram

The U-C phase diagram has been determined.[7,12] The high uranium section of the phase diagram has been determined in some detail.[39] Three compounds exist: UC, U_2C_3, and UC_2.

U-C-N Phase Diagram

The U-C-N phase diagram has been studied at 1800°C.[40] UC and UN form solid solutions. This has been further confirmed by study of the UC-UN system.[41]

UC-Al

There is no reaction to the melting point of Al.[42]

UC-Be

There is no reaction up to 600°C.[42] There is a reaction after 12 hr, 15 kg/mm^2, at 650°C.[20]

UC-Cr

No mutual solubility was found.[45]

UC-Mo

There is no reaction unless excess carbon is present.[6]

UC-Nb

Probably compatible at 500°C.[44]

UC-Ni

Two distinct diffusion zones form after 10 minutes at 1000°C. One zone was identified as U_6Ni.[20]

UC-Re

A eutectic exists at 1850°C. Re does not form a carbide and should not react with UC.[6]

UC-Si

USi_3 is formed around 1000°C.

UC-Stainless Steel (Type 300)

No reaction was observed during thermal cycling tests up to 1100°C, 13 hours.[43] Stainless steel was embrittled in a UC-NaK-SS compatibility test: at 600°C for 2 weeks; reasons were not established. UC is reported compatible up to 1000°C; at 1100°C there is 0.004 in. penetration.[44] UC appeared to react with stainless steel during the irradiation of UC-stainless steel fuel plates above 540°C but below 1000°C.[24]

UC-Ta

There is no reaction at 1800°C in 2 hours.[25]

UC-Ti

At 1100°C there is 0.005 in. penetration in 6 days; at 1200°C there is marked attack.[44]

UC-Zr

There is a reaction after 12 hr 15 kg/mm^2, at 650°C.[20] There is a reaction at 1000°C.[46]

UC-UC_2-Be_2C

The phase diagram at 1700°C has been studied.[50] Partial solubilities exist between the beryllium and uranium carbides.

UC-CR_3C_2

X-ray studies show partial solubility. Beginning with 20 mole % Cr_3C_2 there is only a single ternary phase.[47]

UC-HfC

X-ray studies indicate a continuous series of solid solutions.[6]

UC-Mo_2C

Mo_2C is slightly soluble in UC; 5 and 10 mole % Mo_2C are heterogeneous.

UC-NbC

X-ray studies indicate a continuous series of solid solutions.[47] The melting point curve and lattice spacing of alloys were determined.[49]

UC-TaC

X-ray studies indicate a continuous series of solid solutions.[47] The melting point curve and lattice spacing of alloys were determined.[49]

UC-ThC

X-ray studies indicate a continuous series of solid solutions.[61] Ternaries with ZrC were studied and found to be solid solutions.[45]

UC-TiC

X-ray studies indicate a solubility of about 10 mole % of TiC. As TiC content is increased, an increasing amount of UC_2 was observed. The solution of TiC in UC is effected with a contraction of the crystalline lattice but the parameters of the mixed phase rich in UC do not decrease as much as the additive law would permit. The observations also indicate that the specimens were not in a state of equilibrium.[47]

UC-VC

Partial solubility exists in the system. The solubility of UC in VC is slight; however, the solubility of VC in UC is significant. X-rays showed a miscibility gap.[47]

UC-WC

Up to 10 mole % WC appears to be soluble in UC.[47]

UC-ZrC

X-ray studies indicate a continuous series of solid solutions.[47,48,45] The melting point curve and lattice spacing of alloys were determined.[49]

Reactions with Liquids

Water

Sintered compacts of UC and UC_2 disintegrated in boiling water (1 atm. pressure) in less than 1 hour.[27] UC_2 decomposes slowly at room temperature and rapidly when heated.[3] In the ab-

sence of air, a green hydroxide is produced. In the presence of air the product is grayish black. The carbon is converted to $\frac{1}{3}$ gaseous and $\frac{2}{3}$ liquid and solid hydrocarbons. The effect of Fe, Si, W, N, O, and H_2 on the corrosion rate of UC in 60°C water was studied. Fe and W appears to have an adverse effect while hydrogen and oxygen appear to have a beneficial effect.[24] The carbide reacted with water vapor at dark red heat with ignition to form a black oxide. UC decomposed completely in moist air within a week.

PuC was not attacked by cold water but it effervesced steadily in hot water and precipitated the hydroxide.[16] The gases produced were methane and hydrogen with smaller quantities of ethane, butanes, acetylene, and ethylene. Pu_2C_3 was less stable to hydrolysis in the atmosphere than PuC, but it was less easily hydrólized by boiling water.

Acids

The reaction of UC, UC_2, PuC and Pu_2C_3 with acids such as HNO_3, HCl, and H_2SO_4 produced hydrogen, acetylene, ethylene, ethane and other hydrocarbons.[6,3] Concentrated acids react only slowly at room temperature, and more rapidly when heated. Dilute acids react more rapidly. Reaction of UC with H_3PO_4 was slow at room temperature but rapid when heated.[3] U_2C_3 reacted slightly with H_2SO_4, HNO_3 up to 170°C, vigorously with HCl at 75°C; it did not react with $HC_2H_3O_2$ up to 170°C.[2] The reaction between PuC and cold HNO_3 was slight; when heated with HNO_3 containing some NaF, there was a steady evolution of gas, and carbon was deposited.

Alkalis

UC_2 decomposed readily in alkalis.[9]

NaK

Compatibility tests of UC with NaK up to 700°C and 8 weeks showed no serious attack; some weight loss was observed.[51,52] At 800°C UC was reported compatible with NaK for one month.[44]

Na

UC has good stability in Na up to about 500°C.[42]

Bi

Uranium carbide did not appear to react with Bi at 600°C in a 3-hour test.

Zn

UC is wetted by molten Zn.[20]

Pb

UC is not wetted by molten Pb.[20]

Sn

UC is not wetted by molten Sn.[20]

Organic Coolants

UC did not appear to be attacked in Santowax R at 400°C for a few days.[53] No corrosion was detected on UC after 5 hours in diphenyl, and terphenyls up to 350°C.[20] A 50 mg/cm^2-hr weight loss occurred on UC in glycerine at 100°C.[20]

Reaction with Gases

Air and Its Components

UC and UC_2 react readily with oxygen and water vapor at room temperature. The carbides are pyrophoric at room temperature if the surface area is sufficiently large; according to one source a particle size of 40 μ or less.[32] Dense UC_2 ignites in air or O_2 at about 400 °C and burns to U_3O_8 and CO_2. After 5½ hours in 600 °C air U_2C_3 was found to have disintegrated into granules still containing material with a metallic appearance. PuC oxidized slowly as it was heated to 300 °C in air.

Reaction of UC_2 with O_2, N_2, and water vapor has been studied.[27] The reactions follow the general equation $W = Kt^n$, where W = weight gain, K = rate constant, t = time, n = 1 for the linear law and 0.5 for the parabolic law. The reactivity of UC_2 with water vapor followed the linear law.

Reactivity of UC_2 with oxygen followed the parabolic rate to 250 °C. At 300 °C oxidation proceeded anisothermally, and the temperature of the specimen rose to 1000 °C in less than one minute. Preliminary results on the reaction of UC with O_2 show that a parabolic rate is followed at somewhat more rapid rate than UC_2. PuC burned brightly in oxygen at 400 °C.

Reactivity of UC_2 with nitrogen followed the parabolic rate to 700 °C. After 12 hours at 1100 °C the carbide was completely converted to nitride.

F_2

No reaction occurred between UC_2 and F_2 at room temperature but slight heating resulted in an explosive reaction.[3]

Cl_2

At 350 °C, UC_2 and Cl_2 reacted to form a volatile chloride. At 600 °C UO_2 + UC_2 reacted with Cl_2 to form UCl_4 leaving a large residue. At 800 and 1000 °C higher uranium chlorides were produced.[3]

Br_2

A reaction occurred between UC_2 and Br_2 above 300 °C. UBr_4 was formed at 900 °C.[3]

I_2

U_2C_3 reacted with I_2 at 600 °C to give UI_4. I_2 vapor at a partial pressure of 100 mm passed over UC_2 at 500 °C forms UI_4.[3]

NH_3

At red heat UC_2 decomposition takes place.[3]

H_2S

UC_2 ignited at 600 °C in H_2S, and formed a sulphide.[3]

CO_2

UC oxidizes rapidly in CO_2 at 500 °C; the rate is invariant to 830 °C.[42] U-UC is analogous to U, but UC appears better than U. A UC specimen oxidized at "a rate of 0.6%" in 6 hr at 500 °C, whereas U metal oxidized at "a rate of 6%."[31]

H_2

UC is compatible with hydrogen to high temperatures if no second phases are present.[44]

4.2.3 Effects of Radiation

Arc cast UC samples irradiated in NaK up to 6400 MW-d/T at maximum temperatures up to 1000°C have been relatively stable.[30,54,56,25] Density decreases of 0.6 to 2.5% have been measured; some of this may have been due to internal cracks. Cracking has been noted but it has not been severe. Changes in diameter have been negligible. Fission gas release was very small and could be accounted for by recoil from the fuel surface. Some surface attack was noted on the UC. This was attributed to NaK of insufficient purity. The data are based on four samples in two capsules.

Post-irradiation heating of a sample of UC irradiated to a low burnup released 0.7% of the Xe^{133} in 67 hours at 927°C.[55]

Estimates of in-pile "effective" thermal conductivity for arc cast UC operating between ~540-820°C are 0.021-0.025 cal/g-sec-°C.[56] The out-of-pile conductivity was measured to be 0.05-0.06 cal/g-sec-°C.

Plates of 24 w/o UC-stainless steel dispersions have been irradiated 2-6 a/o burnup. Slight swelling of the plates was noted; the UC particles had some internal porosity after irradiation. The UC and stainless steel appeared to have reacted chemically. Temperatures were above 540 but below 1000°C.[24]

4.3 CARBIDE POWDER PREPARATION

4.3.1 Uranium Oxide-Carbon Reaction

The first objective of the experimental work was the preparation of high purity uranium monocarbide (stoichiometric composition 95.2% U and 4.8% C) by heating mixtures of uranium oxides (UO_2 and U_3O_8) and carbon according to the reactions:

$$UO_2 + 3C \longrightarrow UC + 2CO$$
$$U_3O_8 + 11C \longrightarrow 3UC + 8CO$$

The UO_2 was Mallinckrodt's minus 200 mesh ceramic grade powder (natural uranium). U_3O_8 was made by heating the MCW UO_2 in air at 800°C to constant weight. The carbon was R. T. Vanderbilt Co's Thermax Thermatomic Carbon, an amorphous carbon made by the thermal decomposition of methane. It had an ash content of 0.05% and an average particle size of 1 to 2 microns.

All of the reaction mixtures were made as follows: stoichiometric amounts of uranium oxide (UO_2 or U_3O_8) and carbon were ball-milled for 2 hr in a rubber-lined mill with stainless steel balls to an average particle size of 5 microns for the uranium oxide. Pellets 0.6-in. in diameter and 0.75-in. long were cold-pressed at 20,000 psi from the mix.

The following reaction procedures were investigated:

1. heating the reaction mix in an induction furnace in an argon atmosphere,
2. heating the reaction mix in a ceramic tube furnace in an argon atmosphere,
3. heating the reaction mix in an induction furnace under vacuum.

Reaction in Induction Furnace in Argon

The pellets of the reaction mixtures were loaded in a graphite crucible in the induction furnace (Fig. 4.1) and heated in an argon atmosphere. The temperature range covered was 1750 to

1950 °C, with holding periods of from 15 min to 4 hr. The atmosphere could not be sufficiently controlled to produce a satisfactory product.

Typical results were as follows:

Chemical Analyses, %*

U	93.35
Combined C	4.84
Uncombined C	0.08
Fe	0.75
N + O, by diff.	0.98
Total	100.00

X-Ray Analyses

Major phase, UC
Weak to moderate pattern, UC_2
Weak pattern, UO_2

The high iron content resulted from crushing the carbide in a cast iron mortar. By crushing in a tool steel mortar it was found possible to reduce the iron contamination to less than 0.1%.

Reactions in the Ceramic Tube Furnace in Argon

According to the results of the x-ray and chemical analyses, a better product was obtained by carrying out the reaction in a ceramic tube furnace (Fig. 4.2) in an argon atmosphere. X-ray analysis of the products obtained in this furnace by heating a stoichiometric mixture of UO_2 and carbon at different temperatures and holding periods are shown in Table 4.1.

Table 4.1 — Reactions of UO_2 + 3C in Muffle Furnace

Experiment No.	Reaction Temp, °C	Reaction Time	X-Ray Analysis of Reaction Products
1	1400	4 hr	Major phase, UO_2 Faint to weak patterns, UC and UC_2
2	1700	20 min	Major Phase, UC Very faint patterns, UO_2 and UC_2
3	1700	90 min	Major phase, UC Very faint pattern, UC_2
4	1750	30 min	Major phase, UC Very faint patterns, UC_2 and UO_2

At 1400 °C the reaction is very slow, and even after 4 hr the major phase is still UO_2. In the temperature range of 1700 to 1750 °C the reaction of the same small amounts of reaction materials (about 30 g) reaches near completion rapidly.

*Chemical analysis techniques are described in Section 7.3

The results of the chemical analysis of the reaction product from experiment 2 were as follows:

	Percent
U	94.44
Combined C	4.86
Uncombined C	–
N	0.21
Fe	0.22
O, by difference	0.27
Total	100.00

A comparison of the results of the x-ray analyses shows a weak to moderate pattern of UC_2 and a weak pattern of UO_2 in the induction furnace and only a very faint pattern of UO_2 and UC_2 in the ceramic tube furnace. The results of the chemical analyses indicate, for about the same amount of combined carbon, higher uranium and lower oxide and nitride contents in the ceramic tube furnace than in the induction furnace.

Reaction in Vacuum Induction Furnace

A sketch and photograph of the vacuum induction furnace are shown in Figs. 4.3 and 4.4. The vacuum pump was a four-stage mechanical booster pump, model KMB-30, purchased from Kinney Manufacturing Company and had a capacity of 30 cfm. At room temperature, a pressure of about 10 microns was obtained in the whole system. The pressure increased to about 100 microns at an operating temperature of 1900°C, due to release of CO and the degassing of components.

The pellets, pressed from the reaction mixtures (UO_2+3C) and (U_3O_8+11C), were loaded in the induction furnace in a graphite crucible. The vacuum furnace was pumped down to a pressure of about 10 microns. The temperature was then raised to the desired operating temperature and held for the desired period of time. The furnace was allowed to cool off overnight under continuous pumping. Table 4.2 summarizes the results obtained of the reaction experiments in the vacuum induction furnace.

The best results were obtained with the (UO_2+3C) mixture in the temperature range 1750 to 1800°C. With U_3O_8, there is a tendency to form more UC_2. The results obtained with the 550 g mixture, experiment 12, at 1800°C for 4 hr, are quite encouraging. The oxygen and nitrogen values on this material were determined by National Research Corporation by the vacuum fusion method.

In all the synthesis experiments, the uranium monocarbide obtained by the different methods was oxidized very rapidly when exposed to the air and was also pyrophoric in fine powder form. Special precautions had to be taken during unloading the furnace and transportation to the glove-box. All subsequent operations (crushing, preparing samples for x-ray and chemical analysis, loading mills, etc.) were done in the glove-box in an argon atmosphere. In many cases it was observed that the quality of the atmosphere in the glove-box was not satisfactory, and attempts are being made to improve the atmosphere.

4.4 CARBIDE PELLET FABRICATION

4.4.1 Pressing and Sintering

The following procedure was usually used for forming the green pellets: the uranium carbide was crushed and dry-milled for 4 hr with stainless steel balls in a rubber-lined ball mill to an average particle size of about 5 microns. The powder was then mixed with 7 weight % alcohol and 0.5 weight % Carbowax 6000. After evaporating the alcohol, 0.5 in. × 0.5 in. pellets were pressed at 40,000 psi.

Table 4.2 — Reactions in Vacuum Induction Furnace

Experiment No.	Reaction Mixture	Reaction Temp, °C	Reaction Time, hr	Results of X-Ray Analysis	Results of Chemical Analysis, %	
5	UO_2 + 3C (32 g)	1650	2	Major phase, UC Faint patterns, UO_2 and UC_2	U Combined C Uncombined C	93.69 4.55 0.07
6	U_3O_8 + 11C (32 g)	1650	2	Major phase, UC Strong pattern, UC_2 Faint pattern, UO_2	U Combined C Uncombined C	92.74 6.63 0.07
7	UO_2 + 3C (32 g)	1750	1	Major phase, UC Faint patterns, UO_2 and UC_2	U Combined C Uncombined C N Fe	94.61 4.75 0.07 < 0.10 < 0.01
8	U_3O_8 + 11C (32 g)	1750	1	Major phase, UC Faint to weak pattern, UO_2 Faint pattern, UC_2	U Combined C Uncombined C N Fe	94.57 4.52 0.15 < 0.10 < 0.01
9	UO_2 + 3C (100 g)	1750	1	Major phase, UC Faint pattern, graphite Very faint patterns, UC_2 and UO_2	U Combined C Uncombined C N Fe	94.98 4.65 trace < 0.10 < 0.01
10	UO_2 + 3C (32 g)	1850	1	Major phase, UC Weak pattern, UC_2 Faint pattern, UO_2	U Combined C Uncombined C	94.51 4.36 0.06
11	U_3O_8 + 11C (32 g)	1850	1	Major phase, UC Strong pattern, UC_2 Weak pattern, UO_2	U Combined C Uncombined C	92.81 6.21 0.04
12	UO_2 + 3C (550 g)	1800	4	Major phase, UC Faint pattern, UO_2 and UC_2 solid solution	U Combined C Uncombined C Fe *N *O	94.89 4.80 0.08 < 0.01 0.003 0.24

*Values determined by National Research Corporation by vacuum fusion method.

Table 4.3 summarizes the results of the sintering experiments obtained in:

1. the induction furnace in an argon atmosphere,
2. the ceramic tube furnace in an argon atmosphere,
3. the vacuum induction furnace.

The results of the sintering experiments in the induction furnace (Fig. 4.1) in argon were very inconsistent probably due to a contaminated atmosphere. In experiment 1 the pellets were partially oxidized; in experiment 2, the pellets were fractured; in experiment 3, however, the pellets had a clean metallic appearance. The high density obtained in experiment 2 is probably due to pick-up of nitrogen in the induction furnace. This presumption is supported by the fact that in experiment 4, in the ceramic tube furnace, the tube was broken and high density was obtained. A sample of this pellet was sent to National Research Corporation for nitrogen and oxygen determination. The nitrogen content was 1.82% and the oxygen content 0.09%. The sintered pellets with lower density have a much lower nitrogen content. A photomicrograph of a similar pellet is shown in Fig. 4.5. A two-phase structure is present consisting of UC_2 and U(C,N) solid solution.

There is also an indication that sintering in the ceramic tube furnace in argon improves the quality of the material. This is illustrated by the following chemical analyses before and after sintering of the product in experiment 6.

Chemical Analysis before Sintering, %		Chemical Analysis after Sintering, %	
U	94.22	U	95.21
Total C	4.87	Total C	4.80
Fe	0.24	Fe	0.16
N*	0.04	N*	0.02
O*	0.63	O*	0.04

After sintering, the oxygen was decreased considerably and the uranium content increased. These results, together with the synthesis experiments, indicate that it would be possible to make good quality uranium monocarbide in the ceramic tube furnace in an argon atmosphere.

Except for the experiments in which nitrogen contamination was evident, densities higher than about 10 g/cc have not yet been obtained in the sintering experiments.

Several UC pellets having bulk densities of between 9 and 10 g/cc are planned for use in preliminary studies of UC cladding compatibility. These had the following chemical analysis:

Pellet	%
U	94.79
Total C	4.83
Free C	0.05
Fe	0.24
N	< 0.10

A photomicrograph of a pellet is shown in Fig. 4.6. An essentially single phase structure of UC is present. The small dark areas are voids.

*Values obtained by National Research Corporation by vacuum fusion.

Table 4.3 — Sintering Experiments with Uranium Monocarbide

Experiment No.	Furnace and Atmosphere	Sintering Temp, °C	Sintering Time	Sintered Density, g/cc (Theor.13.63)	X-Ray Analysis of Sintered Pellet	Chemical Analysis of Sintered Pellet,%	
1	Induction, argon	1800	1 hr	9.15			
2	Induction, argon	1850	1 hr	13.1			
3	Induction, argon	1950	1 hr	10.55			
4	Ceramic tube, argon	1800	30 min	13.05	Major, UC Weak patterns, UO_2 and UC_2	U Total C Fe *N *O	94.14 3.96 0.15 1.82 0.09
5	Ceramic tube, argon	1800	30 min	8.57	Major, UC Very faint pattern, UC_2 and UO_2 solid solution	U Total C Fe N	94.88 4.72 0.06 < 0.10
6	Ceramic tube, argon	1800	1 hr	10.01	Major UC Faint pattern, UC_2 Indication of UO_2	U Total C Fe *N *O	95.21 4.80 0.16 0.02 0.04
7	Induction, vacuum	1750	30 min	8.84	Major, UC Weak pattern, UC_2 Faint pattern, UO_2	U Total C	94.34 5.35
8	Induction, vacuum	1800	30 min	9.40	Major, UC Faint patterns, UC_2 and UO_2 Very faint pattern, UO_2 solid solution	U Total C Fe *N *O	94.22 4.87 0.24 0.04 0.63
9	Induction, vacuum	1900	1 hr	10.03	Major, UC Weak to faint pattern, UO_2 and UC_2	U Total C Fe N	94.70 4.75 < 0.01 < 0.10

*Values of N and O determined by National Research Corporation by vacuum fusion.

4.4.2 Hot Pressing

One hot pressing was made in a graphite mold at 1800°C, resulting in a pellet with a bulk density of 12.6 g/cc. X-ray analysis indicated that the UC_2 content had increased moderately due to intimate contact with the graphite mold. An aluminum nitride mold has been made for further hot pressing experiments.

4.5 METALLOGRAPHY

Carbide pellets were sectioned by a diamond wheel, with the sample and wheel submerged in cutting oil. Oxidation of the sample during the cutting operation was prevented this way, and the pyrophoricity hazard was reduced. Specimens were mounted by casting and setting a polyester resin around them. The procedure was used because it is simple, and does not require an elevated temperature.

Specimens were polished with 600 grit SiC paper, diamond paste Grades 15, 6, and 1, and finally a grade containing diamond particles 1 μ or smaller. Cutting oil was used as a lubricant in all cases, and the specimens were kept out of contact with air and moisture as much of the time as possible. Eventually, the PuC-UC specimens will be polished in a helium atmosphere. Photomicrographs of stoichiometric UC and UC containing nitrogen are shown in Figs. 4.5 and 4.6.

4.6 COMPATIBILITY

In order to study possible fuel-cladding interactions under conditions similar to those which would prevail in an actual fuel element, a series of diffusion capsule tests will be made. In these capsules the carbide fuel material will be held in contact with various cladding materials at 650 to 800°C for periods up to several months. Following this, the capsules will be sectioned and the carbide-cladding interface examined by metallography, x-ray diffraction, and autoradiography. The interaction of uranium carbide with type 304 stainless steel, 2¼% Cr-1% Mo steel, Inconel-X, niobium, Zircaloy-2, Hastelloy-B, and beryllium will be studied initially.

The diffusion capsule design is shown in Fig. 4.7. The carbide and cladding materials are held in contact by means of the stainless steel insert. Continued contact at elevated temperatures is assured since the stainless steel has an appreciably higher coefficient of thermal expansion than the Inconel container. The diffusion capsules are ready for assembly.

4.7 THERMAL CYCLING TESTS

The effect of thermal cycling on fuel carbides containing excess amounts of uranium metal will be studied, to see whether or not the uranium metal additions have any deleterious effects on the dimensional stability of the material. The pellets will be sealed under vacuum in small Inconel capsules and then cycled between 540 and 1100°C. The specimens will be wrapped with tantalum foil to prevent interaction between the carbide and capsule.

In order to achieve more rapid cycling than possible by simply allowing the specimens to heat and cool with the furnace, the furnace is kept at a constant temperature and the capsules moved in and out of the hot zone. This is accomplished automatically by means of an Inconel carriage attached to a solenoid-actuated air cylinder. The solenoid responds to the signals of a Wheelco temperature controller which in turn responds to the signals of a control thermocouple located in a well of the capsule being cycled. The equipment has been constructed and set up.

4.8 REFERENCES FOR SECTION 4

1. R. Keiffer et al., The Preparation of Uranium Monocarbide and Its Behaviour Compared with Other High Melting Carbides, IGRL-T/C-52 (Nov. 1957).
2. M. W. Mallet, A. F. Gerds, and D. A. Vaughan, Uranium Sesquicarbide, AECD-3060 (Jan. 31, 1950).
3. Report on the Carbides of Uranium: UC, UC_2, and U_2C_3, NEPA-273 (Sep. 15, 1947).
4. G. T. Seaborg, "The Transuranium Elements," McGraw-Hill Book Company, Inc., New York (1949).
5. W. H. Zachariasen, The Crystal Structure of Plutonium Sesquicarbide, Acta Cryst., 5:17(1952).
6. M. Bowman, Los Alamos Scientific Laboratory, Personal Communication, (August 1959).
7. M. W. Mallet, A. F. Gerds et al., J. Electrochem. Soc., 99:197 (1952).
8. K. Whitehead, L. D. Brownlee and R. Raine, Metropolitan-Vickers, Res. Reports C-864, C-892, C-893.
9. J. Baker, Uranium Carbide, NEPA-138 (Dec. 31, 1946).
10. Leo Brewer, LeRoy A. Bromley, Paul W. Gilles, and Norman L. Lofgren, The Thermodynamic Properties and Equilibria at High Temperatures of Uranium Halides, Oxides, Nitrides and Carbides, BC-82 (Sep. 20, 1945).
11. E. Epremian, Uranium Compounds for New High Temperature Fuels, TID-7546, Book 2 (Mar. 1958).
12. F. A. Rough and A. A. Bauer, Constitution of Uranium and Thorium Alloys, BMI-1300 (June 2, 1958).
13. M. P. Ames Laboratory Reports CT-686 (May 22, 1943); CN-1495 (Mar. 10, 1944) and CC-1514 (Mar. 1944).
14. T. A. Butler, R. Fischer and A. S. Newton, M. P. Ames Laboratory CC-164 (May 14, 1943).
15. W. R. Martini, A. Compilation of the Vapor Pressure Data for the Elements from Br to U and their Oxides and Carbides, NAA-SR-215 (Mar. 20, 1953).
16. J. L. Drummond, B. J. McDonald, Heather M. Ockenden, and G. A. Welch, The Preparation and Properties of Some Plutonium Compounds, Part VII Plutonium Carbides, J. Chem. Soc. p. 4785 (Dec. 1957).
17. J. Lemons, Los Alamos Scientific Laboratory, Personal Communication (Aug. 1958).
18. L. M. Litz, A. B. Garrett, and Frank C. Croxton, Preparation and Structure of Carbides of Uranium, J. Am. Chem. Soc., 70:1718 (May 1948).
19. R. E. Rundle, N. C. Baenziger, A. S. Wilson, and R. A. McDonald, Structure of Carbides, Nitrides and Oxides of Uranium, J. Am. Chem. Soc., 70:99 (1948).
20. A. Boettcher and G. Schneider, "Some Properties of Uranium Monocarbide,"Second United Nations International Conference on the Peaceful Uses of Atomic Energy, A/Conf. 15/P/964.
21. A. E. Austin and C. M. Schwartz, Structure of UC_2, Progress Relating to Civilian Applications During June 1958, p. 40, BMI-1273 (July 1, 1958).
22. W. H. Zachariasen, The Crystal Structure of PuN and PuC, Acta Cryst. 2:388 (1949). (Also ANL-4070, Oct. 14, 1947)
23. A. A. Bochvar et al., "Interaction Between Plutonium and Other Metals In Connection with Their Arrangement in Mendeleev's Periodic Table," Second United Nations International Conference on the Peaceful Uses of Atomic Energy, A/Conf. 15/P/2197 (July 1958).
24. Progress Relating to Civilian Applications During June 1959, BMI-1357.
25. Progress Relating to Civilian Applications During May, 1959, p. 51, BMI-1346,(June 1, 1959).
26. A. C. Secrest Jr., et al., Preparation and Properties of Uranium Monocarbide Castings, BMI-1309 (Jan. 2, 1959).
27. A. B. Tripler, Jr., et al., Further Studies of Sintered Refractory Uranium Compounds, BMI-1313 (Jan. 27, 1959).
28. L. Brewer, M. P. Berkeley CC-672 (May 15, 1943).

29. E. Barnes et al., "The Preparation, Fabrication and Properties of Uranium Carbide and Uranium-Uranium Carbide Cermets," Metallurgy and Fuels, Vol. V, Progress in Nuclear Energy, McGraw-Hill Book Co., Inc. (1956).
30. C. A. Smith and F. Rough, Properties of Uranium Monocarbide, NAA-SR-3625 (June 1, 1959).
31. J. Dubuisson et al., "The Preparation of U-UC Cermets and Stoichiometric Monocarbide by Sintering Under Stress," Second United Nations International Conference on the Peaceful Uses of Atomic Energy, A/Conf. 15/P/1162.
32. E. Barnes et al., The Preparation, Fabrication and Properties of UC and U-UC Cermets, AERE-M/R-1958.
33. A. Secrest et al., Casting Techniques for the Preparation of Uranium Monocarbide, Progress Relating to Civilian Applications During March 1958, p. 69, BMI-1259 (Apr. 1, 1958).
34. A. C. Secrest et al., Casting Techniques for the Preparation of Uranium Monocarbide, Progress Relating to Civilian Applications During June 1958, p. 45, BMI-1273 (July 1, 1958).
35. G. A. Meyerson, "Proceedings of the Second United Nations International Conference on the Peaceful Uses of Atomic Energy," Vol. 6, p. 564 (Sep. 10, 1958).
36. R. J. Ackermann and R. J. Thorn, "High Temperature Thermodynamic Properties of Reactor Materials," Second United Nations International Conference on the Peaceful Uses of Atomic Energy, A/Conf. 15/P/715 (June 1958).
37. O. Kubachewski, and E. L. Evans, "Metallurgical Thermochemistry," John Wiley and Sons, Inc., New York (1958).
38. O. H. Krikorian, High Temperature Studies, UCRL-2888 (1955).
39. B. Blumenthal, Constitution of Low Carbon U-C Alloys, ANL-5958 (Feb. 2, 1959).
40. A. Austin and G. Gerds, The Uranium-Nitrogen-Carbon System, BMI-1272 (June 23, 1958).
41. R. A. J. Sambell and J. Williams, The Uranium Monocarbide/Uranium Mononitride System, AERE-M/R-2654 (Sep. 1958).
42. P. Murray and J. Williams, "Ceramic and Cermet Fuels," Second United Nations International Conference on the Peaceful Uses of Atomic Energy, A/Conf. 15/P/318 (July 1958).
43. A. C. Secrest, E. L. Foster, and R. F. Dickerson, Casting Techniques for the Preparation of Uranium Monocarbide, Progress Relating to Civilian Applications During July, 1958, p. 43, BMI-1280 (Aug. 1, 1958).
44. R. W. Nichols, Ceramic Fuels – Properties and Technology, Nucl. Eng., (Aug. 1958).
45. O. S. Ivanov, and T. A. Badajeva, "Phase Diagrams of Certain Ternary Systems of Uranium and Thorium," Second United Nations International Conference on the Peaceful Uses of Atomic Energy, A/Conf. 15/P/2043 (July 1958).
46. A. Accary, R. Caillat, Development of Ceramic Fuel Elements in France, from the book by H. Hausner and J. Schumar, "Nuclear Fuel Elements," Rheinhold Publishing Corp., New York, (1959).
47. H. Nowotny et al., The Preparation of UC and its Reactions with Carbides of the Refractory Transition Metals, R. de Metallurgie 55:453 (1958), AEC-TR-3415 (May 1958).
48. W. Witteman, J. Leitnaker and M. Bowman, The Solid Solubility of Uranium Monocarbide and Zirconium Carbide, LA-2159 (Apr. 1958).
49. L. D. Brownlee, The Pseudo-Binary Systems of UC with ZrC, TaC, and NbC, J. of the Inst. of Metals, 87:58 (Oct. 1958).
50. M. Burdick et al., An X-Ray Study of the System UC-UC_2-Be_2C, J. of Res. of the NBS, 54:4 (Apr. 1955).
51. R. B. Price et al., Irradiation-Capsule Design for Uranium Monocarbide, Progress Relating to Civilian Applications During March 1958, p. 70, BMI-1259 (Apr. 1, 1958).
52. R. B. Price and W. H. Goldthwaite, Irradiation of Uranium Monocarbide, Progress Relating to Civilian Applications During November, 1958, p. 45, BMI-1304 (Dec. 1, 1958).
53. H. Pearlman, A. I., Personal Communication (Aug. 1959).
54. S. Alfant, G. Lamale, A. W. Hare, and F. A. Rough, Postirradiation Examination of Uranium Monocarbide, Progress Relating to Civilian Applications During November, 1958, p. 46, BMI-1304 (Dec. 1, 1958).

55. R. Lieberman et al., Fission-Product Release from Irradiated Uranium Monocarbide, Progress Report Relating to Civilian Applications During August, 1958, p. 38, BMI-1286 (Sep. 1, 1958).
56. Progress Relating to Civilian Applications During March 1959, p. 73, BMI-1330.
57. F. A. Rough, Evaluation of Uranium Monocarbide as a Reactor Fuel, Progress Relating to Civilian Applications During May 1958, p. 63, BMI-1267 (June 1, 1958).
58. A. B. Tripler, Jr., M. J. Snyder, and W. H. Duckworth, Preparation, Fabrication and Physical Properties of Uranium Compounds, Progress Report Relating to Civilian Applications During September, 1957, p. 43, BMI-1226 (Oct. 1, 1958).
59. J. B. Melehan et al., Literature Survey for the Appraisal of UC as a Possible Nuclear Fuel Progress Report Relating to Civilian Applications During August, 1958, p. 14, BMI-1286 (Sep. 1, 1958).
60. F. Rough, Private Communication (Aug. 1959).
61. H. Nowotny et al., Zur Kenntnis des Teilsystems UC-ThC, Planseeberichte fuer Pulvermetallurgie, 5:102 (1957).

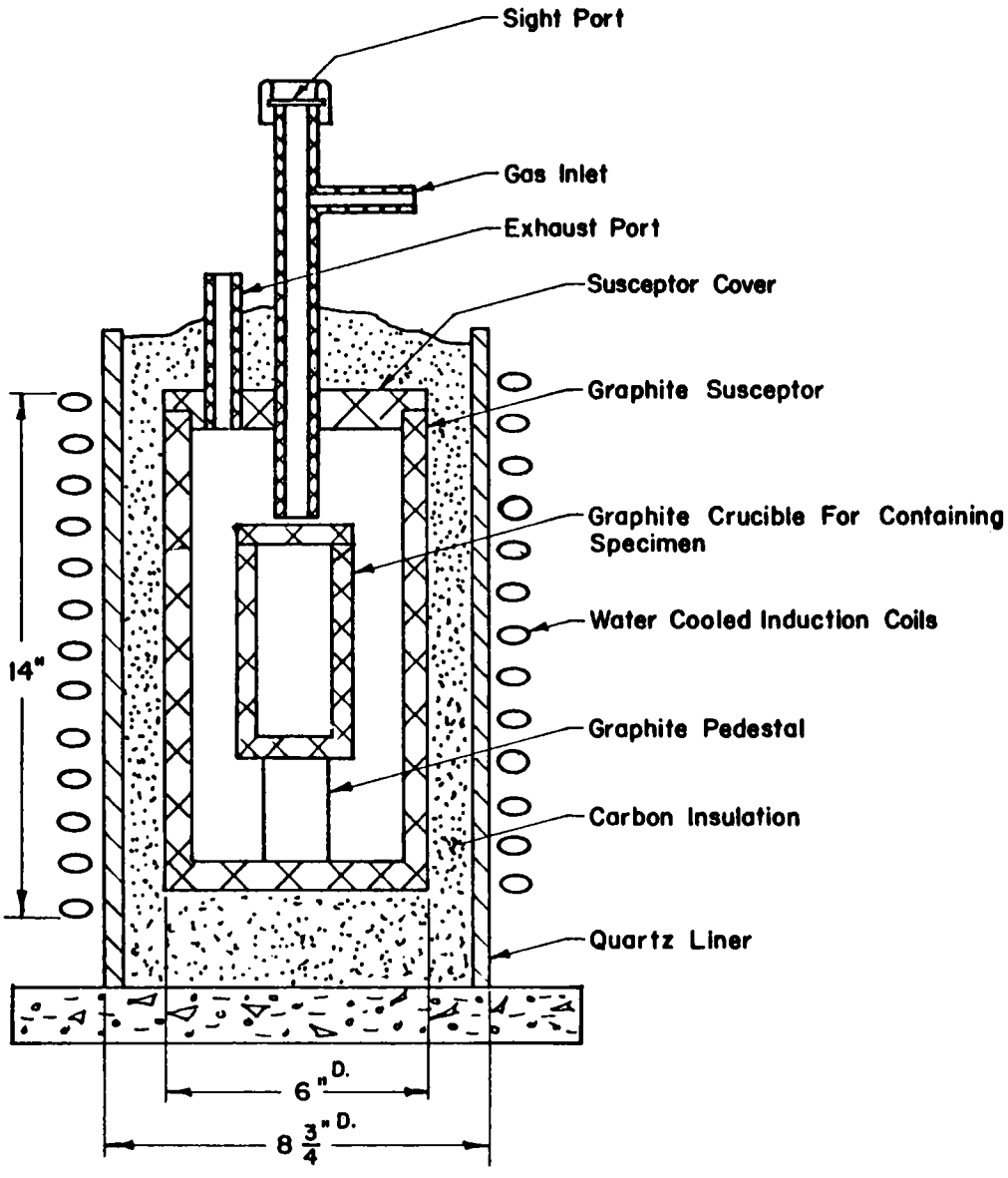

Fig. 4.1 — Sketch of atmosphere induction furnace

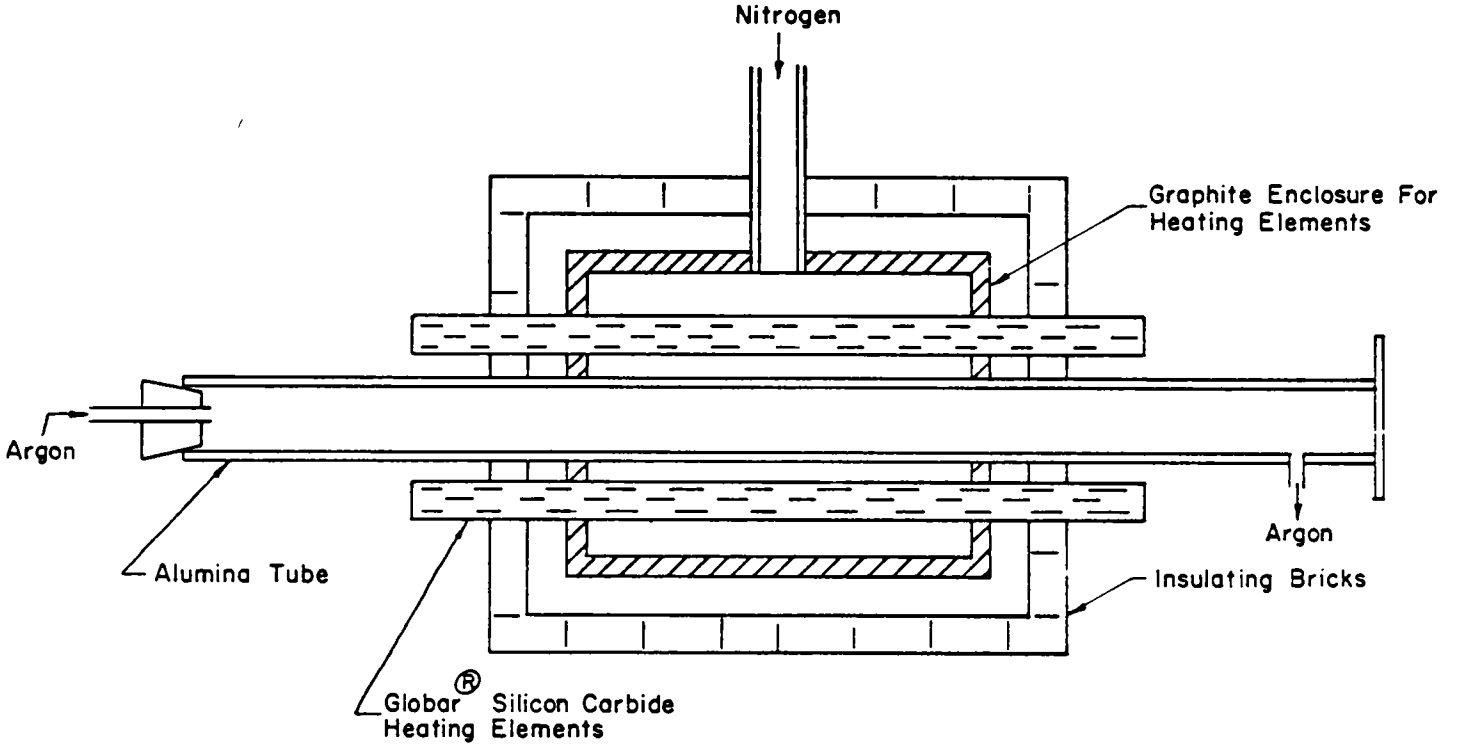

Fig. 4.2 — Horizontal tube furnace for temperatures up to 1800 °C

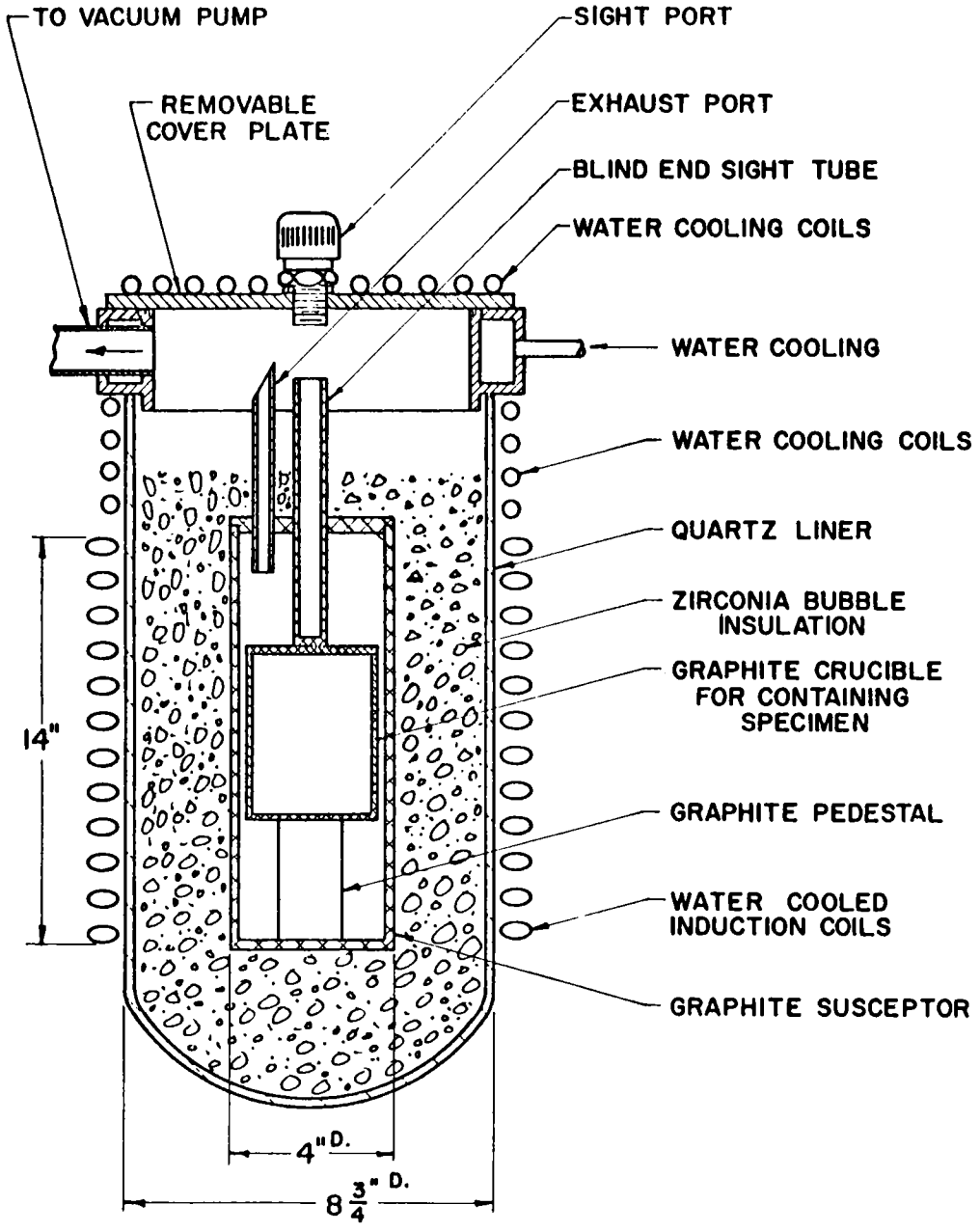

Fig. 4.3 — Sketch of vacuum induction furnace

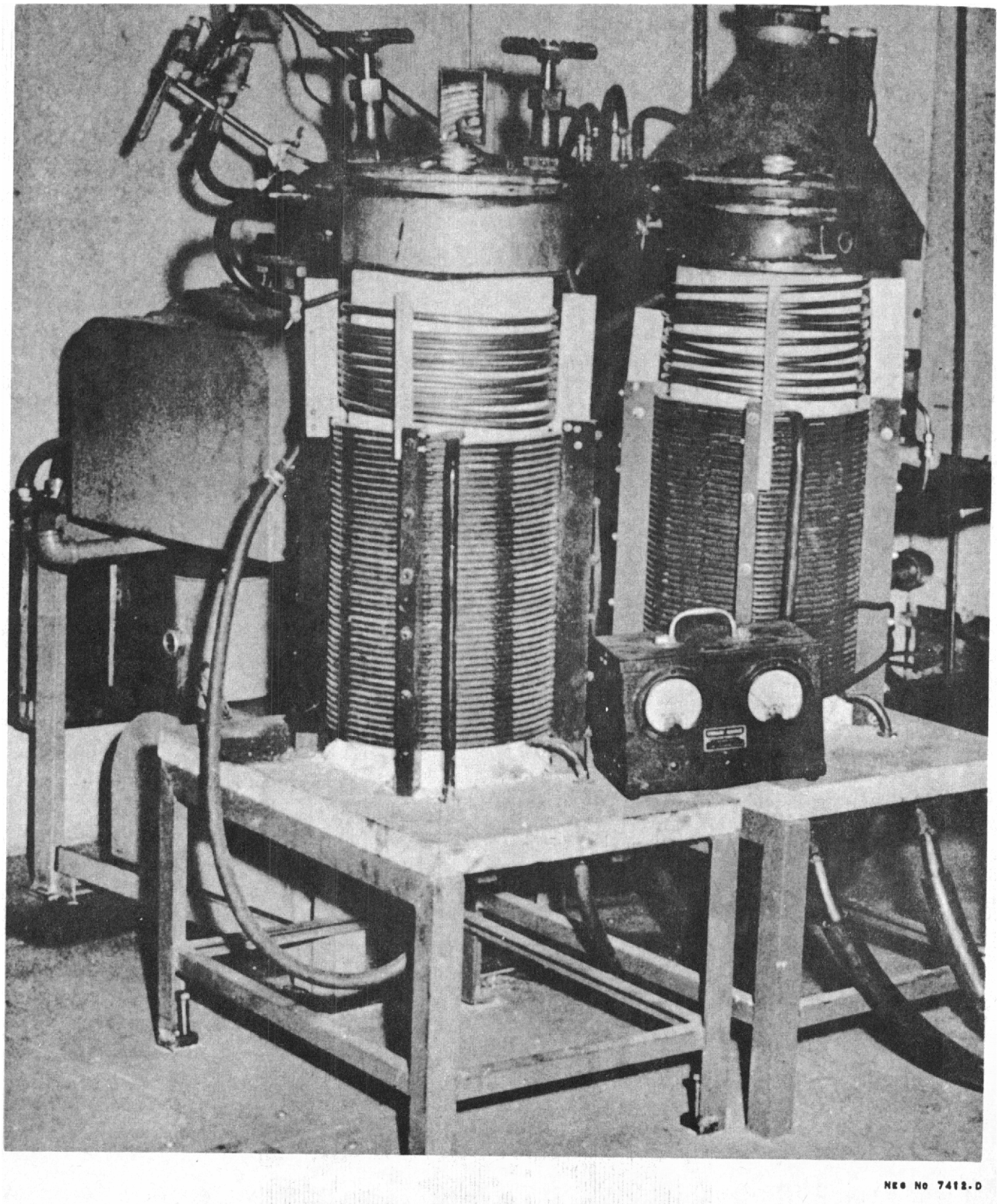

Fig. 4.4 — Vacuum induction furnace

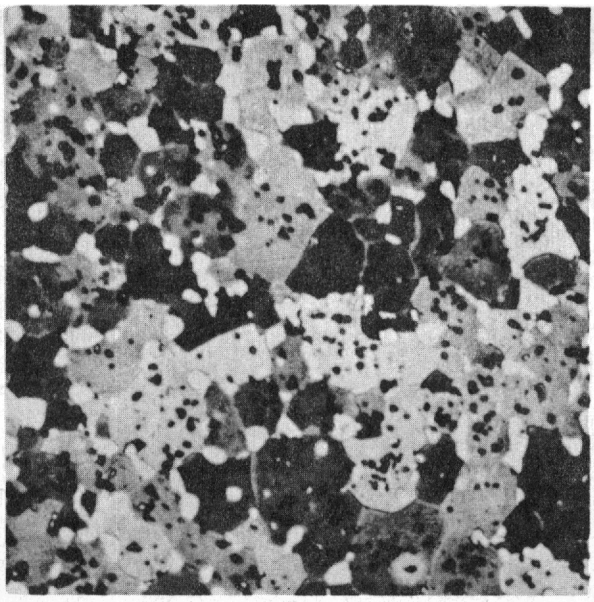

Fig. 4.5 — Sintered UC with nitrogen impurity – 500× – nitric acid-acetic acid-water etch – (Experiment 4, Table 4.3). The matrix phase is U(C,N) solid solution. The light phase is UC_2. The dark spots are voids.

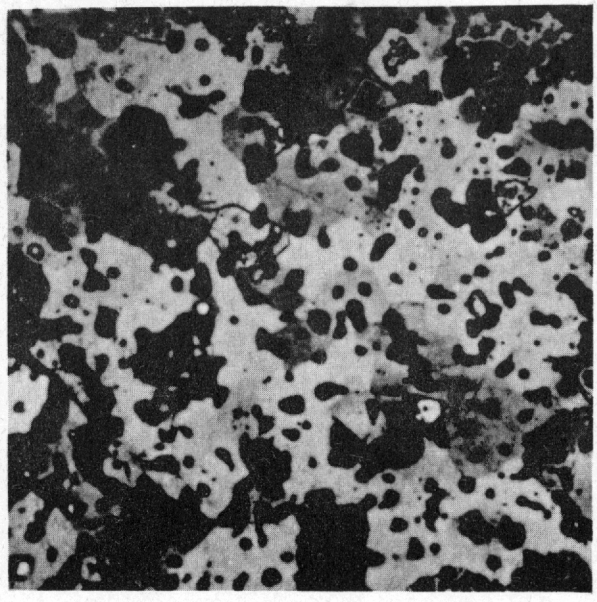

Fig. 4.6 — Sintered UC – 500× – nitric acid-acetic acid-water etch – (Experiment 6, Table 4.3). The major phase is UC. The dark spots are voids.

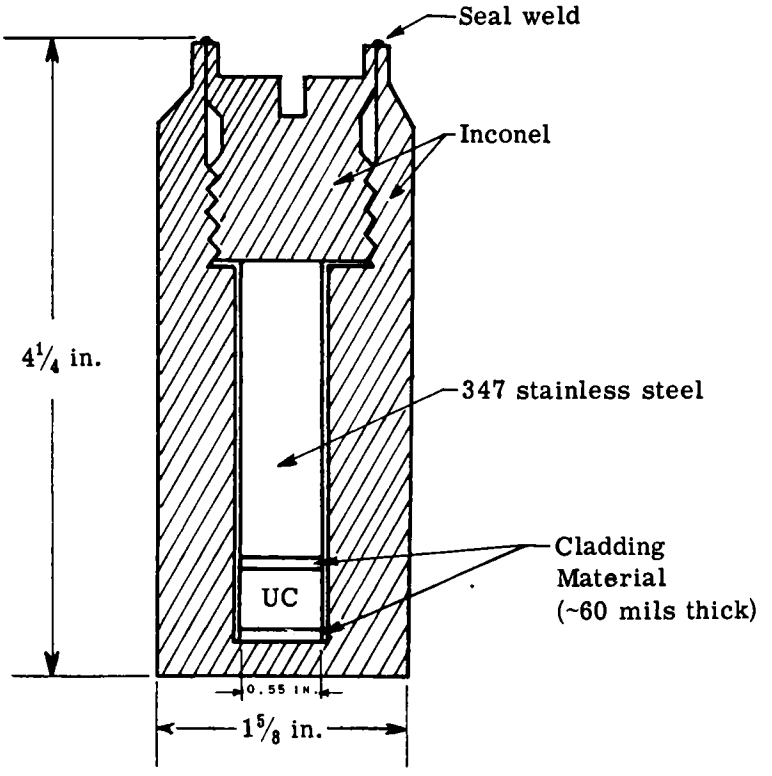

Fig. 4.7 — Diffusion capsule

5. FUEL REPROCESSING

5.1 INTRODUCTION

The major problem in reprocessing uranium carbide-plutonium carbide fuels by liquid-liquid extraction methods is anticipated to be dissolution of the spent fuel. While uranium carbide is expected to dissolve readily in conventional solvents such as nitric acid, the solubility of uranium carbide-plutonium carbide is unknown. The probable behavior of the irradiated fuel containing fission products is still more difficult to predict. Laboratory studies on the dissolution of pellets of uranium carbide and uranium carbide-plutonium carbide with selected simulated fission products may provide guidance for methods of attack on the difficult problems of dissolution of the irradiated fuel.

5.2 DEJACKETING (LITERATURE STUDY)

The many shapes and types of compositions proposed for nuclear fuels, and the many types of cladding materials advocated, preclude the use of a single simple decladding method for all types of fuel elements. Therefore, the decladding process may follow one of the several courses discussed below.

5.2.1 Mechanical Decladding

Rolling, milling, extrusion, abrasion cutting, electrical discharge cutting and shearing are some of the mechanical decladding methods that have been tested. Rolling and shearing combinations have been used to weaken fuel element cladding. Special tools which penetrate only the jacket have been designed. These separate the cladding from the core of the fuel element. Fuel material adhering to the cladding may be either dissolved with the clad and recovered or preferentially dissolved and combined with the core dissolution streams.

Mechanical decladding has several advantages:

1. Reagents needed to dissolve the fuel are generally less corrosive than those needed for chemical decladding, thus requiring less expensive dissolution equipment.
2. There is less material to dissolve, thus resulting in smaller waste volumes and increased plant capacity.
3. Concentrations of undesirable chemicals are reduced, leading to greater efficiency in the subsequent separation steps.

The main disadvantage of mechanical decladding concerns the removal of the cladding pieces from the dissolvers employed to recover adhering fuel material. The use of special equipment or of a subsequent chemical dissolution of the cleaned cladding pieces is required.

5.2.2 Selective Fuel Dissolution

Depending on the design and nature of the fuel core it is frequently possible to preferentially dissolve the core material without affecting the cladding. Thus in leaching tests on stainless steel

clad UO_2 fuel sections ($\frac{3}{8}$ in. D and $1\frac{1}{2}$ in. L) the sections were cleaned of UO_2 by 10M HNO_3 in 25 min.

Advantages and disadvantages of such a technique are similar to those for mechanical decladding (Section 5.2.1).

5.2.3 Complete Dissolution of Fuel and Cladding

Although this is not, strictly speaking, a decladding operation it is frequently the only technique that can be used to expose the fuel. Recovery of the desirable fuel is accomplished by solvent extraction.

5.2.4 Selective Cladding Dissolution

Successful dissolution of the cladding without substantial attack of the fuel has been demonstrated. Types of reagents employed include molten metals, fused salts, alkalies, and acids. With UO_2 fuels clad with such materials as Zircaloy-2, or 304L stainless steel, uranium losses as low as 0.02% have been reported under carefully controlled conditions.

A UO_2 fuel clad with stainless steel was made the electrode in a nitric acid solution. Under specified conditions of voltage, current, pH and temperature, the cladding alone was dissolved electrolytically and uranium recoveries were greater than 99.5%.

5.2.5 Selective Volatility

Alloy type fuels such as U, U-Zr-Nb-Sn, U-Zr and U-Zircaloy-2 clad with Zr or Zircaloy-2 may be reacted with anhydrous HCl at 300°C. The $ZrCl_4$ formed sublimes while UCl_3 remains behind since it has, at this temperature, a vapor pressure of less than 10^{-11} atm. Some fuel elements can be declad in less than 3 hr by this method. The residue of the chlorination is then dissolved in water and stripped of HCl by distillation with concentrated HNO_3.

5.3 DISSOLUTION (EXPERIMENTAL STUDY)

UC. Whole or crushed UC pellets can be easily dissolved in 6M HNO_3. The reaction is exothermic and can be controlled by adjusting the acid concentration. It is advisable to heat the solution near the end of the reaction to avoid the small residue that would otherwise be left. In cases where the solution was not heated this residue amounted to 0.03 to 0.06 w/o of the original sample, calculated as U_3O_8.

UC and Simulated Fission Products ("Fisside"). A few UC pellets were made up containing simulated fission products to find out whether they affect the solubility of the pure UC. The "fisside" is not expected to reproduce the solubility problems of a real irradiated carbide; the latter is probably more difficult to dissolve. It is hoped that the "fisside" will give some measure of the problem that might arise with irradiated fuel.

The simulated fission products were limited to relatively stable carbide formers. The amounts to be present after 40% plutonium atom burnup of 20 w/o PuC-80 w/o UC were calculated; the method of calculation is shown in Section 7.2.

The composition of pellets by weight percent is shown below:

Constituent	%	Constituent	%	Constituent	%
UC	96.28	NbC	0.02	ZrC	0.64
LaC_2	0.25	CeC_2	0.58	MoC	0.72
YC_2	0.06	Pd+C	0.61	RuC	0.84

All the elements were added as carbide, with the exception of Pd metal powder and a stoichiometric amount of carbon. The carbides were mixed by milling together for 4 hr in a rubber-lined mill with stainless steel balls. Green pellets were pressed at 40,000 psi using Carbowax 6000 as a temporary binder. The pellets were sintered in a vacuum furnace at 1800°C for 1 hr resulting in a bulk density of about 8 g/cc.

A sample pellet was ground to -100 mesh with a hardened steel mortar and pestle. The powder (11.5361 g) was accurately weighed in a 300-ml Pyrex beaker. The uncovered sample was deliberately allowed to stand in the well ventilated hood and observed to determine its short term pyrophoric tendencies. There was no evidence of warmup in a 10 min period.

Small increments (about 5 ml) of 8N nitric acid were added. Following each addition there was a rapid evolution of gas; the reaction was highly exothermic. The foam formed with each addition of acid quickly subsided. Additions of nitric acid were made until very little gas evolution was observed. The beaker containing the sample was mounted on a hot plate equipped with a motor and glass stirring rod. The sample was stirred with heating to 100°C for one hour. A total of 80 ml of 8M HNO_3 was added to the sample. This is about a 600% excess of nitric acid.

The dark-colored solution was filtered through a sintered glass Gooch crucible by suction. The residue was washed with water and dried at 120°C. The black residue weighed 0.4896 g and amounted to 4.24% of the starting sample. The residue was then treated in a platinum dish with 1 ml of 40% HF and 0.5 ml of concentrated HNO_3, and heated to dryness. About 5 ml of concentrated HNO_3 was added with heating on a sand bath for 1 hr. After cooling, 10 ml of water was added. The sample was filtered, water-washed, and dried. The residue weighed 0.2433 g; 2.10% of the original sample thus remained undissolved. The residues contain uranium. Quantitative uranium analyses are in progress.

5.4 FISSION PRODUCT SEPARATION (LITERATURE STUDY)

From a literature study it was concluded that liquid-liquid extraction with TBP is preferable to hexone or ion exchange methods. Other complexing agents have been studied. Although some of these look promising their economic value has not as yet been established.

For certain analytical procedures requiring the separation of uranium from plutonium, thenoyltrifluoracetone will be used. This reagent is, however, not recommended for a commercial operation.

5.5 BIBLIOGRAPHY FOR SECTION 5

U. S. Patent 2,879,130 (1959).

U. S. Patent 2,880,636 (1959).

F. L. Culler and R. E. Blanco, Dissolution and Feed Preparation for Aqueous Radiochemical Separation Processes, Second United Nations International Conference on the Peaceful Uses of Atomic Energy, A/Conf. 15/P/1930 (Sep. 1958).

V. R. Cooper, Quarterly Report, HW-57582 (Sep. 25, 1958).(Classified).

A. F. Boeglin and J. A. Buckham, Effect of Geometrical Shape on the Continuous Dissolution of Aluminum in Mercury – Catalyzed in Nitric Acid, IDO-14425 (Dec. 31, 1957).

W. E. Shuler and T. H. Siddall, III, Reprocessing of Power Reactor Fuels. First Quarterly Progress Report to January 1, 1958, DP-283 (Apr. 1958).

Patent 2,882,124, Assignee G. T. Seaborg (Apr. 14, 1959).

J. R. Flanary and J. H. Goode, Recovery of Enriched Uranium from UO_2-Stainless Steel Fuel Elements by Solvent Extraction, Ind. and Eng. Chem. 51:23-6 (1959).

E. L. Anderson, Jr., Fuel Reprocessing by Aqueous Methods, Nucleonics 15(10):72 (1957).

J. J. Shefcik and A. M. Platt, Preliminary Darex Flow Sheet, HW-58600 (Dec. 18, 1958).

G. R. Jasny et al., Recovering Uranium from Unirradiated Fuel Element Scrap, Ind. and Eng. Chem. 50:1777 (Dec. 1958).

E. S. Occhipinti, comp., Reprocessing of Power Reactor Fuels – Fourth Quarterly Progress Report July 1 to October 1, 1958, DP-338 (Feb. 1959).

V. R. Cooper, Quarterly Report, HW-58708, (Dec. 31, 1958). (Classified).

F. G. Kitts and B. C. Finney, Development of Batchwise and Semicontinuous Darex Flow Sheets Using 61 Weight percent HNO_3, CF-58-11-106, (Nov. 19, 1958).

C. E. Stevenson, Idaho Chemical Processing Plant – Technical Progress Report for July through September, 1958, IDO-14457 (Feb. 2, 1959).

E. E. Erickson, Continuous Dissolver Theory-I. Development of General Relationships for a Tube-Flow Flooded Dissolver, IDO-14450 (Nov. 24, 1958).

E. E. Erickson, Continuous Dissolver Theory-II. Application of Tube-Flow Dissolver Theory to Data from a 2-inch, Continuous Flooded Dissolver, IDO-14451 (Jan. 14, 1959).

J. L. Straughn and W. B. Tarpley, NYO-7925 (May 1958).(Classified).

O. W. Parrett and K. L. Rohde, The Effect of Silicon in the Reprocessing of a Uranium-Aluminum Alloy, IDO-14441 (July 28, 1958).

F. G. Kitts, A Continuous Darex Process Flowsheet, CF-57-10-89 (Oct. 1957).

F. G. Kitts and J. J. Perona, A Preliminary Study of Presolvent Extraction Treatment of Stainless Steel Uranium Fuels With Dilute Aqua Regia, CF-57-6-125 (Rev.)(Oct. 11, 1957).

E. S. Occhipinti, comp., Reprocessing of Power Reactor Fuels – Second Quarterly Progress Report for January 1 to April 1, 1958, DP-318 (Sept. 1958).

E. E. Voiland, Problems Associated with the Chemical Processing of Aluminum-Silicon-Plutonium Fuel Materials, HW-54819 (Apr. 1, 1958).

F. S. Martin and M. J. Waterman, Head-End Processes for Dissolving Stainless Steel-UO_2 Dispersion Type Fuel Elements. I.Carbide and Nitride Treatments. II.Anodic Dissolution, AERE-C/R-2454 (Jan. 1958).

L. M. Ferris, Decladding of PWR Blanket Fuel Elements with Aqueous Ammonium Fluoride Solutions, ORNL-2558 (Oct. 9, 1958).

E. S. Occhipinti, comp., Reprocessing of Power Reactor Fuels – Third Quarterly Progress Report, April to July 1, 1958, DP-319 (Dec. 1958).

C. E. Stevenson, Technical Progress Report for January through March 1958, Idaho Chemical Processing Plant, IDO-14443 (Sept. 15, 1958).

C. W. Pierce and B. Manowitz, Reprocessing of Power Reactor Fuels. The Enrico Fermi Fast Breeder Reactor Fuel Progress Report No. 1, BNL-511(T-124)(June 1958).

W. E. Clark and A. H. Kibbey, Hydrofluoric Acid Decladding of Zirconium-Clad Power Reactor Fuel Elements, ORNL-2460 (Nov. 7, 1958).

J. L. Swanson, The Zirflex Process, Second United Nations International Conference on the Peaceful Uses of Atomic Energy, A/Conf. 15/P/2429 (June 1958).

L. Küchler and W. Schüller, Reprocessing of Nuclear Fuels, Chem. Abstracts 53(7) 5890(Apr.10, 1959) Nukleonik 1, 112-24(1958) in German.

CEP's 1959 Special Nuclear Report, Chem. Eng. Prog., p. 65(Feb. 1959).

J. K. Davidson et al, The Fast Oxide Breeder – The Fuel Cycle, KAPL-1757 (July 1, 1957).

Fuel Elements Conference Held in Paris, November 18-23, 1957, pp 369-442, 526, 542, TID-7546 Book 2 (Mar. 1958).

Progress Report on Solid Fuels, Nucleonics 17 (5):100 (May 1959).

S. Glasstone, "Principles of Nuclear Reactor Engineering," p. 764, Van Nostrand, New York (1955).

Patent No. 2,871,176 (1959)

News Roundup, Nucleonics 17 (4):26 (Apr. 1959).

European Atomic Fuels Grow, Special Report, Chem. and Eng. News, p. 64 (July 27, 1959).

Research – Inventions Wanted, Chem. and Eng. News, p. 40 (June 8, 1959).

Reactor Fuel Processing, 1(1):5 (Feb. 1958); 1(3):4 (July 1958); 2(1):7 and 2(1):9 (Jan. 1959); 1(1) (Feb. 1959); 2(1) (Apr. 1959).

6. PLUTONIUM FACILITY DESIGN AND CONSTRUCTION

6.1 INTRODUCTION

The Carborundum Company is designing and constructing a facility to be used for fabricating the fuel and studying "cold" reprocessing. The design of the facility is complete and its components are being built. The construction of the facility is expected to be complete in November 1959. NDA is designing and constructing a facility to be used for fuel evaluation, specimen preparation, irradiation, post irradiation examination, and "hot" reprocessing. The design of the pre-irradiation facility is nearly complete. Fabrication of the chemistry boxes is complete. The construction of the pre-irradiation facility and equipment is expected to be completed in March 1960. The equipment for post-irradiation examination will be designed in 1960, and built in 1961.

The design of these facilities was strongly influenced by the advice of Argonne National Laboratory, Los Alamos Scientific Laboratory, the AEC New Brunswick Laboratory, Oak Ridge National Laboratory, and the Savannah River Operations. Their assistance is sincerely appreciated.

6.2 HEALTH AND SAFETY

6.2.1 Introduction

Safe operation of the facility in which unirradiated plutonium or plutonium-bearing materials is handled requires that provision be made to combat the hazards of toxicity, pyrophoricity, and nuclear reactivity associated with the element. The containment philosophy of performing all operations within sealed glove-boxes provides assurance that the spread of contamination is limited; concurrently it provides a means to surround the materials with an inert atmosphere and reduce the pyrophoricity hazard. Strict accountability procedures to control amounts of fissionable material handled or stored in each operation will be exercised.

A report detailing all the experimental procedures will be issued and approved prior to initiation of actual plutonium handling.

6.2.2 Background Information

The health hazard of plutonium is due to its high alpha activity and to its ready absorption in the bones, 18% of the inhaled plutonium and 70% of that entering the bloodstream being retained.[1] The alpha particles of this retained plutonium produce intense local damage to the bone marrow. The effective half life of plutonium is approximately 120 yr and hence it is a cumulative poison in the bone. The maximum permissible quantity of plutonium which may accumulate in the body during the working lifetime is set at 0.6 μg. As a consequence of this, the permissible occupational tolerance level (maximum permissible level) of plutonium in air is 2.0×10^{-12} μc/cc or 3.2×10^{-11} g/m^3 based on continuous exposure for 40 hr/wk for 50 yr.[2] This corresponds to between

two and three one-micron particles of plutonium metal in a cubic meter of air. The 40 hr/wk tolerance level of plutonium in drinking water is 10^{-4} μc/ml. The permissible surface contamination is approximately 1000 disintegrations/min for 75 cm^2 of area.[3]

6.2.3 Hazard Control

Carborundum Facility

Tight, smooth, steel-panelled walls and monolithic vinyl flooring are conducive to containment of contamination, to good housekeeping, and to fire prevention. The room will have its own ventilation and air-conditioning system, with air exhausted through absolute filters. There will be a sprinkler system within the plutonium room, as well as in the adjacent areas.

Entrance of personnel to the working area is through a change room where protective clothing and shoe covers are obtained. Normal exit is also through this room. An alpha counter for monitoring clothing and personnel is available in this room. The room also has a shower, wash basin, and containers for contaminated clothing and shoe covers.

Waste water from the shower and sinks will be pumped through a filter to remove particulate matter, and then into holding tanks where it will be tested for activity before disposal.

The glove-box system will have the following safety features: inlet and exit gas stream filters, vacuumtight transfer and glove port covers, over and under pressure alarm systems for each box, temperature alarm systems, and an automatic exhaust system to operate in the event of accidental leakage into the glove-box system.

Personnel working on the project will be checked with a urinalysis once every three months and a blood test once every six months. All personnel will be checked prior to initiation of operations. Fecal samples will be taken in the event of a contamination incident. Persons working in the glove-boxes will wear surgeons' gloves inside arm-length neoprene gloves. After removal from the glove-boxes, hands will be immediately monitored by alpha counters located at strategic positions around the room.

Air samples will be taken during working hours and checked for activity. Equipment outside the glove-boxes, furniture, floors, etc., will also be monitored. Scott Air Packs will be available for use in carrying out hazardous operations such as changing gloves on the boxes.

Criticality will not be a problem since not more than 200 g of plutonium will be in the facility at any one time.

An operating manual is being prepared.

NDA Facility

Hard finish paint on smooth noncombustible walls and waxed hard finish paint on concrete floors will permit easy decontamination of rooms if necessary. The laboratory will have its own continuous ventilation system with room air exhausted to a stack through Fiberglas and absolute filters at a rate of four room changes per hr. Standby components will be available to replace equipment for routine maintenance or during an emergency. Air monitors will be employed to detect buildup of contamination in the laboratory or in the effluent stream. A health physicist will routinely survey the area for radioactive contamination and will monitor all handling operations. All materials leaving the facility will be monitored by the health physicist. Water from showers, sinks, and laundry will be filtered, retained in tanks, and monitored before disposal.

The health physicist will routinely monitor soil, water, vegetation, and wildlife from the areas surrounding the laboratory building.

The glove-boxes will have safety features similar to those described above.

Personnel entering the alpha areas will wear shoe covers, protective clothing, and head covering. Surgeons' gloves will be worn during operations with plutonium materials. Respirators will be readily available and will be used during potentially hazardous operations or during emergencies. Eating, drinking, or smoking will be prohibited in the operations area. Upon leaving the facility, all clothing will be monitored, removed, stored, and laundered if necessary. Personnel will be monitored before entering the change room.

Personnel working on the project will be checked with a urinalysis every three months and a blood test every six months, or as needed in the event of a contamination incident.

All of the materials of construction in the facility are fire-resistant, but local fires may occur. In the event of a fire, operators will be trained so that prompt corrective action can be taken. All working areas within the containment system will be provided with suitable fire extinguishing material within easy reach of operators. Good housekeeping procedures will be followed to minimize the accumulation of combustible materials in and around the laboratory.

6.3 FACILITY FOR FUEL CARBIDE FABRICATION AND COLD REPROCESSING AT THE CARBORUNDUM COMPANY

6.3.1 Laboratory

The laboratory for handling alpha-active materials is located on the fourth floor of the Carborundum Central Research Building in Niagara Falls, New York. It consists of an alpha-handling area and a personnel change area. Fig. 6.1 shows the equipment layout and room plan of the facility. Approximate inside dimensions are 14 ft wide, 48 ft long and 8½ ft high. Walls and ceiling will be enameled steel paneling, while a vinyl floor covering will be laid over the present tile floor.

The layout shows three entrances into the area; however, the door on the east side of the room will be used for all normal traffic in and out of the facility. The large double door on the south wall will be used only for movement of large equipment into the area, especially during initial equipment setup in the room. When not in use, the door will be locked and sealed. The small door on the south wall is for an emergency exit only and can only be opened from the inside. All doors have explosion-proof windows installed in them to permit inspection of the room without entering it.

In the southeast corner of the work room are two 50-gal tanks. All water from the shower and sinks will be pumped through two filters to these tanks, checked for contamination level, and diluted (if required) before being passed to the drain.

The six glove-boxes, as well as other permanent equipment, are shown in their approximate positions. Most of the helium purification system will be set in an adjacent room on the south side of the new room between the large door and the emergency exit. The two tanks shown near glove-box No. 6 are gas storage tanks and are a part of the helium purification system.

6.3.2 Box Design

The Carborundum alpha box is made of an aluminum extrusion frame having safety glass front and back, and aluminum panels on the remaining sides. The front, back and side panels are vertical. The aluminum panels are welded to the aluminum extrusions, and the glass panels are sealed to the extrusions by means of O-rings. Glove ports are sealed to the safety glass by O-rings; the box is accessible from two sides. The glove ports are of the ANL design; the aluminum extrusions are of a modified ANL design (Fig. 6.2).

Boxes 1, 2, and 6 are air-atmosphere boxes while 3, 4, and 5 are helium-atmosphere boxes. (See Fig. 6.1.) All boxes, with the exception of 6, will have glove ports on both sides. The six boxes are similar in design. Boxes 1 through 5 are 3 ft high, $3\frac{1}{2}$ ft deep, and vary in length from $3\frac{1}{2}$ to 6 ft. Box 6 is 3 ft high, 2 ft deep, and $3\frac{1}{2}$ ft long. Gas, water, and power lead-throughs are provided.

6.3.3 Box Arrangement

Boxes 1 through 5 are connected in-line, in the center of the laboratory space. The box line will be accessible from all sides. Boxes 1 through 5 will have 16 in. diameter transfer ports on both ends to allow passage of material from one box to another. Box 6 will have one 14 in. diameter transfer port. All transfer ports will have internal lock, O-ring sealed sliding doors. A vacuum lock will connect boxes 2 and 3 so that material can be transferred from the air box system to the helium box system without contaminating the latter with air. All other box connections will be made by a plastic sleeve arrangement between ports and with a metal inner sleeve for rigidity. Plastic pouches will be used on the ends of boxes 1 and 5 to transfer materials into and out of the system.

Table 6.1 gives a summary of The Carborundum Co. boxes.

Table 6.1 — Summary of The Carborundum Co. Boxes

No.	Name	Atmosphere	Function
1	Chemistry box	Once-through air	Sample preparation for analysis. Separation of U from Pu.
2	Chemistry box	Once-through air	Macro and micro U and Pu analysis
3	Chemistry box	Recirculating He	Carbon analysis. Density measurements.
4	Fabrication box	Recirculating He	Crushing, grinding
5	Fabrication box	Recirculating He	Carbide synthesis, pressing, sintering
6	Low level chemistry box	Once-through air	Alpha counting, fluorimetry, x-ray camera loading area

6.3.4 Box Outfitting

Box 1 – Chemistry Box

The box will be used to dissolve nonirradiated fuel materials, recover uranium and plutonium from simulated fission products and other interfering ions, and to separate uranium from plutonium where necessary. In addition to these operations this box will be used to store the required reagents and to concentrate excess volumes of solvents by evaporation.

For chemical analysis the separations will be performed by a solvent extraction technique using separatory funnels and a mechanical shaker.

The box will have an air atmosphere.

Box 2 – Chemistry Box

This box will be used for uranium and plutonium analysis. Aliquots of uranium and of plutonium solutions previously separated in box 1 will be transferred to box 2 for chemical analysis.

Macro concentrations of these elements will be determined principally by oxidation-reduction titrimetric methods, although visual end-point titrations using suitable indicators or spectrophotometric methods will be considered where applicable.

In those cases where the samples contain nitrate ions the samples will be converted to the sulfates by fuming with sulfuric acid. The uranium and plutonium ions will then be reduced by means of a lead or Jones reductor. In the case of uranium ion the valence state will be adjusted to +4 by passing air through the solution and titrating to the +6 state with ceric sulfate. With plutonium solutions the +3 form will be titrated directly to the +4 state with ceric sulfate. With such a method it is necessary to ascertain the absence of Fe and other non-U and non-Pu reducible ions in the solutions prior to the reduction step. The presence of such interfering ions will be eliminated in the solvent extraction procedure employed in box 1.

Micro amounts of uranium will be determined by a fluorimetric technique while micro amounts of plutonium will be quantitated by alpha counting. Such samples will be prepared in box 2 and analyzed in box 6. Uranium samples contained in suitable planchets will be evaporated to dryness under infrared heat, heated to 1000°C to destroy any possible organic matter and twice fused with NaF. Plutonium samples extracted as the thenoyl trifluoroacetone complex will be evaporated to dryness on suitable planchets.

In order to carry out the proposed operations the box will contain a Fisher automatic titrimeter with dual controls, a Sargent-Malmstadt automatic potentiometric titrator, a National vacuum oven, a thermoelectric muffle furnace, a hot plate-magnetic stirrer, a heat lamp, a mechanical stirrer, and miscellaneous equipment.

The box will have an air atmosphere.

Box 3 – Chemistry Box

This box will be used for carbon analyses and density measurements.

Samples for carbon analysis will be weighed and transferred to the carbon combustion furnace with suitable catalysts and ignited in a stream of oxygen. The carbon dioxide will be collected in ascarite and weighed. For density measurements the samples in pellet form will be weighed under liquid immersion in calibrated pycnometers.

This box will contain a Mettler analytical balance and a Fisher carbon train.

Due to the pyrophoric nature of the carbide powders in question and the instability of surfaces of carbide compacts in air, this box will contain a helium atmosphere.

Box 4 – Fabrication Box

This box will be used for crushing and grinding powder at various stages of the carbide preparation and fabrication. A tool steel mortar and pestle will be used for crushing the reaction product from the UC synthesis; the powders will be milled in a Fisher Minimill; the pellets will be centerless ground on an adaptation of a roller lapping machine obtained from the Spitfire Tool Company.

The box will be operated in a helium atmosphere.

Box 5 – Fabrication Box

This box will be used for the synthesis of carbides, cold pressing, sintering, or hot pressing. Equipment will include a hydraulic laboratory press and a combination sintering-hot press furnace. The furnace is illustrated in Fig. 6.3. Power leads sufficient to carry 15 kw will be installed.

The box will be operated in a helium atmosphere.

Box 6 – Low Level Chemistry Box

This box will be employed for alpha counting of micro plutonium samples, for fluorimetric analysis of micro amounts of uranium and to load the x-ray camera for x-ray diffraction studies. The x-ray diffraction determinations will be performed outside the boxes. This box will contain the probe of an alpha counter, the head of a fluorimeter, and an x-ray camera.

An air atmosphere will be used in the box.

6.3.5 Gas Systems

Helium

Fig. 6.4 is a schematic of the helium purification and recovery system with one helium glove-box (box 3) shown on the diagram. The section enclosed by the dotted line shows the portion of the helium purification system which is duplicated for each helium box. The total helium flow in the system will be 20 cfm and with three helium boxes will distribute approximately 6 to 7 cfm through each box.

The gas flow in the system is described below, beginning with the gas circulating pumps. First, the gas enters the suction side of the pumps. Two pumps are operated in parallel so that continuity of operation can be maintained even though one pump may be out of the circuit for servicing or repair. Each pump has a capacity of 20 cfm and a head of 6 lb pressure. The pump motor and bypass relief valves all are housed in a tank containing a water-cooled helium atmosphere, thereby producing a zero-leakage circulation system.

The helium leaves the gas circulating pumps at a pressure of 5 to 6 lb and flows through the high-temperature getter columns. The columns are operated at about 900°C. The purification system contains four 3 in. diameter, high-temperature columns operating in parallel. These columns are individually equipped with temperature control and with flow indication and control. In addition, each column is provided with a separate temperature alarm system that is interlocked with solenoid control valves on each of the three helium boxes, so that should a large amount of air enter the system, there would be an immediate shutdown. Each of these purification towers contains 10 lb of zirconium turnings. Each of the getter columns is individually valved so that the column may be removed from the system, the cartridge replaced, and the getter evacuated.

The purified gas leaving the high-temperature getter columns next passes through a single, low-temperature titanium getter column to remove any hydrogen which may have accumulated in the helium. The column operates at about 400°C. Periodically, the low-temperature titanium getter will be valved-off, heated to high temperature with internal heaters, and evacuated to remove the hydrogen and regenerate the getter.

Following the low-temperature titanium getter are two storage tanks having a combined capacity of about 100 ft^3.

The gas flow from the storage tank is manifolded back to the three glove-boxes and then flows through a rotameter and differential pressure controller which keeps the flow constant after it has once been set manually. The flow then goes through the inlet air filter on each of the boxes. The gas leaves the box through two filters, mounted in parallel, on the side opposite from the inlet. One filter will be a standby, to be used when a filter change is required. Ball-seal valves are provided upstream from the inlet filter and downstream from the exit filters so that the entire box can be shut off from the system.

Following the two isolation valves after the absolute exit gas filters on each box will be a second container enclosing a second absolute gas filter in series with the two filters contained on the box and serving as secondary protection against the exit of plutonium dust from the system.

After this filter, the gas passes through a back-pressure control valve and then to a gas take-off which allows a very small flow of gas, less than 1/10 cfh, to flow through a cold-cathode discharge-type gas analyzer. The analyzer gives a measure of the total impurities, and also serves to detect any abnormally high level of impurities (such as oxygen) that would come through with the helium. The gas then passes through a solenoid valve to the suction side of the circulating pumps.

The alarm system on the cold-cathode discharge analyzer will operate to open a solenoid valve leading to the suction manifold and, at the same time, close the solenoid valve leading to the suction inlet of the helium circulating pumps. These two solenoid valves will be located downstream from the air-operated, diaphragm-sealed, back-pressure control valve. The function of this back-pressure control valve is to keep the pressure constant in the glove-boxes. It responds to a signal received from the manometer control and differential pressure-control relay. The two solenoid valves referred to would be interlocked in such a manner that an abnormally rapid temperature increase in any of the four getter columns would open the helium flow from the box to the air stack. The abnormal temperature increase would be indicated by a separate alarm thermocouple operating through a temperature indicator relay controller. Location of the back-pressure control valve, before the two solenoid valves, insures that the back pressure in the box will be maintained correct even though the exhaust goes to the stack, where the pressure drop may be different than the suction inlet pressure at the helium pumps. A one-way valve will be provided in the line leading to the air exhaust stack to prevent the backflow of air into the helium system, should, for any reason, the suction pressure at the air exhaust stack be greater than either the box pressure or the helium inlet pressure.

Air

The flow control system of the three air boxes is different and is as follows: Downstream from the isolation valves, on the parallel exit air filters, will be located a flow control valve properly sized to provide a flow rate of 20 cfm when the boxes are operating at 2 in. of water below atmospheric pressure. Regulation of flow and of box pressure will be by manual control, i.e., by setting the exhaust valve at the exit and the inlet rotameter valve, to produce the desired flow and inlet box pressure. The air from the three air boxes will then go to a manifold, through the absolute filter, and the exhaust fan and up the stack.

An oil-filled manometer will be provided on the box for measuring pressure, providing safety protection, and providing an alarm in the case of overpressurizing or underpressurizing of the box. On the box side, the manometer will be equipped with an absolute filter and with the high and low-level alarm contacts necessary to operate an automatic warning system. This same manometer and alarm system will also be provided on the three helium boxes and will integrate with the helium recovery-circulation system. The above combination of pressure-indicating, and over and underpressure warning system will provide absolute protection against breakage of the glass by any failure which would either overpressurize or underpressurize the box. Pressure limits in the helium boxes are -0.5 to -1.5 in. of water.

A 100 cfm fan will be used in the exhaust line to pull the required air through the air boxes and to exhaust the helium boxes in the event of a break or overpressurizing of the boxes. An absolute filter will be mounted before the fan to minimize the contamination of the gas entering the stack.

6.4 FACILITY FOR CARBIDE EVALUATION AT NDA

6.4.1 Laboratory

The laboratory for alpha active materials will be located in the NDA Hot Laboratory Building, Pawling, New York. It will consist of an alpha handling area, an alpha service area, a personnel

change area and an area for shipping, receiving, storing, packaging and reprocessing radioactive materials. The general layout is shown in Fig. 6.5.

The alpha handling area to the north of and separated from the gamma facilities by a floor to ceiling wall, will be approximately 28 ft × 32 ft × 20 ft high. The walls will be a smooth surface construction. The concrete floor will be painted. The area will contain the glove-boxes and hoods.

The alpha service area, a 19 ft × 16 ft room, will be west of the alpha handling area and provide for storage of auxiliary equipment such as the helium mass spectrometer leak detector, welding machine, chemistry or other materials, and also for alpha material storage. This area will also provide work space for general maintenance of equipment and boxes.

North of the alpha handling area, a 12 ft × 16 ft building will house the helium purification system, with the associated control system.

The personnel change area, which is accessible from either the alpha or gamma facilities, will be equipped for personnel and clothing monitoring, clothing storage, showers and sinks, and a locker room. Normal traffic in and out of the facility will be through this area. Emergency exits will be on the north and south wall of the alpha handling area.

Located south of the Hot Laboratory Building is a ramp for shipping and receiving radioactive materials. A 20 ft × 20 ft building, located off this ramp, will be used to package radioactive material in concrete and to reprocess shower, sink, and laundry water. (All liquids containing large concentrations of plutonium will be processed in boxes.)

The alpha handling and service areas have a common ventilating system designed to provide four complete room atmosphere changes per hr. The room air is drawn through a Fiberglas filter and an absolute filter located at floor level and is discharged through a 50 ft high by 16 in. diameter stack. There are two stack blowers: one for continuous operation and the second for standby. In addition to room ventilation, the blower provides a suction head of 0.55 in. H_2O below atmospheric for removal of excess box pressure. See Section 6.4.5.

6.4.2 Box Design

The working boxes, shown in Fig. 6.6 are 4 ft long by 3 ft deep by 3 ft high, and are constructed of carbon steel welded on the outside; there is additional welding on the interior floor to wall joint and 6 in. up the sides, to provide for easy decontamination in case of a spill. The basic box is provided with two sloping 1 ft × 3 ft viewing windows, one 1 ft × 3 ft ceiling window for lighting, two 16 in. transfer ports and four 8 in. glove ports. All windows are of fire resistant plastic, type 5009FS.* Each window is set in a frame constructed of structural Z cross-section iron. The only preparation of the window sealing surfaces is to sandblast off the mill scale and paint to prevent rusting. The area under the O-ring is coated with a latex rubber compound which sets to the shape and pits of the iron. The box interior is covered with Liquid Tile,† an acid and fire resistant coating. The box exterior is painted with Amercoat.‡

The boxes have been leak tested, to date, by shrouding the outside with helium, maintaining the inside at a 1 to 2 in. negative pressure and locating a leak detector sniffer in the box. Since atmospheric air contains 4 ppm helium, it was used as a standard. The leak rate was determined to be less than 0.001% of box volume per hour. Each box is designed to contain a specific process, as described in Section 6.4.4.

---

* Trade name of Rohm & Haas Company, Philadelphia, Pa.

† Trade name of Evershield Products, Joppa, Md.

‡ Trade name of Amercoat Corporation, South Gate, Calif.

6.4.3 Box Arrangement

The boxes will be arranged in an "L" shape as shown in Fig. 6.5. The corner of the "L" will be used for transferring material in or out of the line. The boxes will be connected to each other by a plastic bag-tunnel arrangement which permits them to be safely removed from the line if necessary. Two hoods will be located against the south wall of the alpha handling area.

6.4.4 Box Outfitting

Table 6.2 lists the working boxes by name, number, and function. A more detailed description is given below.

The chemistry boxes (S-202, 203, and 204) have been completed. All the equipment for the boxes has been received or is on order. A fourth box is nearly completed; it is currently being used as a "mockup" box. The chemistry boxes are shown in their temporary setup on Fig. 6.6.

Table 6.2 — Summary of NDA Boxes and Hoods

No.	Name	Atmosphere	Function
S-104	Welding box	Recirculating He	Welding and leak detection
S-105	Weighing box	Recirculating He	Weight measurements
S-106	Cutoff box	Recirculating He	Sectioning, mounting, rough polishing
S-107	Polishing box	Recirculating He	Polishing, etching, and metallography
S-108	——	Recirculating He	Future expansion
S-114	Transfer box	Once-through He	Transfer operation between boxes
S-202	Chemistry box	Once-through air	Separation of U from Pu (low level), U sample preparation for analysis
S-203	Chemistry box	Once-through air	Separation of U from Pu (high level), U and Pu analysis
S-204	Chemistry box	Once-through air	Carbon analysis, PuC-UC dissolution
S-205	Furnace box	Once-through air	Thermal cycling, dilatometry
S-206	——	Once-through air	Future expansion
S-207	Air transfer box	Once-through air	
Hood No. 1	Counting hood	Once-through air	Alpha counting
Hood No. 2	Furnace hood	Once-through air	Fuel-clad compatibility tests

Box S-104 – Welding Box

The function of this box is to provide a facility for welding and leak testing. Fuel pellets will be welded into tubing for irradiation specimens, and diffusion couples will be welded for out-of-pile testing. The leaktightness of the welds will be checked with a helium mass spectrometer leak detector.

The equipment for welding will consist of a rigid, inert electrode welding torch, adjustable for gap and angle of weld. A variable speed mechanism will rotate the tube. The capacity will be 1 in. diameter 32-in. long tubes or larger diameter, short tubes.

The equipment for leak testing will consist of a mass spectrometer leak detector outside the box, and a sample holder inside the box. The line from the sample holder to the mass spectrometer leak detector will contain a millipore filter to keep the instrument from being contaminated.

Box S-105 – Weighing Box

This box will be employed to weigh plutonium containing materials preparatory to various chemical analyses. A Mettler analytical balance will be used. Samples for carbon analysis will be prepared here by placing them in tubes and sealing them by crimping. A recirculating helium atmosphere will be used.

Box S-106 – Cutoff Box

The function of this box is to provide a facility for the initial steps of metallographic sample preparation. Specimens will be sectioned, mounted, and rough polished.

Equipment will consist of a cutoff wheel capable of sectioning carbide samples submerged in oil. The machine will be similar to the one presently in use on UC. A low temperature setting resin will be used for mounting specimens. A rough polishing wheel, with recirculating, non-aqueous coolant will also be installed in this box.

Recirculating helium atmosphere will be used.

Box S-107 – Polishing Box

Final polishing, etching, and metallographic examination will be done in this box. Two polishing wheels will be available. The box will contain an ultrasonic cleaning tank while the power unit for this tank will be mounted outside the box. A metallograph will be adapted so that it can be used to view samples inside the box. The metallograph itself will be mounted outside the box. The sample will be separated from the objective by a sealed optical flat.

Recirculating helium atmosphere will be used.

Box S-114 – Transfer Box

In addition to transfer operations, this box will be used for alpha counting and heat sealing vinyl pouches. An alpha survey meter probe and a heat sealer will be included in the box.

Box S-202 – Chemistry Box

This box will be employed to prepare samples for the fluorimetric analysis of uranium and for alpha counting of plutonium contaminated waste streams. Uranium and plutonium will be separated from each other and interfering impurities, by solvent extraction and by ion exchange methods. Aliquots of the samples will be evaporated on planchets and monitored for alpha contamination by means of an alpha survey meter prior to the transfer to the counting hood. Only samples showing less than about 10,000 counts/min will be taken out of the hood for precise alpha counting or fluorimetric measurements.

Necessary equipment which will be contained in this box includes alpha survey probe, shaker, separating funnels, ion exchangers, and infrared lamps.

The atmosphere in the box will be once-through air.

Box S-203 – Chemistry Box

This box will be employed for the separation of uranium from plutonium during reprocessing studies and for the analysis of pellets. The chemical analysis of macroquantities of uranium and of plutonium solutions will be performed by an oxidation-reduction titrimetric method using the reaction of ceric sulfate on U^{+4} or Pu^{+3}. The uranium will be oxidized by titration to the hexavalent state and the plutonium to the quatrivalent form. The separation and purifications of uranium and plutonium will be performed by solvent extractions and by ion exchange. Provisions

will be included to recover and reprocess undissolved material such as free carbon and undissolved uranium and plutonium containing crud with the aim of studying the material balance of the process.

Equipment to be contained in this box includes a Jones reductor, ion exchange columns, a Sargent-Malmstadt automatic titrator, a filter stand, and solvent extraction equipment.

The atmosphere in the box will be once-through air.

Box S-204 – Chemistry Box

This box will be employed to dissolve samples, evaporate and fume acid solutions and to analyze samples for their carbon content. Samples for carbon analysis will be heated by induction heating in an oxygen atmosphere. The generator for the induction heater will be located below the box and the leads to the work coil will be brought into the box through the floor by means of appropriate seals. The combustion gases (CO_2) will be absorbed in barium hydroxide which will be titrated with acid after a filtration step.

A once-through air atmosphere is planned for this box. Provision will be made to employ an inert atmosphere in the box in cases where it will be necessary to manipulate pyrophoric, powdered materials.

Hood No. 1 – Counting Hood

The hood will be used to alpha count planchets which may contain plutonium. In addition, planchets which may contain a dried layer of uranium will be flamed, subjected to two NaF fusions, and analyzed fluorimetrically.

The equipment provided for this hood includes a flowing gas proportional alpha counter, a fluorimeter, and two blast burners. A once-through air atmosphere will be used.

Hood No. 2 – Furnace Hood

The hood will be used to run fuel-clad compatability tests. The diffusion couples are described in Section 4.6. Sealed and leak tested couples will be taken out of the box train and placed in a metallic furnace tube. The furnace tube will be sealed with a flange and O-ring, then placed in the furnace in the hood. At the conclusion of the test the furnace tube will be disassembled in the box train.

6.4.5 Gas Systems

Three gas systems have been designed to provide the desired atmosphere within the gloveboxes:

1. A once-through air system for the chemistry boxes and one transfer box.
2. A once-through helium system for the second transfer box.
3. A recirculating helium system for the metallurgical boxes. These systems are designed to perform the following basic functions:

   Maintain the boxes at a slight negative pressure at all times.
   Keep at a minimum any alpha bearing material suspended in the box atmosphere.
   Provide an inert atmosphere with low oxygen contamination within the metallurgical boxes.

Helium

Working Boxes

The metallurgical boxes are all provided with an inert helium atmosphere. Helium is supplied from a dual manifold connected to a total of ten high-pressure helium bottles. A pressure switch located on the high-pressure side of the gas regulator provides an alarm when the bottle pressure falls below 50 psig. Adequate time is then available for helium bottle replacement. Helium is continuously recirculated at a rate of 5 to 6 cfm through each working metallurgical box. A stand-by blower is provided to insure continuous operation of the system. Both helium blowers are completely sealed units to prevent gas leakage. An absolute filter, placed at the blower suction, removes any gas-borne particulate matter. The helium system pressure is controlled at 0.4 to 0.6 in. of water below atmospheric pressure.

The excess pressure bleed-off is identical to that provided on the air-atmosphere working boxes. Instead of a continuous in-flow of helium, however, makeup gas is provided by two additional air-operated, solenoid-actuated valves. The signal for actuating these valves is obtained from pressure switches set at 0.6 and 0.7 in. of water vacuum.

Since a low oxygen content is required in the helium atmosphere, a 2 cfm side stream is continuously withdrawn and passed through a refrigerated activated charcoal bed. Based on assumptions of a certain number of transfers and the maximum allowable leakage, a bed operating at -100°F will keep the oxygen content below 100 ppm (by volume) and the nitrogen content below 1800 ppm. An oxygen analyzer is provided so that the oxygen content of the gas can be continuously recorded and an alarm furnished when the O_2 concentration exceeds 500 to 600 ppm. The charcoal beds will be regenerated by flowing a stream of hot air around the units while maintaining a vacuum on the columns. Three beds are provided so that one may be regenerated while another is operating and a third is available for emergency service.

The -100°F operating temperature of the charcoal columns will be provided by a mechanical refrigeration unit. A second unit is provided for standby service. In addition to cooling the charcoal, the refrigerant flows through a finned pre-cooler placed at the base of the charcoal bed. The pre-cooler brings the entering helium to operating temperatures as well as condensing any water vapor present.

The use of a mechanically refrigerated charcoal bed over a liquid nitrogen-cooled charcoal bed was chosen because of its considerably lower cost. The higher impurity level of the -100°F system compared to the -300°F system is not expected to be harmful to the planned operations.

Transfer Box

The helium transfer box serves the dual function of reducing contamination migration and diluting any air that is brought into the system. All transfers are done by bagging. To keep down gas-borne alpha contamination and minimize oxygen content, a continuous helium bleed of 3 cfh (corresponding to one box volume per 8-hr day) enters the box. A check valve prevents any back-flow into the helium line. The pressure control system, which is identical to that provided for the air atmosphere transfer box, discharges the excess helium to the stack and maintains the box at 0.4 in. of water below atmospheric pressure.

Air

Transfer Box

The air transfer box and the working air atmosphere boxes are separately provided with a continuous small in-flow of room air at 5 to 6 cfm. This air, which is removed by means of the

pressure control system, serves to keep suspended alpha-bearing material at a low level. An absolute filter on the air intake insures that alpha contamination cannot be carried into the room through the bleed line.

Working Boxes

The working air boxes are normally maintained at approximately 0.4 in. of water below atmospheric pressure. This is accomplished by means of a sensitive pressure switch located in the exit manifold of the boxes which is activated when the manifold pressure approaches 0.4 in. below atmospheric pressure. The switch operates a solenoid which in turn activates an air operated ball valve located in the line to the suction side of the stack blower. An orifice is placed in this line to the stack so that the rate at which the valve cycles can be controlled. To provide backup in case of failure of the primary control valve and to provide adequate flow capacity in case of a glove break, two additional pressure switch-control valve assemblies are provided in parallel. These are set for operation at 0.3 in. and 0.2 in. of water vacuum, respectively. The valves and lines are sized so that in case of glove breakage a flow of 30 cfm can be maintained. This air flow quantity assures a linear velocity of 100 ft/min across the full area of the glove port.

The pressure control system for the air transfer box is essentially the same as that for the working boxes except that only two pressure control valves are provided. These switch-valve assemblies are set for operation at 0.4 and 0.3 in. of water vacuum, respectively. Again the normal control valve (0.4 in. setting) is provided with an orifice so that its rate of cycling can be controlled. The backup valve, when open, can provide the 30 cfm flow required in case of a glove break. An alarm is provided to indicate when the backup valve is open.

Introduction and removal of all material from the air atmosphere working boxes is done by bagging through the air transfer box. The transfer of material between the transfer box and the working boxes is also by means of bagging. The atmosphere within the transfer box can thus be kept at a lower contamination level than the working boxes.

6.4.6 Irradiation Test Design

Test Objectives

In order for PuC-UC fuel to reduce fuel cycle costs, several conditions must be met. The fuel has to be able to achieve high burnup, high operating temperatures, and high power. At least 2 a/o burnup is desirable at fuel temperatures above 1200°F with maximum dimensional stability of the fuel and minimum release of fission products. Power should be at least equivalent to presently planned fuels. The objective of the irradiation program is to determine whether the high burnup, temperature, and power required can be achieved.

The test will measure temperatures, burnup, power, and dimensional stability of the fuel. In addition, measurements of in-pile effective thermal conductivity, fission gas pressure, and fission gas release will be attempted.

Specimen Description

The fuel specimens will be stainless steel or niobium-clad cylinders about 0.250 in. OD, with about 3 in. fueled length. The length is limited by the test reactor and capsule design. The fuel will be in the form of pellets, 0.191 in. OD, with an L/D ratio of about 1.0, stacked one atop the other inside the tube. Space not taken up by fuel will be filled with one atmosphere helium at room temperature. Void space will be left inside the tube, above the fuel stack. The volume will be determined by considerations of stress in the clad due to temperature rise and estimated fission gas release. The lower temperature specimens will have a central thermocouple measuring the

planned 1900°F central temperature. The cladding will be niobium. The higher temperature capsules will not have a central thermocouple, but will have a pressure probe attached to measure internal gas pressure during operation. The cladding will be stainless steel.

Test Conditions

A total of eight capsules will be irradiated. Two capsules containing UC specimens will be irradiated in 1960, and six capsules containing PuC-UC specimens will be irradiated in 1961. The detailed design of the two UC capsules is being completed currently and their description is given in Table 6.3. Capsules 3 through 8 will test 20% PuC-80% UC fuel; test conditions contemplated are presented in Table 6.4.

Test Reactor

The Westinghouse Test Reactor (WTR) was chosen for the irradiation tests for the following reasons:

1. Geographic proximity. The location of the WTR near Pittsburgh, Pennsylvania is 2000 to 3000 miles closer than test reactors with comparable neutron fluxes, such as MTR, ETR, and GETR. Considerable savings in communications, and transportation of personnel and heavy equipment can be made by use of the WTR.
2. Highest available fast flux. PuC-UC fuel is intended for reactors having a high fast flux. Since high energy neutrons have a major effect on material properties, it is important to irradiate the fuel in a fast flux representative of power reactor operating conditions. The WTR has facilities for irradiation in the center of its fuel elements, thus making a high fast flux available, equalled only in the ETR. Suitable space in the ETR is committed for long term, high priority work, and the operating power during this period is uncertain.
3. Predictability of flux. The WTR is installing cobalt flux suppressors in the core. It is hoped this will reduce the maximum-to-average flux ratio and reduce the flux suppression caused by experiments. The flux in an experimental hole will then be much less dependent on neighboring experiments, and will be predictable within much closer limits.
4. Cost. Irradiation costs are comparable to other high flux test reactors.

Capsule Design Description

Capsule No. 1

Detailed design of the capsule is currently in progress. The capsule consists of an outer and inner shell separated by fins and a helium annulus. The outer shell, or jacket, is $16\frac{1}{2}$ in. long by 1.125 in. OD. It is sealed at the bottom with a welded plug, 1/4 in. thick, and at the top by the welded conduit adapter plug. The conduit is approximately 27 ft long by 3/4 in. OD, and is attached by means of a Swagelok connector to an aluminum terminal box.

The inner capsule, containing the two fuel specimens, heaters, monitor wire well, and thermocouple wells, is a stainless steel finned tube sealed at both ends by welded plugs. The inner capsule is filled with sodium and helium cover gas at one atmosphere room temperature pressure. Operating pressure is about three atmospheres absolute inside the container due to helium expansion. A sodium fill tube, four heater leads, and the thermocouple wells are brazed into the top plug. A single thermocouple well is brazed into the bottom plug.

A stainless steel sleeve, 1.5 in. OD, surrounds the outer jacket, with an annular space between jacket and sleeve of 0.090 in. The sleeve serves to support the capsule in the reactor basket, while providing an annulus of the proper size to permit cooling water flow around the capsule jacket. The capsule sleeve is designed to fit inside a WTR size "W" basket.

Table 6.3 — Description of UC Capsules

	Lower Temperature Capsule (Capsule 1)	Higher Temperature Capsule (Capsule 2)
Specimen	UC, 3½% enriched. Niobium clad. Two specimens per capsule.	UC, 3½% enriched. Stainless steel clad. One specimen per capsule.
Burnup, % of Total Uranium Atoms	2	2
Maximum Fuel Temperature	1900°F (1040°C)	2600-2900°F (1430-1600°C)
Clad Surface Temperature	1000°F (540°C)	~1760°F (960°C)
Power, kw/ft	14	14-18
Test Reactor	WTR*	WTR*
Thermal Flux, nvt (depressed)	1.2×10^{14}	1.2×10^{14}
Fast Flux, nvt	1×10^{15}	1×10^{15}
Irradiation Time, Calendar Months	~6	~6
Instrumentation		
Temperature (recorded continuously)	Central and surface thermocouples	Surface thermocouples
Temperature control (continuous)	Heater	Heater
Fission gas release (periodic manual reading)	——	In-pile pressure measurement
Burnup	Flux monitors	Flux monitors
Post-Irradiation Examination	Visual and dimensional examination of clad sample. Photography of samples. Puncture of clad and fission gas release measurement. Visual and dimensional examination of fuel pellets. Counting of flux monitors. Dissolution studies for reprocessing.	

* Westinghouse Test Reactor.

Table 6.4 — Capsule Test Conditions

	Burnup		Maximum Fuel Temperature, °F	Instrumentation, Post-Irradiation Examination
	% of Pu atoms	% U+Pu atoms		
Capsule 3	20	~4	1900	As in Capsule 1
Capsule 4	20	~4	2600-2900	As in Capsule 2
Capsule 5	40	~8	1900	As in Capsule 1
Capsule 6	40	~8	2600-2900	As in Capsule 2
Capsule 7	To be determined		1900	As in Capsule 1
Capsule 8	To be determined		2600-2900	As in Capsule 2

During irradiation, control of the specimen temperature is achieved by varying the electrical power input to the heaters. The instrument used to maintain heater control is a recorder-controller, operating with a motor-driven variable autotransformer equipped with a potentiometer slide wire control unit. The single setpoint available in the recorder portion of the recorder-controller is used to activate a high-temperature alarm signal. The control console is also equipped with a multipoint strip-chart recorder, watt hour meter, voltmeter, ammeters, and switchgear necessary for power control.

Capsule No. 2

Basically, Capsule No. 2 is the same as Capsule No. 1, except for inclusion of the pressure measuring device, the deletion of one specimen, and a higher operating temperature. Design of the pressure measuring probe is currently in progress.

6.4.7 Capsule Heater Tests

Fuel temperature is an important variable for an irradiation test. A constant test temperature is important, for meaningful extrapolation of the test data to a fuel element design. Large temperature drops result from loss of fission heat during long burnup tests, and large temperature changes can result from test reactor power changes and flux depression from neighboring experiments. The NDA temperature controlled capsule uses a small, sheathed, ceramic-insulated, electrical heater to control the temperature at a constant level. The test temperature depends on the reliability of the capsule heater; for this reason out-of-pile performance tests of the heaters were made to provide information on the reliability and possible methods of failure of the heaters. Since the heater reliability is a problem common to the Sponge Fuel Project [Contract AT(30-1)-2303, Project III] as well as this project, the tests were financed jointly.

A dummy capsule was constructed in which two heaters were immersed in sodium with helium cover gas. The inner and outer shell configuration was representative of the actual capsule design. The heater specifications were as follows:

Heater Length	68 in.
Heater Sheath, OD	0.056 in.
Heater Coil, OD	0.875 in.
Heater Max. Power Rating	2000 watts
Voltage at Max. Power	208 volts
Current at Max. Power	9.6 amp

At the start of the test, one heater failed due to overheating the terminal joining one of the heater leads to the electrical conductor wire. The remaining heater operated cyclically for 25 days at an average power of 1600 watts and a maximum temperature of 1170°F. The heater was cycled on and off eight times in the course of the test, in order to simulate reactor shutdowns. The heater was still operable when the test was terminated.

An improved heat transfer correlation was also obtained from temperature and power measurements made during calibration runs on the dummy capsule. The calibration runs were conducted in a water flow test rig which simulated reactor operating conditions.

6.5 REFERENCES FOR SECTION 6

1. G.K. Williamson, D.M. Poole, and J.A. Marples, A Description of Some Facilities for the Study of Plutonium and Its Alloys, AERE M/R 1990 (1956).
2. "Maximum Permissible Body Burdens and Concentrations of Radionuclides in Air and Water for Occupational Exposure," Handbook 69, National Bureau of Standards, Department of Commerce (June 5, 1959).
3. Jette and Coffinberry, Plutonium and Its Alloys, Chap. 1.15, General Properties of Materials, "Reactor Handbook," Vol. 3, Sec. 1 (Mar. 1955).

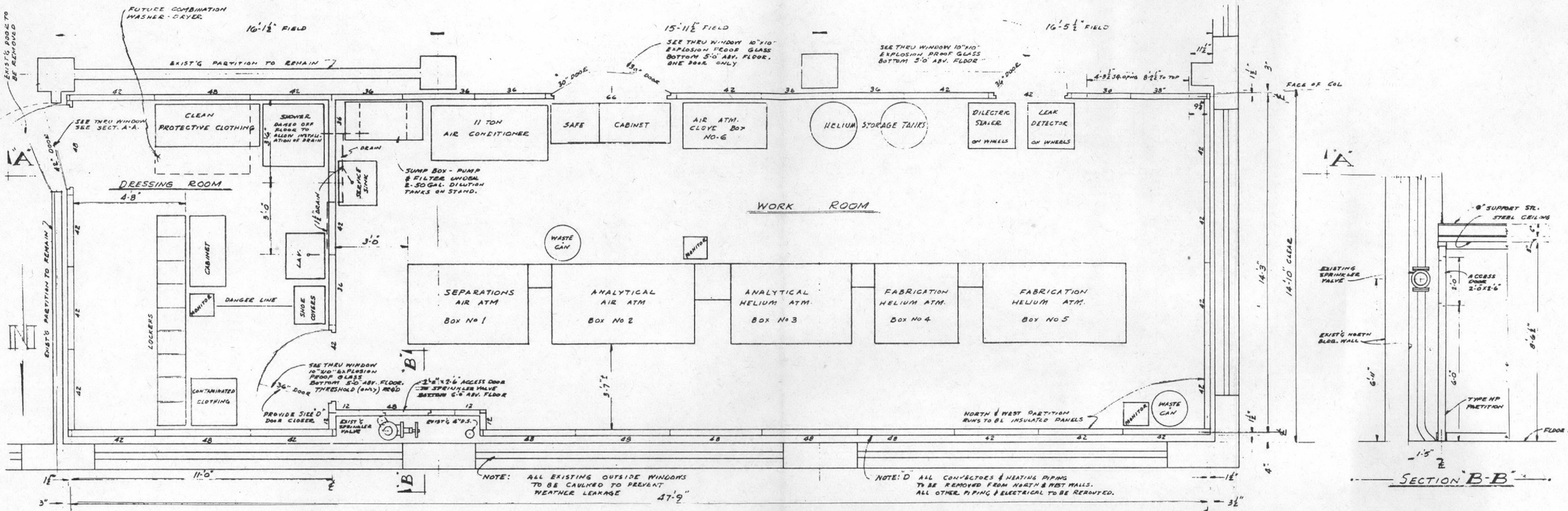

REF. DWGS:

No 34655	AIR COND; VENTILATION; PLUMBING
34656	EXHAUST PLENUM DETAILS
34657	PLUMBING DETAILS
34658	GLOVE BOX PIPING & AIR DUCT DETAILS

Fig. 6.1 — Plutonium handling facilities – research and development – equipment layout – The Carborundum Co.

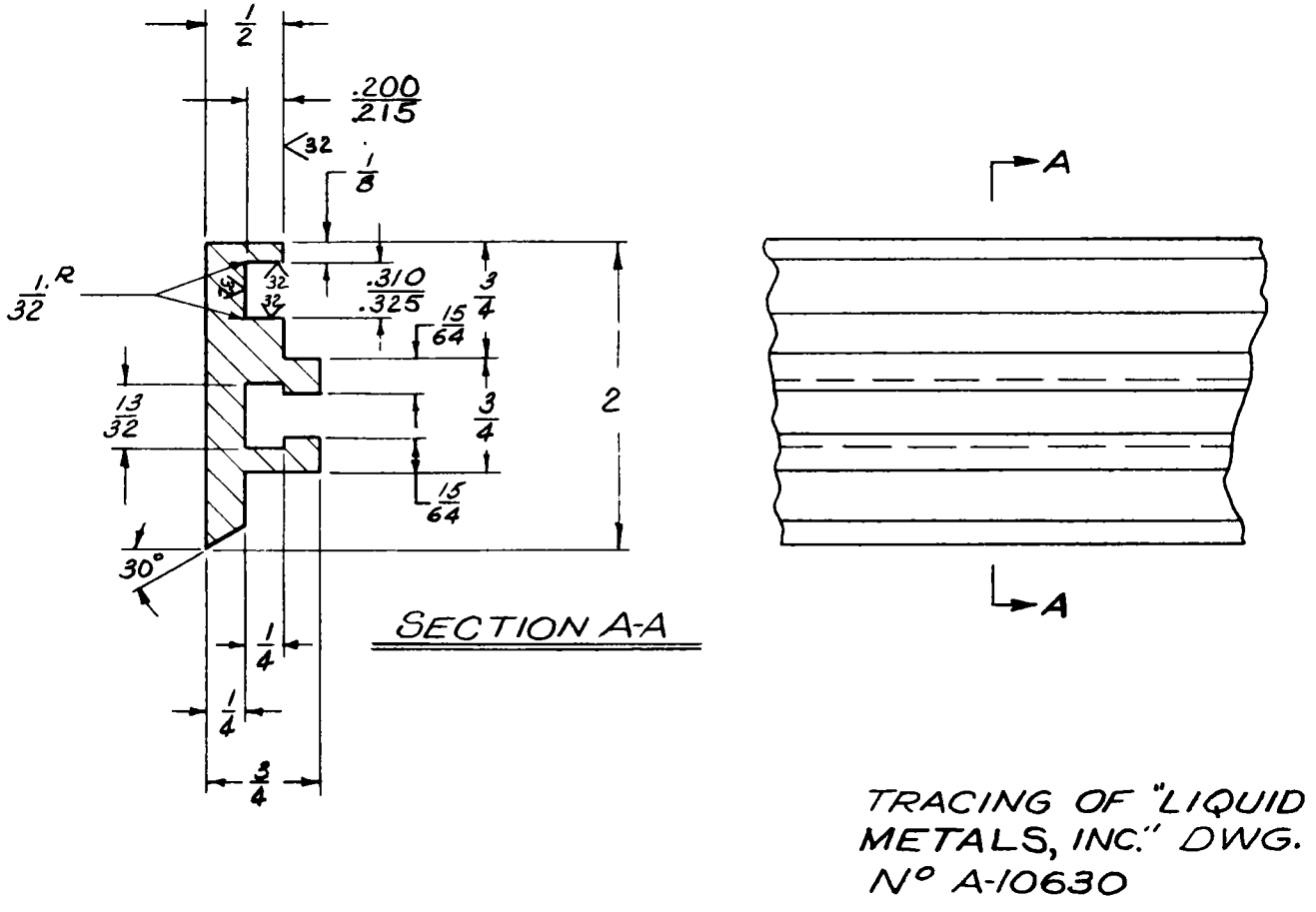

MATERIAL - 6061 T6 ALUMINUM

Fig. 6.2 — Special extrusion – The Carborundum Co.

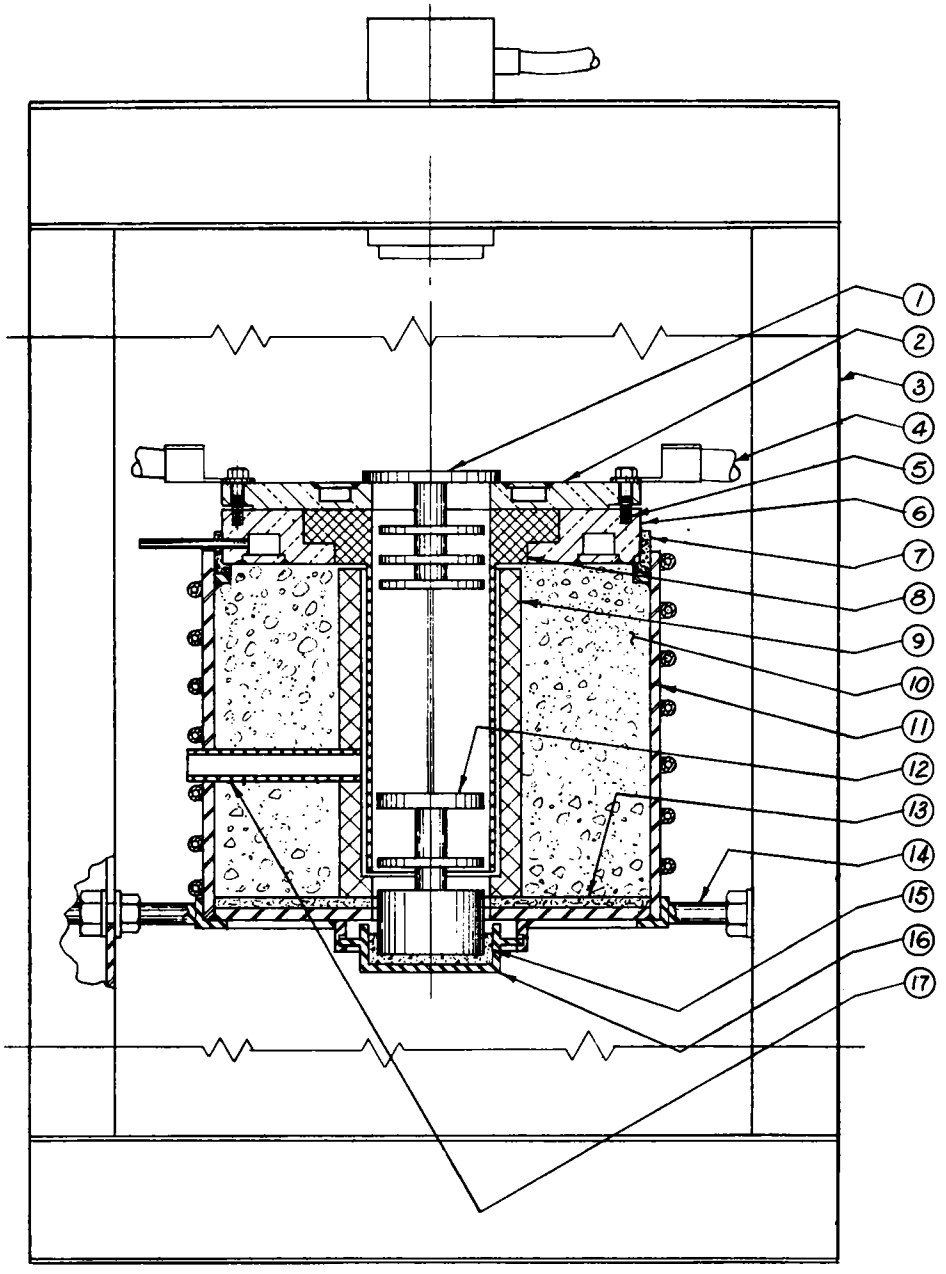

MATERIAL LIST

REQ'D	PART NO.	DESCRIPTION	MAT'L	PATT. NO.	REMARKS
1	R-1133-1	COVER	CARBON		
1	" 2	UPPER CONTACT PLATE	COPPER		
1	" 3	PRESS FRAME	STEEL		W/PHOTO-POWER
	" 4	POWER LEAD			
4	" 5	1/4-20 HEX. HD. MACH. SCR.	COPPER		STD.
1	" 6	LOWER CONTACT PLATE	"		
1	" 7	INSULATING RING	TRANSITE		
1	" 8	HAIRPIN ELEMENT	GRAPHITE		
1	" 9	INSULATING CYLINDER	CARBON		
1	" 10	INSULATION (BULK)	ZIRCONIA		
1	" 11	SHELL (WATER COOLED)	STEEL		
1	" 12	PEDESTAL	CARBON		
1	" 13	BASE INSULATOR	FIBERFRAX		
1	" 14	FURNACE SUPPORT	STEEL		
1	" 15	LINER	TRANSITE		
1	" 16	RETAINER CUP	STEEL		
1	" 17	SIGHT TUBE	GRAPHITE		
	" 18	HAIRPIN ELEMENT	"		ALTERNATE
	" 19	INSULATING CYLINDER	CARBON		"

NOTE: DETAILS -18 & -19 TO BE USED AS ALTERNATES OF DETAILS -8 & -9

Fig. 6.3 — Assembly of hairpin element furnace for sintering or hot pressing – The Carborundum Co.

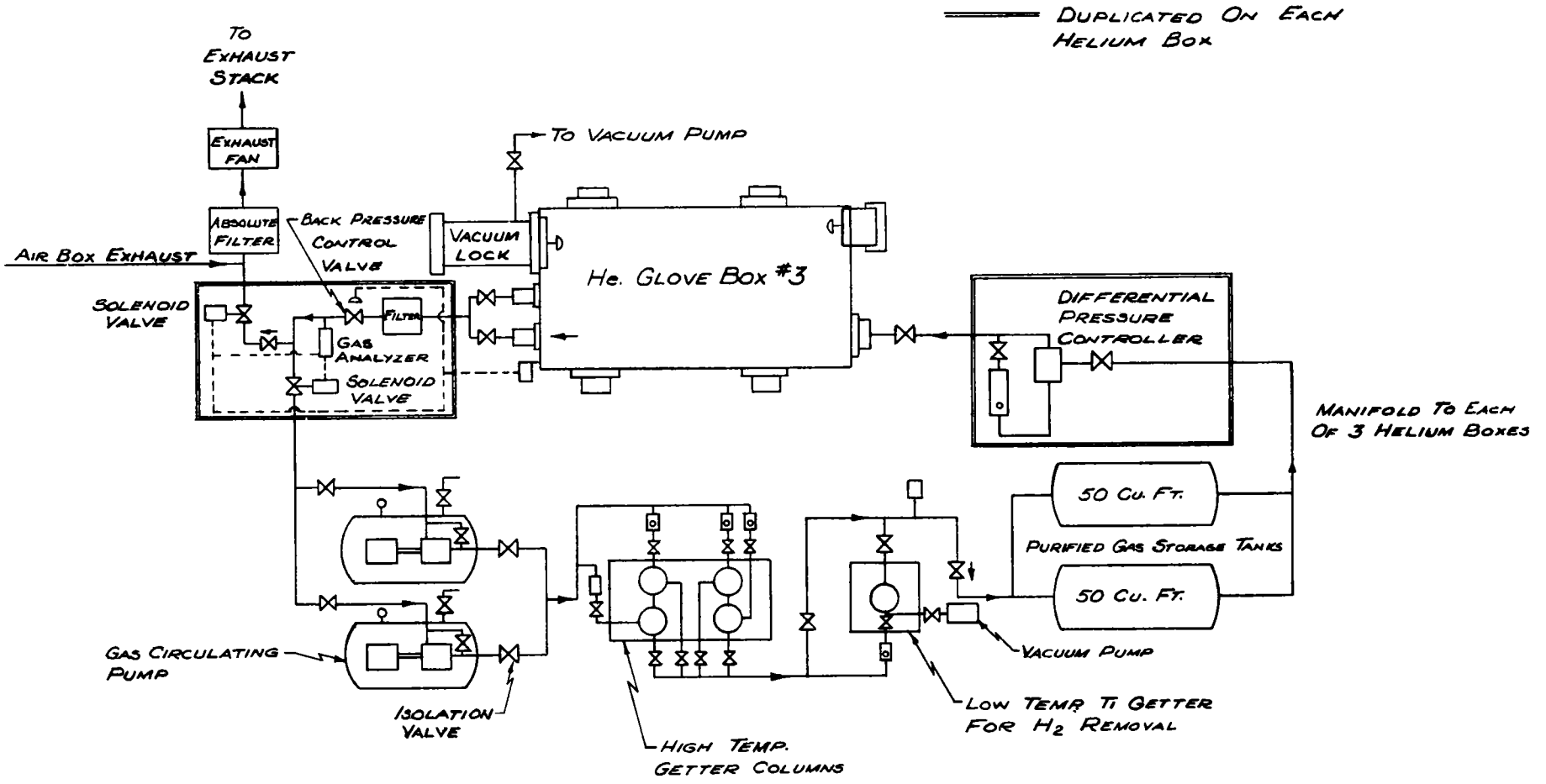

TRACING OF "LIQUID METALS, INC." DRAWING #A-10622 (8/10/59)

Fig. 6.4 — Helium purification and recovery system and glove-box – The Carborundum Co.

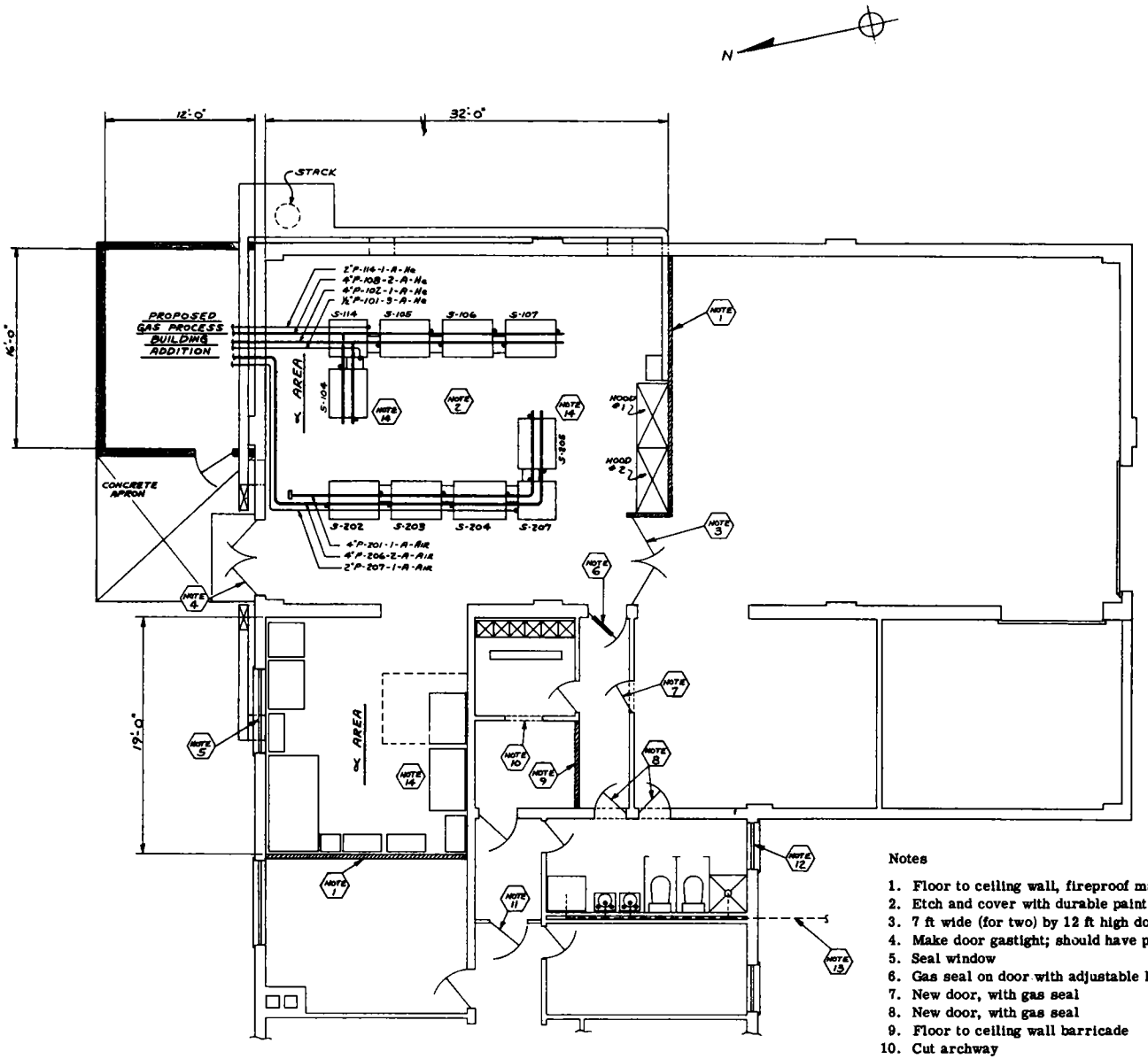

Notes

1. Floor to ceiling wall, fireproof material
2. Etch and cover with durable paint
3. 7 ft wide (for two) by 12 ft high double doors with gas seals
4. Make door gastight; should have panic bar on inside
5. Seal window
6. Gas seal on door with adjustable louvers on door
7. New door, with gas seal
8. New door, with gas seal
9. Floor to ceiling wall barricade
10. Cut archway
11. New door with gas seal and adjustable louvers on door
12. Seal window
13. Run drain from washing machine, sinks, and shower to waste process building basement
14. Air inlets

Fig. 6.5 — Pawling hot laboratory – modifications layout – ground floor plan

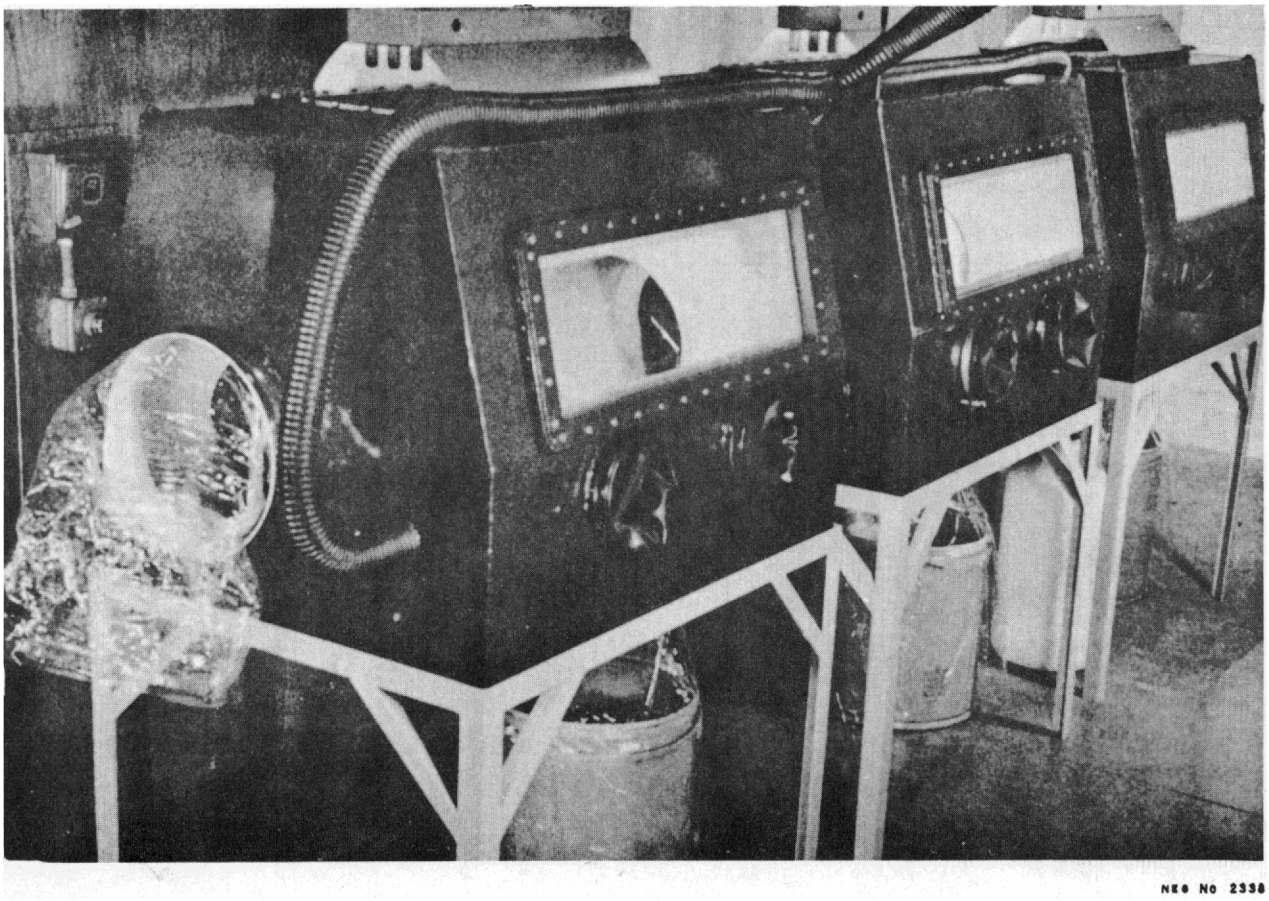

Fig. 6.6 — Chemistry boxes for NDA plutonium facility

7. APPENDIX

7.1 COST CALCULATIONS

The cost calculations were patterned after a method outlined by the Edison Electric Institute.* A sample cost estimate for a UC-fueled EFFBR (reactor B, Tables 3.5 and 3.7) is presented below; the symbols used correspond to those defined in the footnote. Background information follows.

Reactor Characteristics	Core	Blanket
Fuel material	UC	U-2¾% Mo
Content, KgU fresh fuel	1438	40,000
Enrichment, %	27.9	depleted (0.36)
Power, Mw	265	35
Specific power, S, tKw/KgU	152	0.875
Breeding ratio	0.259	0.906
Burnup, B, %	2.0	0.1

Station efficiency: Y = 33%
Plant utilization factor: X = 0.8.

The core and blanket were treated separately. Yearly costs were obtained for each and combined to determine the overall fuel cycle cost.

The average fuel residence time, T_r, in the reactor (core or blanket) is estimated in the following way:

$$T_r = \frac{25.2B}{SY}$$

where T_r = average fuel residence time in the reactor, years
B = burnup (percent of fissionable and fertile atoms fissioned before fuel discharge)
S = specific power at full power, (tKw/KgU input)
Y = plant utilization factor

$$T_{r\text{-core}} = \frac{(25.2)(2)}{(0.8)(184)} = 0.343 \text{ yr}$$

$$T_{r\text{-blanket}} = \frac{(25.2)(0.1)}{(0.8)(0.875)} = 3.60 \text{ yr}$$

---

* Survey of Initial Fuel Costs of Large U.S. Nuclear Power Stations, EEI-59-150 (Dec. 1959).

7.1.1 Net Fuel Material Cost, C_m

1. C'_u, value of U required for fresh fuel assuming 1.5% processing losses.

$$C'_{u\text{-core}} \text{ at 27.9\% enrichment} = 4573 \frac{\$}{\text{KgU}} \times 1.015 \frac{\text{KgU required}}{\text{KgU input}} = 4640 \frac{\$}{\text{KgU input}}.$$

$$C'_{u\text{-blanket}} = 4.85 \frac{\$}{\text{KgU input (depleted U)}}.$$

2. C''_u, value of U recovered from spent fuel assuming 1.5% processing losses.

$C''_{u\text{-core}}$ [based on 2% burnup, 0.9 occurring in U^{235}, and 1.2 atoms U^{235} destroyed per U^{235} fission $(1+\alpha \approx 1.2)$].

$$U^{235} \text{ destroyed} = 0.02 \times 0.9 \times 1.2 = 0.022 \frac{\text{atoms destroyed}}{\text{atom U input}}$$

$$U^{235} \text{ left} = 0.279\text{-}0.022 = 0.257 \frac{\text{atoms } U^{235}}{\text{atom U input}}$$

$$U^{238} \text{ fissioned} = 0.02 \times 0.10 = 0.002 \frac{\text{atoms } U^{238} \text{ fissioned}}{\text{atom U input}}$$

$$U^{238} \text{ captures} = 0.022 \times 0.259 = 0.006$$

$$\text{Total U destroyed} = 0.022 + 0.002 + 0.006 = 0.030$$

$$\text{Final enrichment} = \frac{0.257}{0.970} = 0.265$$

Based on 1.5% processing loss and 3.0% destroyed

$$C''_{u\text{-core}} \text{ at 0.265 enrichment} = 4334 \frac{\$}{\text{KgU}} \times 0.955 \frac{\text{Kg recovered}}{\text{KgU input}} = 4140 \frac{\$}{\text{KgU input}}$$

$$C''_{u\text{-blanket}} = 4.85 \text{ \$/KgU input.}$$

3. Net U cost, C_u, is the value of U required minus the value of U recovered.

$$C_u = (C'_u - C''_u)$$

$$C_{u\text{-core}} = 4640\text{-}4140 = 500 \text{ \$/KgU input}$$

$$C_{u\text{-blanket}} = 0$$

4. Credit for Pu recovered, C_{Pu}, assuming 1% losses in processing.

Core:

$$\text{Pu formed} = 0.022 \frac{\text{KgU}^{235} \text{ destroyed}}{\text{KgU input}} \times 0.259 \frac{\text{KgPu formed}}{\text{KgU}^{235} \text{ destroyed}} = 0.0057 \frac{\text{KgPu formed}}{\text{KgU input}}.$$

$$C_{Pu} \text{ at } 30\ \$/gm = 0.0057 \times 30{,}000 \times 0.99 = 170\ \frac{\$}{KgU \text{ input}}.$$

Blanket:

$$\text{Pu formed} = 0.022\ \frac{KgU^{235} \text{ destroyed}}{KgU \text{ input into core}} \times 0.906\ \frac{KgPu \text{ formed in blanket}}{KgU^{235} \text{ destroyed}}$$

$$\times\left(\frac{1438}{0.343}\right)\frac{KgU \text{ in core}}{yr} \times\left(\frac{3.60}{40{,}000}\right)\frac{yr}{KgU \text{ in blanket}} = 0.00752\ \frac{KgPu \text{ formed in blanket}}{KgU \text{ input to blanket}}.$$

$$C_{Pu\text{-blanket}} \text{ at } 30\ \$/gm = 0.00752 \times 30{,}000 \times 0.99 = 223\ \frac{\$}{KgU}.$$

5. Net fuel material cost C_m.

$$C_m = C_u - C_{Pu}$$

$$C_{m\text{-core}} = 500\text{-}170 = 330\ \$/KgU \text{ input into core.}$$

$$C_{m\text{-blanket}} = -223\ \$/KgU \text{ input into blanket.}$$

7.1.2 Fuel Fabrication Cost, C_f

Core:

1. Cost of converting UF_6 to UO_2

$$C_{f\text{-}1 \text{ core}} = 100\ \frac{\$}{KgU}$$

2. Cost of converting UO_2 to UC powder

$$C_{f\text{-}2 \text{ core}} = 10\ \frac{\$}{KgU}$$

3. Cost of fabricating UC powder to UC pellets, assuming 2% losses

$$C_{f\text{-}3 \text{ core}} = 11 + (0.02 \times 4573) = 102\ \frac{\$}{KgU}$$

4. Cost of stainless steel

$$C_{f\text{-}4 \text{ core}} = 2.50\ \frac{\$}{KgU}$$

5. Assembly and inspection

$$C_{f\text{-}5 \text{ core}} = 120\ \frac{\$}{KgU}$$

6. Shipping cost of fresh fuel

$$C_{f-6 \text{ core}} = 2 \frac{\$}{KgU}$$

7. Total core fabrication cost

$$C_{f-core} = 100 + 10 + 102 + 2.50 + 120 + 2 = 336.5 \frac{\$}{KgU}$$

Blanket:

1. Cost of converting UF_6 to metal

$$C_{f-1 \text{ blanket}} = 11 \frac{\$}{KgU}$$

2. Cost of extrusion and fabrication

$$C_{f-2 \text{ blanket}} = 19.2 \frac{\$}{KgU}$$

3. Scrap recovery and loss in fabrication

$$C_{f-2 \text{ blanket}} = 0$$

4. Inspection cost

$$C''_{f-2 \text{ blanket}} = 2.9 \frac{\$}{KgU}$$

5. Subassembly hardware

$$C'''_{f-2 \text{ blanket}} = 28.8 \frac{\$}{KgU}$$

6. Shipping fresh fuel

$$C_{f-3 \text{ blanket}} = 2 \frac{\$}{KgU}$$

7. Total blanket fabrication cost

$$C_{f-blanket} = 11 + 19.2 + 2.9 + 28.8 + 2 = 63.9 \frac{\$}{KgU}$$

7.1.3 Spent Fuel Processing Cost, C_p

1. Cost of shipping spent fuel and recovered and converted materials

$$C_{p-1} = 5 \frac{\$}{KgU}$$

2. Cost of recovery of pure U and Pu nitrates from spent UC fuel, C_{p-2}. (It is assumed that spent fuel elements from the core and blanket are processed together at yearly intervals.)

Recovery plant costs: \$15,300/day

Recovery plant capacity: 1000 KgU/day

$$\text{Processing time core} = 1438 \text{ KgU} \times \frac{0.985 \text{ KgU processed}}{\text{KgU input}} \times \frac{1 \text{ day}}{1000 \text{ KgU processed}} = 1.42 \text{ days}$$

$$\text{Processing time} = \frac{1.42}{0.343} = 4.14 \text{ days}$$

(It is assumed that total cleanup time is 8 days for combined cores and blanket. 4.1 days are charged to core and 3.9 days to blanket.)

$$C_{p-2} \text{ core} = \frac{15{,}300 \text{ \$/day}(4.1+4.1) \text{ days}}{1438/0.343 \text{ KgU}} = 29.9 \text{ \$/KgU input}$$

$$\text{Processing time blanket} = \frac{1}{3.60} \times 40{,}000 \times 0.985 \times \frac{1}{1000} = 10.9 \text{ days}$$

Plant cleanup time = 3.9 days

$$C_{p-2} \text{ blanket} = \frac{15300(10.9+3.9)}{40{,}000/3.6} = 20.4 \text{ \$/KgU input}$$

3. Conversion of pure uranium nitrate to UF_6, C_{p-3}

$$C_{p-3} \text{ core} = 32 \frac{\$}{\text{KgU processed}} \times 0.985 \frac{\text{Kg processed}}{\text{KgU input}} = 31.4 \text{ \$/KgU input}$$

C_{p-3} blanket = 0

4. Conversion of pure Pu nitrate to Pu metal, C_{p-4}

$$C_{p-4} \text{ core} = 0.0057 \frac{\text{KgPu processed}}{\text{KgU}} \times 1500 \frac{\$}{\text{KgPu processed}} = 8.7 \text{ \$/KgU input}$$

C_{p-4} blanket = 0.00752 × 1500 = 11 \$/KgU input

5. Recovery of Pu and U scrap, C_{p-5} [Taken as 17% of $(C_{p-2}+C_{p-3}+C_{p-4})$]

	Core	Blanket
C_{p-2}	29.9	20.4
C_{p-3}	31.4	0
C_{p-4}	8.7	11
	70.0	31.4

C_{p-5} core = 0.17 × 70.0 = 11.9 KgU input

C_{p-5} blanket = 0.17 × 31.4 = 5.2 KgU input

6. Total spent fuel processing cost, C_p

$$C_{p\text{-core}} = 5 + 29.9 + 31.4 + 8.7 + 11.9 = 86.9 \text{ \$/KgU input}$$

$$C_{p\text{-blanket}} = 5 + 20.4 + 0 + 11 + 5.3 = 41.7 \text{ \$/KgU input}$$

7.1.4 Fuel Cycle Working Capital Costs

1. The average working capital fund required is assumed to be the fuel fabrication cost, plus the cost of fuel purchased if any. Since enriched uranium is leased from the government, the only fuel purchased is the depleted U in the blanket. The average term of working capital fund is assumed to be the average residence time of fuel in the reactor. Cost of working capital fund, C_c, is assumed to be 12% simple interest per fund dollar per year.

$$C_{c\text{-core}} = 337 \text{ \$/KgU} \times 0.12\%/\text{yr} \times 0.343 \text{ yr} = 13.9 \text{ \$/KgU input}$$

$$C_{c\text{-blanket}} = (64+4.85)0.12 \times 3.60 = 29.7 \text{ \$/KgU input}$$

7.1.5 Fuel Material Lease Charge, C_ℓ

1. Value of uranium material leased

$$C'_{u\text{-core}} = 4640 \frac{\$}{\text{KgU input}}$$

2. Term of lease, yr

	Core
Fresh fuel processing time	0.30
Residence time in reactor	0.34
Spent fuel reprocessing time	0.70
	1.34

3. Cost of leasing material at 4% per year

$$C_{\ell \text{ core}} = 4640 \frac{\$}{\text{KgU input}} \times 1.34 \text{ yr} \times \frac{0.04}{\text{yr}} = 250 \frac{\$}{\text{KgU input}}$$

$C_{\ell \text{ blanket}} = 0$ (depleted U is purchased and accounted for under fuel cycle working capital cost)

7.1.6 Total Fuel Cost, M

To obtain total fuel costs for the reactor the unit costs obtained (C_i\$/Kg) must be multiplied by the following constants, and added:

Core:

$$M_{i \text{ core}} = \frac{\$}{\text{KgU input}} \times 10^3 \frac{\text{mill}}{\$} \times \frac{1438 \text{ KgU input}}{0.343 \text{ yr}} \times \frac{\text{yr}}{100 \times 0.8 \times 10^3 \text{ kw } 24 \times 365 \text{ hr}}$$

$$= C_{i \text{ core}} \times \frac{1438}{0.343} \times 0.143 \times 10^{-5} = 0.00598 \, C_{i \text{ core}}$$

M_i = mills/eKw-hr

Blanket:

$$M_{i\ \text{blanket}} = C_{i\ \text{blanket}} \times \frac{40{,}000}{3.60} \times 0.143 \times 10^{-5} = 0.0159\ C_{i\ \text{blanket}}$$

7.1.7 Summary of Costs

	Core		Blanket		Total
	$/KgU	mills/eKw-hr	$/KgU	mills/eKw-hr	mills/eKw-hr
C_u, Net Uranium Cost	500	2.99	0	0	
C_{Pu}, Credit for Pu Recovered	-170	-1.02	-223	-3.55	
C_m, Net Fuel Material Cost	330	1.97	-223	-3.55	-1.58
C_f, Fuel Fabrication Cost	337	2.02	64	1.02	3.04
C_p, Spent Fuel Processing Cost	87	0.52	42	0.67	1.19
C_c, Fuel Cycle Working Capital Cost	14	0.08	30	0.47	0.55
C_e, Fuel Material Lease Cost	250	1.50			1.50
					4.70

7.2 FISSION PRODUCT BUILDUP AT HIGH BURNUP

The buildup of fission products for an EFFBR fueled with PuC-UC (reactor C, Table 3.5) was determined for 40% burnup of the original plutonium (~8 a/o burnup or ~65,000 MW-d/T). This burnup corresponds to a fuel residence time of approximately 1 yr (at 100% plant utilization factor). The results are shown in Fig. 7.1, which is a plot of fission product weight per fuel pin vs cooling time. Fig. 7.2 shows the influence of irradiation time, by plotting the ratio of fission product weight to that for 1 yr irradiation. Only those elements among the fission products which form stable carbides and, therefore, might possibly interfere with chemical reprocessing of the fuel are considered.

In Fig. 7.3 the gross fission product activity and the fission product energy release are given as a function of cooling time, to further aid in assessing difficulties which might arise in the reprocessing steps.

The above data are derived from publications by ANL,* based on plutonium fission in fast reactors.

* Estimation of Fission Product Spectra in Discharged Fuel from Fast Reactors, L. Burns, Jr., and P.G. Dillon, ANL-5742 (July 1957).

7.3 CHEMICAL ANALYSIS TECHNIQUES

7.3.1 Uranium (Gravimetric Analysis at The Carborundum Co.)

A 0.5 g sample contained in a platinum crucible was weighed and ignited at 1000℃. A mixture of hydrofluoric, nitric, and sulfuric acids was added to the cooled sample and evaporated until SO_3 fumes were noticeable. The contents of the crucible were then transferred to a 150 ml beaker with the aid of water. Iron was separated from the uranium by the addition of ammonium hydroxide and ammonium carbonate and the precipitate was repeatedly washed with ammonium carbonate. The filtrate and washings were then acidified with nitric acid and heated to boiling. The uranium was precipitated from the cooled solution with ammonium hydroxide, filtered, and ignited to constant weight at 1000℃. The uranium content of the sample was then calculated on the basis of the weight of the U_3O_8 recovered.

7.3.2 Carbon Analysis

In order to ascertain the completeness of reaction in the formation of UC, it is necessary to determine the combined carbon and the free carbon content of a sample. This has been accomplished by determining the total carbon and free carbon contents and calculating the combined carbon from these values.

Total Carbon Analysis

A measured quantity of iron chips and tin metal was added to a 1 g sample contained in a combustion crucible. The mixture was ignited for a period of 3 min in a Leco induction furnace under oxygen flowing at a rate of 1 liter per min. Carborundum collected the released CO_2 in ascarite contained in weighed Nesbitt absorption bulbs. NDA's method is similar but involves smaller quantities of material and the CO_2 is collected in barium hydroxide. The barium carbonate is filtered and washed. The remaining barium hydroxide and washings are titrated with acid.

Free Carbon Analysis

One gram of the carbide sample was dissolved in 50 ml containing 3 volumes of HNO_3 to 5 volumes of water and heated on a sand bath until the carbides were decomposed. The resulting sample was filtered through a Gooch filter containing a previously ignited asbestos pad. The residue was washed with $HCl:H_2O$(1:20), then with hot water and dried at 110℃. The graphitic carbon content was determined by the combustion method described above.

7.3.3 Nitrogen Analysis

A 1 g sample was weighed on tared aluminum foil and placed in a stainless steel boat containing 25 g of previously melted potassium hydroxide. The charge was inserted into a furnace equipped with a stainless steel tube and heated to 500-600℃. After 40 min of fusion the ammonia produced from the nitrides was flushed by passing argon through the train and scrubbed through a hot 20% sodium hydroxide solution. The condensate from this scrub solution was collected in a 50 ml boric acid solution and titrated with 0.10N sulfuric acid.

7.3.4 Iron Analysis

The iron content of precipitates described in Section 7.3.1 was determined colorimetrically with thiocyanate.

7.3.5 Proposed Future Methods

Volumetric Uranium Analysis (NDA)

The procedure for the determination of macro amounts of uranium involved the dissolution of carbide pellets in acid, the removal of interfering cations by cupferron and fuming with sulfuric acid. This technique has been used at NDA on other projects and is proposed for this project. The resulting solution was then passed through a Jones reductor and aerated. Titration of U^{+4} to U^{+6} with standard ceric sulfate using Ferroin (1,10-phenanthroline-ferrous sulfate) as a visual indicator resulted in a precision of 0.03%. Using a potentiometric method with a platinum mesh electrode and a saturated calomel fiber type electrode to produce a titration curve revealed that the proper rate for the addition of ceric sulfate was strongly temperature dependent. Thus at room temperature a waiting period of about 20 min was necessary to obtain a constant voltage reading after each addition of titrant. The waiting period at 60-70°C was only 5 min. On the other hand, a rather rapid titration at room temperature will result in a good end point even though intermediate points along a titration curve may not represent the true shape of the curve.

Fluorimetric Uranium Analysis

Concentrations of uranium in waste streams are usually small and require large volume reductions or micro-analytical techniques. This technique has been used at NDA on other projects and is proposed for use on this project. Micro amounts of uranium (10^{-3} to 10^{3} μg) may best be determined fluorimetrically. The method consists of evaporating a small aliquot (0.1 ml) of a uranium containing solution on a platinum planchet which is then flamed to burn any possible organic matter. Sodium fluoride (100 mg) is then added to the sample and is fused two successive times; the planchet is then analyzed fluorimetrically and compared to standards. Each sample, blank and standard is run in triplicate. Precisions of the order of 2% or better have been regularly obtained with this technique.

Plutonium

Phases of the program involving PuC will require the analysis of samples for plutonium. Waterbury and Metz* fume plutonium solutions with perchloric acid and titrate the cooled Pu^{+6} solutions potentiometrically with ferrous sulfate. The advantage of this method is that reducible ions such as iron do not interfere. The use of hot perchloric acid in a glove-box is not advisable unless one takes special precautions to prevent its contact with organic matter. Such precautions would include the use of special hoods or self-contained glass apparatus. For this reason it has been decided to titrate Pu^{+3} to Pu^{+4} with ceric sulfate after appropriate chemical separation of plutonium from interfering ions.

A solution containing uranium, plutonium, and reducible ions such as Fe^{+3} is made to 10M with respect to nitric acid and extracted with thenoyl trifluoroacetone (TTA) dissolved in xylene. Under these conditions the ferric complex is extracted in the organic phase while the U^{+6} and Pu^{+4} remain in the aqueous phase. The aqueous solution is then diluted to 2M HNO_3, reduced with hydroxylamine, then oxidized with sodium nitrite and extracted with TTA. Under these conditions Pu^{+4} goes into the organic phase and U^{+6} remains in the aqueous phase.

Aliquots of the resulting aqueous or organic phases may then be evaporated to dryness for the fluorimetric analysis of uranium or for alpha counting of the plutonium, respectively. When macro quantities are involved, the uranium aqueous phase or the plutonium (after back extraction into water with 10M HNO_3) may be fumed with sulfuric acid and passed through a Jones reductor, as described above, for subsequent volumetric analysis. In the case of plutonium the air oxidation step is omitted and the Pu^{+3} titrated potentiometrically to the +4 state.

---

*G.R. Waterbury and C.F. Metz, Anal. Chem. 31:1144 (1959).

Another approach for macro analysis of uranium and plutonium involves the separation of interfering cations such as iron by cupferron and separating the uranium from the plutonium by means of ion exchange using Dowex 1A.* Under the conditions of the method uranium is not adsorbed and the adsorbed plutonium may be eluted with a reducing agent such as hydroxylamine.

---

*C.F. Metz, Anal. Chem. 29:1748 (1957).

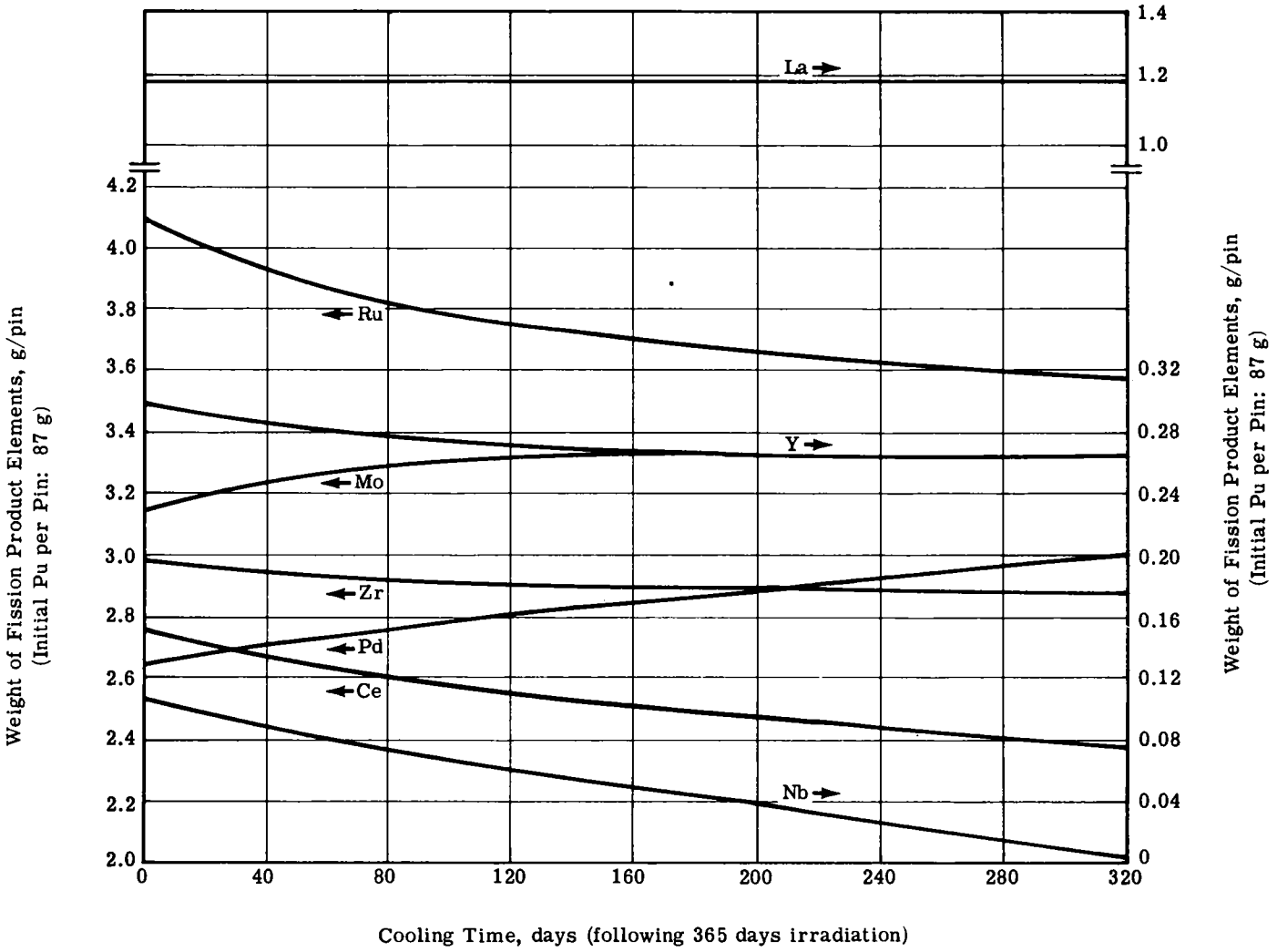

Fig. 7.1 — Weight of fission product elements vs cooling time – 40% Pu burn-up in PuC-UC reactor (Reactor C, Table 3.5)

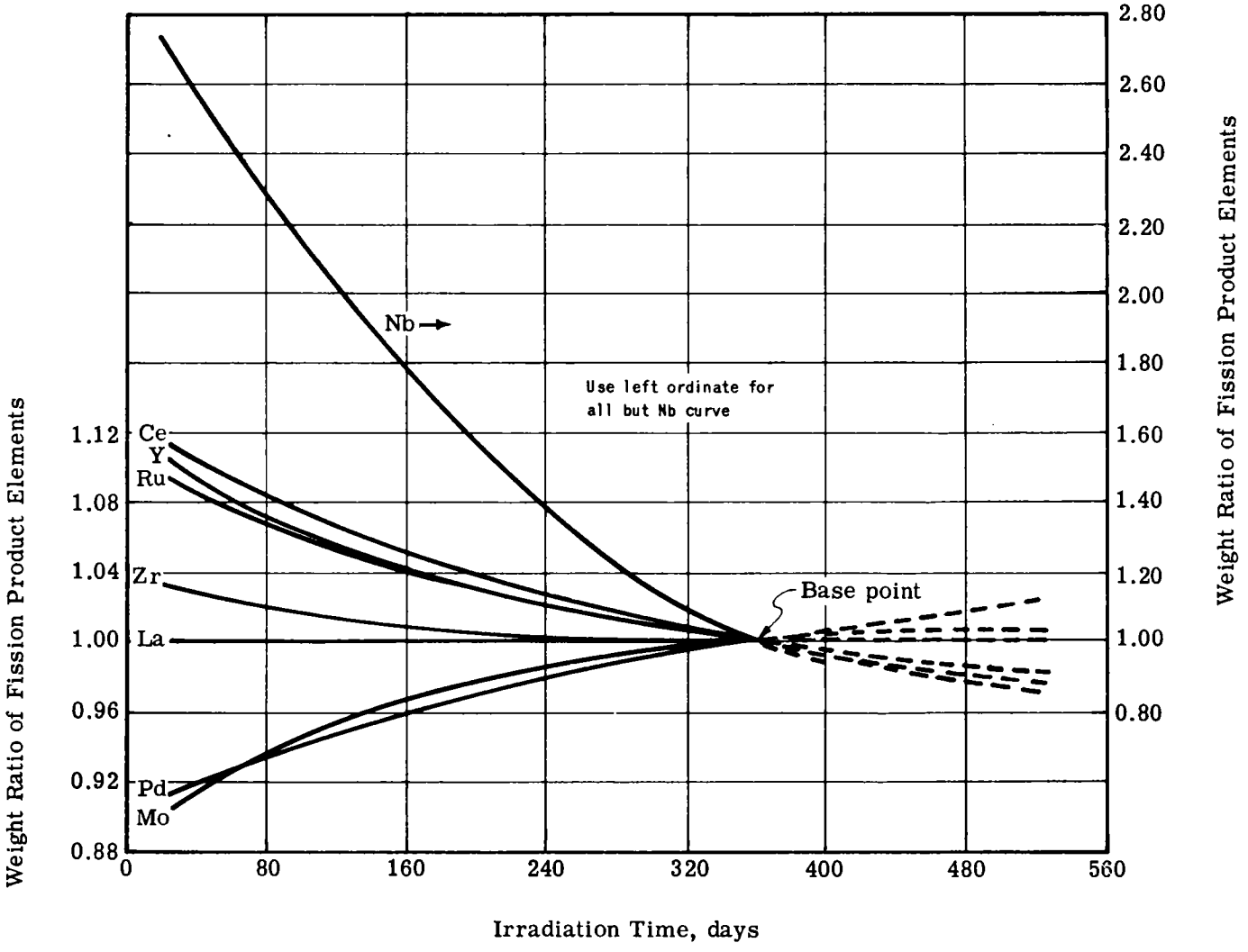

Fig. 7.2 — Ratio of fission product weight for variable irradiation times to weight at 365 day irradiation. Cooling time = 100 days. 40% of original Pu^{49} atoms burned out. (Reactor C, Table 3.5)

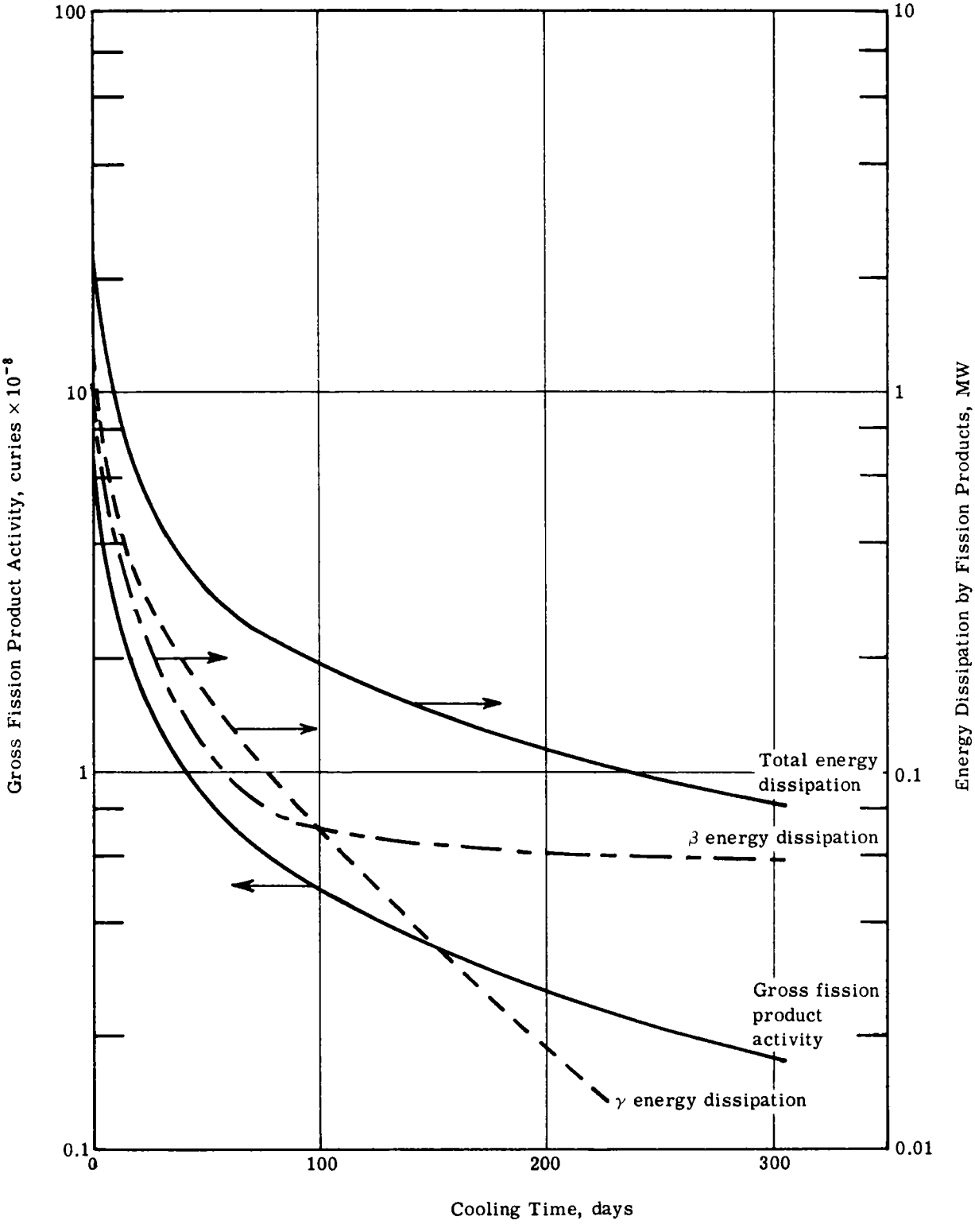

Fig. 7.3 — Fission product activity and energy dissipation of fission products vs time of cooling – 40% Pu^{49} burnout – 365 day irradiation (Reactor C, Table 3.5)